

# Crepant Resolutions of $\mathbb{C}^3/\mathbb{Z}_4$ and the Generalized Kronheimer Construction (in view of the Gauge/Gravity Correspondence)

UGO BRUZZO <sup>a,g</sup>, ANNA FINO <sup>b,g</sup>, PIETRO FRÉ <sup>c,f,g</sup>,  
PIETRO ANTONIO GRASSI <sup>d,f,g</sup> AND DIMITRI MARKUSHEVICH <sup>e,g</sup>

<sup>a</sup> SISSA (Scuola Internazionale Superiore di Studi Avanzati),  
via Bonomea 265, 34136 Trieste, Italy;  
INFN (Istituto Nazionale di Fisica Nucleare), Sezione di Trieste;  
IGAP (Institute for Geometry and Physics), Trieste  
e-mail: bruzzo@sissa.it

<sup>b</sup> Dipartimento di Matematica G. Peano, Università di Torino,  
Via Carlo Alberto 10, 10123 Torino, Italy  
e-mail: annamaria.fino@unito.it

<sup>c</sup> Dipartimento di Fisica, Università di Torino, via P. Giuria 1, 10125 Torino, Italy  
e-mail: pfre@unito.it

<sup>d</sup> Dipartimento di Scienze e Innovazione Tecnologica, Università del Piemonte Orientale,  
viale T. Michel 11, 15121 Alessandria, Italy  
e-mail: pietro.grassi@uniupo.it

<sup>e</sup> Department de Mathématique, Université de Lille, Bâtiment M2,  
Cité Scientifique, 59655 Villeneuve-d'Ascq, France  
e-mail: dimitri.markouchevitch@univ-lille.fr

<sup>f</sup> INFN (Istituto Nazionale di Fisica Nucleare), Sezione di Torino

<sup>g</sup> Arnold-Regge Center for Algebra, Geometry and Theoretical Physics,  
via P. Giuria 1, 10125 Torino, Italy

February 18, 2019; revised June 6, 2019

## Abstract

As a continuation of a general program started in two previous publications, in the present paper we study the Kähler quotient resolution of the orbifold  $\mathbb{C}^3/\mathbb{Z}_4$ , comparing with the results of a toric description of the same. In this way we determine the algebraic structure of the exceptional divisor, whose compact component is the second Hirzebruch surface  $\mathbb{F}_2$ . We determine the explicit Kähler geometry of the smooth resolved manifold  $Y$ , which is the total space of the canonical bundle of  $\mathbb{F}_2$ . We study in detail the chamber structure of the space of stability parameters (corresponding in gauge theory to the Fayet-Iliopoulos parameters) that are involved in the construction of the desingularizations either by generalized Kronheimer quotient, or as algebro-geometric quotients. The walls of the chambers correspond to two degenerations; one is a partial desingularization of the quotient, which is the total space of the canonical bundle of the weighted projective space  $\mathbb{P}[1, 1, 2]$ , while the other is the product of the ALE space  $A_1$  by a line, and is related to the full resolution in a subtler way. These geometrical results will be used to look for exact supergravity brane solutions and dual superconformal gauge theories.

# Contents

<b>1</b>	<b>Introduction</b>	<b>2</b>
<b>2</b>	<b>The <math>\mathbb{C}^3/\mathbb{Z}_4</math> model, its McKay quiver and the associated Kronheimer construction</b>	<b>6</b>
2.1	The McKay quiver diagram and its representation . . . . .	7
2.2	The locus $\mathbb{V}_6 \subset \mathcal{S}_{\mathbb{Z}_4}$ . . . . .	9
2.3	The holomorphic quiver group $\mathcal{G}_{\mathbb{Z}_4}$ and the gauge group $\mathcal{F}_{\mathbb{Z}_4}$ . . . . .	9
2.4	The moment map equations . . . . .	10
<b>3</b>	<b>Properties of the moment map algebraic system and chamber structure</b>	<b>13</b>
3.1	Generalities on the chamber structure . . . . .	14
3.2	The solvable lines located in $\zeta$ space . . . . .	15
3.3	The Kähler potential of the quotient manifolds . . . . .	16
<b>4</b>	<b>Toric geometry description of the crepant resolution</b>	<b>20</b>
4.1	An initial cautionary remark . . . . .	20
4.2	The singular variety $Y_0 = \mathbb{C}^3/\mathbb{Z}_4$ . . . . .	21
4.3	The full resolution $Y$ of $Y_0 = \mathbb{C}^3/\mathbb{Z}_4$ . . . . .	21
4.4	The partial resolution $Y_3$ . . . . .	27
4.5	The degeneration $Y_{EH}$ . . . . .	30
4.6	Summary: the exceptional divisor, curves and homology 2-cycles . . . . .	33
<b>5</b>	<b>Chamber Structure and the tautological bundles</b>	<b>34</b>
5.1	The stability chambers . . . . .	35
5.2	Edges . . . . .	38
<b>6</b>	<b>Periods of the Chern classes of the tautological bundles</b>	<b>38</b>
6.1	The fundamental algebraic system and a dense toric chart covering the variety . . . . .	41
6.2	Periods inside the chambers. . . . .	43
6.3	Periods on the walls and on the edges . . . . .	45
6.4	Summary of the chamber and wall structure . . . . .	49
<b>7</b>	<b>The resolved variety <math>Y</math></b>	<b>50</b>
7.1	The two addends of the Kähler potential . . . . .	50
7.2	Exact solution of the moment map equations . . . . .	51
7.3	Induced Kähler geometry of the exceptional divisor $D_c \sim \mathbb{F}_2$ . . . . .	52
7.4	The isometry group of the second Hirzebruch surface and of the full resolution $Y$ . . . . .	56
7.5	Ricci-flat metrics on $Y$ . . . . .	57

<b>8</b>	<b>The partial resolution <math>Y_3</math> and its Kähler geometry</b>	<b>57</b>
8.1	Construction of the Kähler geometry of $Q_2$ . . . . .	57
8.2	The Kähler potential addends . . . . .	58
8.3	Interpretation . . . . .	61
8.4	The Kähler geometry of the singular variety $Y_3$ . . . . .	62
<b>9</b>	<b>Summary of the Chamber Structure Discussion</b>	<b>62</b>
<b>10</b>	<b>Conclusions</b>	<b>65</b>
	<b>Appendix: structure of the Hirzebruch surfaces</b>	<b>66</b>
	<b>References</b>	<b>68</b>

## 1 Introduction

The present paper is the next step of an investigation program initiated in [18, 30], whose final aim is to fully elucidate the relation among the physical building blocks of  $D = 3/D = 4$  supersymmetric gauge theories, the mathematical constructions of the generalized McKay correspondence, and the generalized Kronheimer-like resolution of  $\mathbb{C}^n/\Gamma$  singularities.

From the physics side, the context of these investigations is, in a broad sense, the *gauge/gravity correspondence* [1, 19, 26–29, 33, 34, 42, 43, 46]. In particular there are two main paradigms:

- a) The case of M2-branes solutions of  $D = 11$  supergravity where the eight-dimensional space transverse to the brane world volume is taken to be, to begin with, of the form  $\mathbb{C} \times \frac{\mathbb{C}^3}{\Gamma}$ , having denoted by  $\Gamma \subset \text{SU}(3)$  a finite subgroup.
- b) The case of D3-brane solutions of type IIB supergravity where the 6-dimensional transverse space to the brane is taken to be, to begin with, just the singular orbifold  $\frac{\mathbb{C}^3}{\Gamma}$  mentioned in the previous lines.

In both cases the idea is the following. Provided one takes into account also the twisted states, String Theory can comfortably live also on singular orbifolds, on the contrary Supergravity does require smooth manifolds. Hence we are interested in the crepant<sup>1</sup> resolution of the orbifold singularity:

$$Y \longrightarrow \mathbb{C}^n/\Gamma \tag{1.1}$$

and we look for exact solutions of  $D = 11$  or  $D = 10$  type IIB supergravities, respectively of the M2-brane and of the D3-brane type, where the transverse space is, respectively,  $\mathbb{C} \times Y$  or  $Y$ . At the same time we are interested in the construction of the  $D = 3$ , respectively,  $D = 4$  matter coupled supersymmetric gauge theories that become superconformal at a suitable infrared fixed point and are, supposedly, the dual partners of such brane solutions.

---

<sup>1</sup>We recall that a morphism of varieties  $X \rightarrow Y$ , which in particular can be a resolution of singularities, is crepant when the canonical sheaf of  $X$  is the pullback of the canonical sheaf of  $Y$ .

**Matter content of the gauge theory.** As it was strongly emphasized in [18, 30], the mathematical lore on the generalization of the McKay correspondence [48] and of the Kronheimer construction of ALE manifolds [44, 45] enter at this point in an essential way. Indeed the basic starting point of such constructions, *i.e.* the space<sup>2</sup>

$$\mathcal{S}_\Gamma \equiv \text{Hom}_\Gamma(R, \mathcal{Q} \otimes R), \quad (1.2)$$

where  $\mathcal{Q}$  is the given embedding of  $\Gamma$  into  $\text{SU}(n)$  and  $R$  is the regular representation of  $\Gamma$ . The structure of the representation ring of  $\Gamma$  is described by the McKay quiver matrix,<sup>3</sup> and the latter determines the gauge group  $\mathcal{F}_\Gamma$  and the whole spectrum of Wess-Zumino hypermultiplets of the associated gauge theory.<sup>4</sup>

**The McKay quivers.** The quiver matrix admits a representation by means of a quiver diagram and quiver gauge theories have been over the last twenty years the target of a large physical literature (see for instance [6, 7, 11] and all references therein). Quiver diagrams interpreted as a recipe to construct a supersymmetric gauge theory are more general than McKay quivers and up to our knowledge the inverse problem of defining necessary and sufficient conditions which, in the vast class of quivers, select those that are of McKay type is unsolved. Each McKay quiver is associated with a discrete group  $\Gamma \subset \text{SU}(n)$  and its nodes are in one-to-one correspondence with the irreducible representations of  $\Gamma$ . Its lines codify the data to construct the above mentioned space  $\text{Hom}_\Gamma(R, \mathcal{Q} \otimes R)$  which hosts the matter multiplets of the corresponding gauge theory. In a general quiver the lines provide the same information about matter multiplets, yet there is no a priori guarantee that these latter fill a space  $\text{Hom}_\Gamma(R, \mathcal{Q} \otimes R)$  for any suitable  $\Gamma$ . Said differently, any quiver diagram provides information for the construction of a Kähler or HyperKähler quotient. McKay quivers provide information how to resolve a  $\mathbb{C}^n/\Gamma$  by means of a Kähler or HyperKähler quotient defined according with a generalized Kronheimer construction; yet not all (Hyper)Kähler quotients are devised to solve quotient singularities. A notable counterexample is provided by the case where the (Hyper)Kähler quotient provides the resolution of a conifold singularity. The relation between gauge theories of the McKay type and of conifold type is addressed in a forthcoming publication [5].

**The first example: ALE manifolds.** Historically the first case that was fully developed both mathematically and physically is that of the Kleinian singularities  $\mathbb{C}^2/\Gamma$ , where the finite groups  $\Gamma \subset \text{SU}(2)$  admit the celebrated ADE classification (for a comprehensive recent review see chapter 8 of [32]). Relying on the properties of the relevant McKay quiver matrices which, due to the ADE classification, are identified with the extended Cartan matrices of the ADE Lie algebras, and on the recently introduced hyperkähler quotient constructions [39], Kronheimer [44, 45] succeeded in providing an algorithmic construction of all four-dimensional ALE gravitational instantons, the A subclass of which had been previously exhibited by Gibbons and Hawking as multicenter metrics [35, 36], generalizing the first and simplest example of the Eguchi-Hanson one-center metric [25]. ALE-manifolds and more general gravitational instantons were extensively studied and utilized in various capacities in string theory and in supergravity [8–10, 14–16]. The first paper where the Kronheimer construction was applied to 2D-conformal field theories in stringy setups dates back to 1994 [2], while the first example of an exact D3-brane solution of type IIB supergravity with  $\text{ALE} \times \mathbb{C}$  transverse space was produced in 2000 [3].

<sup>2</sup>For the definition of the space (1.2) see [18]. For its realization in the specific model studied in the present paper see eq. (2.10).

<sup>3</sup>See both [18] for the general definition and below, (eq. (2.6)) for the present  $\mathbb{Z}_4$  case.

<sup>4</sup>Singularities  $\mathbb{C}^n/\Gamma$  can have a crepant resolution and fall in the class analyzed in [18] only if  $\Gamma$  acts through its representation  $Q$  as a subgroup of  $\text{SU}(n)$ . It is important to recall that the  $\mathbb{Z}_k$  quotient of  $\mathbb{C}^4$  utilized in the ABJM construction [1] does not satisfy this condition and indeed admits only discrepant resolutions.

The ALE resolutions of Kleinian singularities are hyperkähler manifolds and the Kronheimer construction is based on the hyperkähler quotient. All this goes hand in hand with  $\mathcal{N} = 2$  supersymmetry in  $D = 4$  and  $\mathcal{N} = 4$  (broken to  $\mathcal{N} = 3$  by Chern-Simons couplings [12, 31]) in  $D = 3$ .

**The generalization to three dimensions.** In the second half of the nineties of the last century, a few mathematicians from the algebraic geometry community addressed the generalization of the Kronheimer construction to the case of  $\mathbb{C}^3/\Gamma$  singularities [21, 40, 47, 52–55]. In this case the resolved variety is simply a Kähler manifold and the Kronheimer construction reduces to a Kähler quotient. All this goes hand in hand with  $\mathcal{N} = 1$  supersymmetry in  $D = 4$  or  $\mathcal{N} = 2$  in  $D = 3$ . As we discussed at length in [18] the additional necessary item in the generalized Kronheimer construction, besides the real moment maps, is a universal holomorphic equation which substitutes the holomorphic part of the tri-holomorphic moment maps and amounts to a universal cubic superpotential. Instead the generalized McKay quiver diagrams have the same group theoretical definition as in the  $\mathbb{C}^2$  case although they no longer represent extended Cartan matrices. The choice of the appropriate gauge group  $\mathcal{F}_\Gamma$  follows from the quiver in exactly the same way as in the  $n = 2$  case. Henceforth the finite group  $\Gamma$  and its homomorphism  $\mathcal{Q}$  into  $SU(3)$  provide, once more as in the original Kronheimer case, all the data to construct the corresponding unique supersymmetric gauge theory on the brane world-volume.

**The Ito–Reid theorem and the tautological bundles** The two most important results of the mentioned mathematical activity are:<sup>5</sup>

- 1) the Ito-Reid theorem [40] that relates the generators of the cohomology groups  $H^{(q,q)}(Y)$  of the resolved variety to the conjugacy classes of  $\Gamma$  that in the  $\mathcal{Q}$  homomorphic image have *age*  $q$ .
- 2) the definition [24] of the tautological vector bundles  $E_i \rightarrow Y$  associated with each of the irreducible non-trivial representations  $\mathcal{D}_i$  of  $\Gamma$ , with

$$\text{rank } E_i = n_i \equiv \dim \mathcal{D}_i$$

As we emphasized in [18], the first Chern forms  $\omega_i^{(1,1)}$  of the tautological bundles  $E_i$  usually provide a redundant set of generators for the  $H^{(1,1)}(Y)$  group, whose dimension is fixed by the Ito-Reid theorem. One would like to have a constructive approach to single out both the components of the exceptional divisor  $D_E$  and a good basis of homological compact two-cycles  $\mathcal{C}_I$  ( $I = 1, \dots, \ell$ ) so as to be able to calculate the periods of the  $\omega_i^{(1,1)}$  on them:

$$\Pi_I^i \equiv \int_{\mathcal{C}_I} \omega_i^{(1,1)} \quad ; \quad I = 1, \dots, r = |\Gamma| - 1 \quad ; \quad i = 1, \dots, \ell = \# \text{ of senior c.c.} \quad (1.3)$$

The rationale of the above counting is the following. Because of Poincaré duality between  $H^{(2,2)}(Y)$  and  $H_c^{(1,1)}(Y)$  with compact support, the number of senior classes is equal to the number of  $\omega_i^{(1,1)}$  with compact support.

**Relevance of the cocycles and of the cycles for the gauge/gravity dual pairs.** The above geometrical information is of vital importance for the physical interpretation of the orbifold resolution within the correspondence between supergravity brane solutions and gauge theories on the world volume. The levels  $\zeta$  of the moment maps

---

<sup>5</sup>In view of the previous discussion about McKay quivers as a subclass of the set of all possible quivers, the below listed mathematical results apply only to case of supersymmetric gauge theories derived from a McKay quiver and hence associated with a  $\mathbb{C}^3/\Gamma$  singularity. They do not apply to general quiver gauge theories.

are in the gauge-theory the Fayet-Iliopoulos parameters. On the supergravity side these latter emerge as fluxes of  $p$ -forms partially or fully wrapped on homology cycles of the space transverse to the brane<sup>6</sup>.

More specifically, given the blow-down morphism

$$Y \longrightarrow \mathbb{C}^3/\Gamma \tag{1.4}$$

in order to construct a *bona-fide* M2-brane or D3-brane solution of the relevant supergravity that is dual to the considered world-volume gauge-theory we need a *Ricci flat* Kähler metric on the resolved manifold  $Y$ . This latter, which is clearly identified, both topologically and algebraically, by the Kronheimer construction, is not endowed by the corresponding Kähler quotient with a Ricci-flat metric. The derivation of a Ricci-flat Kähler on  $Y$  is a difficult mathematical problem discussed in a forthcoming publication [5], yet one thing is clear a priori. The parameters of such a Ricci-flat Kähler metric must be into correspondence with the Fayet-Iliopoulos parameters appearing in the Kronheimer construction and should parameterize the volumes of the homology cycles of  $Y$ . When one or more of these cycles shrink to zero a singularity develops. When all cycles shrink to zero we come back to singular orbifold  $\mathbb{C}^3/\Gamma$  both on the supergravity and on the gauge theory side.

**What we do in this paper.** In this article we study a specific nontrivial example of orbifold, whose analysis was only sketched in [18]. It corresponds to a specific embedding:

$$\mathcal{Q} : \mathbb{Z}_4 \longrightarrow \mathrm{SU}(3)$$

In the case of cyclic groups the McKay correspondence and the construction of the desingularizations of the singular quotient can be realized using toric geometry [40]. It is then fairly straightforward to identify the possible resolutions and study in full detail their geometry. In particular, one identifies the toric divisors and curves, including the compact divisors (a copy of the second Hirzebruch surface  $\mathbb{F}_2$  for the full resolution, and the weighted projective space  $\mathbb{P}[1, 1, 2]$  for one of the partial desingularizations). Actually utilizing the equations of the divisors provided by toric geometry we are able, by means of the restriction of the moment map equations to these special loci, to compute the periods of the  $(1, 1)$ -forms  $\omega_{1,2,3}^{(1,1)}$  on the basis of compact cycles in the general case.

The construction of the desingularizations, be it made as a generalized Kronheimer quotient [18, 24], or as an algebro-geometric GIT quotient [23, 40], depends on a set of parameters, living in a linear space, called the *stability parameter space*. This is partitioned in chambers, with the property that the quotient does not change when one moves within the interior of a chamber, while nontrivial topological changes may occur while crossing a wall between two chambers. In Sections 5 to 9 we study in great detail this chamber structure, by means of explicit calculations of the periods of the Chern classes of the tautological bundles on the the cycles that generate the 2-homology of the resolutions.

This geometrical study provides the basis for the construction of an explicit dual pair either in M-theory or in type IIB theory. This we plan to do in a new publication [5]. Further comments on the next steps in our program are left for the conclusions.

---

<sup>6</sup>See in particular [3] for an exemplification of this mechanism in the case of a D3-brane with transverse space  $\mathbb{C} \times \text{ALE}$ .

## 2 The $\mathbb{C}^3/\mathbb{Z}_4$ model, its McKay quiver and the associated Kronheimer construction

The action of the group  $\mathbb{Z}_4$  on  $\mathbb{C}^3$  is defined by introducing the three-dimensional unitary representation  $\mathcal{Q}(A)$  of its abstract generator  $A$  that satisfies the defining relation  $A^4 = \mathbf{e}$ . We set:

$$\mathcal{Q}(A) = \begin{pmatrix} i & 0 & 0 \\ 0 & i & 0 \\ 0 & 0 & -1 \end{pmatrix} ; \quad \mathcal{Q}(A)^4 = \begin{pmatrix} 1 & 0 & 0 \\ 0 & 1 & 0 \\ 0 & 0 & 1 \end{pmatrix} \quad (2.1)$$

Since  $\mathbb{Z}_4$  is abelian and cyclic, each of its four elements corresponds to an entire conjugacy class of which we can easily calculate the age-vector and the ages according with the conventions established in [18]. We obtain:

Conj. Class	Matrix	age-vector	age	name
Id	$\begin{pmatrix} 1 & 0 & 0 \\ 0 & 1 & 0 \\ 0 & 0 & 1 \end{pmatrix}$	$\frac{1}{4}(0,0,0)$	0	null class
$\mathcal{Q}(A)$	$\begin{pmatrix} i & 0 & 0 \\ 0 & i & 0 \\ 0 & 0 & -1 \end{pmatrix}$	$\frac{1}{4}(1,1,2)$	1	junior class
$\mathcal{Q}(A)^2$	$\begin{pmatrix} -1 & 0 & 0 \\ 0 & -1 & 0 \\ 0 & 0 & 1 \end{pmatrix}$	$\frac{1}{4}(2,2,0)$	1	junior class
$\mathcal{Q}(A)^3$	$\begin{pmatrix} -i & 0 & 0 \\ 0 & -i & 0 \\ 0 & 0 & -1 \end{pmatrix}$	$\frac{1}{4}(3,3,2)$	2	senior class

(2.2)

Therefore, according with the theorem of Ito and Reid [40], as reviewed in [18], in the crepant resolution:

$$Y \equiv \mathcal{M}_\zeta \longrightarrow \frac{\mathbb{C}^3}{\mathbb{Z}_4} \quad (2.3)$$

the Hodge numbers of the smooth resolved variety are as follows:

$$h^{(0,0)}(\mathcal{M}_\zeta) = 1 ; \quad h^{(1,1)}(\mathcal{M}_\zeta) = 2 ; \quad h^{(2,2)}(\mathcal{M}_\zeta) = 1 \quad (2.4)$$

Furthermore the existence of a senior class implies that one of the two generators of  $H^{(1,1)}(\mathcal{M}_\zeta)$  can be chosen to have compact support while the other will have non-compact support. As we later discuss studying the resolution with the help of toric geometry, this distinction goes hand in hand with the structure of the exceptional divisor that has two components, one compact and one non-compact.

The character table of the  $\mathbb{Z}_4$  group is easily calculated and it foresees four one-dimensional representations

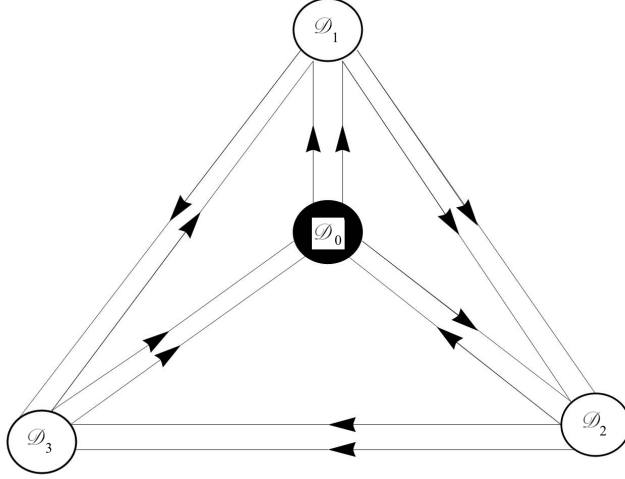


Figure 1: The McKay quiver of the  $\mathbb{Z}_4$  group embedded into  $SU(3)$  according to eq. (2.2).

that we respectively name  $\mathcal{D}_i$ , ( $i = 0, 1, 2, 3$ ). The table is given below.

Irrep \ C.C.	$\mathbf{e}$	$A$	$A^2$	$A^3$
$\mathcal{D}_0$	1	1	1	1
$\mathcal{D}_1$	1	$i$	$-1$	$-i$
$\mathcal{D}_2$	1	$-1$	1	$-1$
$\mathcal{D}_3$	1	$-i$	$-1$	$i$

(2.5)

## 2.1 The McKay quiver diagram and its representation

The information encoded in eqs. (2.2), (2.5) is sufficient to calculate the McKay quiver matrix defined by:

$$\mathcal{Q} \otimes \mathcal{D}_I = \bigoplus_{J=0}^3 \mathcal{A}_{IJ} \mathcal{D}_J \quad (2.6)$$

where  $\mathcal{D}_I$  denotes the 4 irreducible representation of the group defined in eq. (2.5), while  $\mathcal{Q}$  is the representation (2.2) describing the embedding  $\mathbb{Z}_4 \hookrightarrow SU(3)$ . Explicitly we obtain

$$\mathcal{A}_{IJ} = \begin{pmatrix} 0 & 2 & 1 & 0 \\ 0 & 0 & 2 & 1 \\ 1 & 0 & 0 & 2 \\ 2 & 1 & 0 & 0 \end{pmatrix} \quad (2.7)$$

A graphical representation of the quiver matrix (2.7) is provided in fig. 1.

Every node of the diagram corresponds to an irreducible representation  $\mathcal{D}_I$  and, in the Kronheimer construction, to a gauge group factor  $U(\dim \mathcal{D}_I)$ .

As one sees in every node enter three lines and go out three lines. Both the incoming and the outgoing lines are subdivided in a double line in some direction (or from some direction) and a single line to some direction, or from some direction.

This information is sufficient to derive the number of Wess-Zumino multiplets in the corresponding super-

symmetric gauge theory and assign their representations with respect to the three gauge groups (actually four minus one for the barycentric motion) as we will more extensively discuss in the forthcoming paper [5].

From the mathematical viewpoint each line of the diagram corresponds to an independent parameter appearing in the explicit construction of the space  $\mathcal{S}_{\mathbb{Z}_4}$ . This latter is constructed as follows. Let  $R$  denote the regular representation of  $\Gamma$ . We consider the space of triplets of  $4 \times 4$  complex matrices:

$$p \in \mathcal{P}_{\mathbb{Z}_4} \equiv \text{Hom}(R, \mathcal{Q} \otimes R) \Rightarrow p = \begin{pmatrix} A \\ B \\ C \end{pmatrix} \quad (2.8)$$

The action of the discrete group  $\mathbb{Z}_4$  on the space  $\mathcal{P}_{\mathbb{Z}_4}$  is defined in full analogy with the Kronheimer case by:

$$\forall \gamma \in \mathbb{Z}_4: \quad \gamma \cdot p \equiv \mathcal{Q}(\gamma) \begin{pmatrix} R(\gamma)AR(\gamma^{-1}) \\ R(\gamma)BR(\gamma^{-1}) \\ R(\gamma)CR(\gamma^{-1}) \end{pmatrix} \quad (2.9)$$

where  $R(\gamma)$  denotes its  $4 \times 4$ -matrix image in the regular representation.

The subspace  $\mathcal{S}_{\mathbb{Z}_4}$  is obtained by setting:

$$\mathcal{S}_{\mathbb{Z}_4} \equiv \text{Hom}(R, \mathcal{Q} \otimes R)^{\mathbb{Z}_4} = \{p \in \mathcal{P}_{\mathbb{Z}_4} / \forall \gamma \in \mathbb{Z}_4, \gamma \cdot p = p\} \quad (2.10)$$

As we know from the general theory exposed in [18] the space  $\mathcal{S}_{\mathbb{Z}_4}$  must have complex dimension  $3 \times |\mathbb{Z}_4| = 12$  which is indeed the number of lines in the quiver diagram of fig. 1. In the basis where the regular representation has been diagonalized with the help of the character Table (2.5) the general form of the triplet of matrices composing  $\text{Hom}_{\mathbb{Z}_4}(R, \mathcal{Q} \otimes R)$  and therefore providing the representation of the quiver diagram of fig. 1 is the following one:

$$A = \begin{pmatrix} 0 & 0 & 0 & \Phi_{0,3}^{(1)} \\ \Phi_{1,0}^{(1)} & 0 & 0 & 0 \\ 0 & \Phi_{2,1}^{(1)} & 0 & 0 \\ 0 & 0 & \Phi_{3,2}^{(1)} & 0 \end{pmatrix}; \quad B = \begin{pmatrix} 0 & 0 & 0 & \Phi_{0,3}^{(2)} \\ \Phi_{1,0}^{(2)} & 0 & 0 & 0 \\ 0 & \Phi_{2,1}^{(2)} & 0 & 0 \\ 0 & 0 & \Phi_{3,2}^{(2)} & 0 \end{pmatrix} \quad (2.11)$$

$$C = \begin{pmatrix} 0 & 0 & \Phi_{0,2}^{(3)} & 0 \\ 0 & 0 & 0 & \Phi_{1,3}^{(3)} \\ \Phi_{2,0}^{(3)} & 0 & 0 & 0 \\ 0 & \Phi_{3,1}^{(3)} & 0 & 0 \end{pmatrix}$$

The twelve complex parameters  $\Phi_{p,q}^{(J)}$  with  $J = 1, 2, 3$ ,  $p, q = 0, 1, 2, 3$ , promoted to be functions of the space-time coordinates  $\xi^\mu$ :

$$\Phi_{p,q}^{(J)}(\xi)$$

are the complex scalar fields filling the flat Kähler manifold of the Wess-Zumino multiplets in the microscopic lagrangian of the corresponding gauge theory.

## 2.2 The locus $\mathbb{V}_6 \subset \mathcal{S}_{\mathbb{Z}_4}$

As it was explained in the context of the general framework in [18], the  $3|\Gamma|$ -dimensional flat Kähler manifold  $\mathcal{S}_\Gamma$  contains always a subvariety  $\mathbb{V}_{|\Gamma|+2} \subset \mathcal{S}_\Gamma$  of dimension  $|\Gamma| + 2$  which is singled out by the following set of quadratic equations:

$$[A, B] = [B, C] = [C, A] = 0 \quad (2.12)$$

From the physical point of view, the holomorphic equation (2.12) occurs as the vanishing of the superpotential derivatives  $\partial_i \mathcal{W}(\Phi) = 0$  while looking for the scalar potential extrema, namely for the classical vacua of the gauge theory. From the mathematical viewpoint the locus  $\mathbb{V}_{|\Gamma|+2}$  is the one we start from in order to calculate the Kähler quotient  $\mathcal{M}_\zeta$  which provides the crepant resolution of the singularity. At the end of the day  $\mathcal{M}_\zeta$  is just the manifold of classical vacua of the gauge theory.

As discussed in [18], the vanishing locus (2.12) consists of several irreducible components of different dimensions, and  $\mathbb{V}_{|\Gamma|+2} = \mathbb{V}_6$  is the only component of dimension 6. It can be represented in the form  $\mathcal{G}_\Gamma \cdot L_\Gamma$ , where  $\mathcal{G}_\Gamma$  is the holomorphic quiver group, defined in the next Section, and  $L_\Gamma$  is the three dimensional locus that we will shortly characterize. An open part of this principal component  $\mathbb{V}_6$  can be given by the following explicit equations:

$$\begin{aligned} \Phi_{1,0}^{(2)} &= \frac{\Phi_{1,0}^{(1)} \Phi_{0,3}^{(2)}}{\Phi_{0,3}^{(1)}}, & \Phi_{2,1}^{(2)} &= \frac{\Phi_{2,1}^{(1)} \Phi_{0,3}^{(2)}}{\Phi_{0,3}^{(1)}}, & \Phi_{3,2}^{(2)} &= \frac{\Phi_{3,2}^{(1)} \Phi_{0,3}^{(2)}}{\Phi_{0,3}^{(1)}}, \\ \Phi_{1,3}^{(3)} &= \frac{\Phi_{1,0}^{(1)} \Phi_{0,2}^{(3)}}{\Phi_{3,2}^{(1)}}, & \Phi_{2,0}^{(3)} &= \frac{\Phi_{1,0}^{(1)} \Phi_{2,1}^{(1)} \Phi_{0,2}^{(3)}}{\Phi_{0,3}^{(1)} \Phi_{3,2}^{(1)}}, & \Phi_{3,1}^{(3)} &= \frac{\Phi_{2,1}^{(1)} \Phi_{0,2}^{(3)}}{\Phi_{0,3}^{(1)}} \end{aligned} \quad (2.13)$$

## 2.3 The holomorphic quiver group $\mathcal{G}_{\mathbb{Z}_4}$ and the gauge group $\mathcal{F}_{\mathbb{Z}_4}$

Following the general scheme outlined in [18], we see that the locus  $\mathcal{S}_{\mathbb{Z}_4}$  is mapped into itself by the action of the *complex quiver group*:

$$\mathcal{G}_{\mathbb{Z}_4} = \mathbb{C}^* \times \mathbb{C}^* \times \mathbb{C}^* \simeq \mathbf{\Lambda} \equiv \left( \begin{array}{c|c|c|c} \mathbb{C}^* & 0 & 0 & 0 \\ \hline 0 & \mathbb{C}^* & 0 & 0 \\ \hline 0 & 0 & \mathbb{C}^* & 0 \\ \hline 0 & 0 & 0 & \mathbb{C}^* \end{array} \right) ; \quad \det \mathbf{\Lambda} = 1 \quad (2.14)$$

The gauge group of the final gauge theory is the maximal compact subgroup of  $\mathcal{G}_{\mathbb{Z}_4}$ , namely:

$$\mathcal{F}_{\mathbb{Z}_4} = \mathrm{U}(1) \times \mathrm{U}(1) \times \mathrm{U}(1) \simeq \mathbf{\Xi} \equiv \left( \begin{array}{c|c|c|c} \mathrm{U}(1) & 0 & 0 & 0 \\ \hline 0 & \mathrm{U}(1) & 0 & 0 \\ \hline 0 & 0 & \mathrm{U}(1) & 0 \\ \hline 0 & 0 & 0 & \mathrm{U}(1) \end{array} \right) ; \quad \det \mathbf{\Xi} = 1 \quad (2.15)$$

The explicit form of the matrices  $\mathbf{\Lambda}$  and  $\mathbf{\Xi}$  is that appropriate to the basis where the regular representation is diagonalized. In that basis the charge assignments (representation assignments) of the scalar fields are read off from the transformation rule:

$$A(\Phi') = \mathbf{\Xi}^{-1} A(\Phi) \mathbf{\Xi}, \quad B(\Phi') = \mathbf{\Xi}^{-1} B(\Phi) \mathbf{\Xi}, \quad C(\Phi') = \mathbf{\Xi}^{-1} C(\Phi) \mathbf{\Xi} \quad (2.16)$$

Then we consider the locus  $L_{\mathbb{Z}_4}$  made by those triplets of matrices  $A, B, C$  that belong to  $\mathcal{S}_\Gamma$  and are diagonal in the natural basis of the regular representation. In the diagonal basis of the regular representation the same matrices  $A, B, C$  have the following form:

$$\begin{aligned}
A_0 &= \begin{pmatrix} 0 & 0 & 0 & Z^1 \\ Z^1 & 0 & 0 & 0 \\ 0 & Z^1 & 0 & 0 \\ 0 & 0 & Z^1 & 0 \end{pmatrix} ; \quad B_0 = \begin{pmatrix} 0 & 0 & 0 & Z^2 \\ Z^2 & 0 & 0 & 0 \\ 0 & Z^2 & 0 & 0 \\ 0 & 0 & Z^2 & 0 \end{pmatrix} \\
C_0 &= \begin{pmatrix} 0 & 0 & Z^3 & 0 \\ 0 & 0 & 0 & Z^3 \\ Z^3 & 0 & 0 & 0 \\ 0 & Z^3 & 0 & 0 \end{pmatrix}
\end{aligned} \tag{2.17}$$

The fields  $Z^{1,2,3}$  provide a set of three coordinates spanning the three-dimensional locus  $L_{\mathbb{Z}_4}$ . The complete locus  $\mathbb{V}_6$  coincides with the orbit of  $L_{\mathbb{Z}_4}$  under the free action of  $\mathcal{G}_{\mathbb{Z}_4}$ :

$$\mathbb{V}_6 = \mathcal{G}_{\mathbb{Z}_4} \cdot L_{\mathbb{Z}_4} = \begin{pmatrix} \Lambda^{-1} A_0 \Lambda \\ \Lambda^{-1} B_0 \Lambda \\ \Lambda^{-1} C_0 \Lambda \end{pmatrix} \tag{2.18}$$

## 2.4 The moment map equations

Implementing once more the general procedure outlined in [18] we arrive at the moment map equations and at the final crepant resolution of the singularity in the following way.

We refer the reader to [18] for the general definition of the moment map

$$\mu : \mathcal{S}_\Gamma \longrightarrow \mathbb{F}_\Gamma^*$$

where  $\mathbb{F}_\Gamma^*$  denotes the dual (as vector spaces) of the Lie algebra  $\mathbb{F}_\Gamma$  of the gauge group. We recall that the preimage of the level zero moment map is the  $\mathcal{F}_\Gamma$  orbit of the locus  $L_\Gamma$ :

$$\mu^{-1}(0) = \mathcal{F}_\Gamma \cdot L_\Gamma. \tag{2.19}$$

Note that  $L_\Gamma$  is actually  $\mathbb{C}^3$ , so that the image of  $L_\Gamma$  in the Kähler quotient of level zero coincides with the original singular variety  $\mathbb{C}^3/\Gamma$  (cf. Lemma 3.1 in [44]).

Next, as in [18], we consider the following decomposition of the Lie quiver group algebra:

$$\mathbb{G}_{\mathbb{Z}_4} = \mathbb{F}_{\mathbb{Z}_4} \oplus \mathbb{K}_{\mathbb{Z}_4} \tag{2.20}$$

$$[\mathbb{F}_{\mathbb{Z}_4}, \mathbb{F}_{\mathbb{Z}_4}] \subset \mathbb{F}_{\mathbb{Z}_4} ; \quad [\mathbb{F}_{\mathbb{Z}_4}, \mathbb{K}_{\mathbb{Z}_4}] \subset \mathbb{K}_{\mathbb{Z}_4} ; \quad [\mathbb{K}_{\mathbb{Z}_4}, \mathbb{K}_{\mathbb{Z}_4}] \subset \mathbb{F}_{\mathbb{Z}_4} \tag{2.21}$$

where  $\mathbb{F}_{\mathbb{Z}_4}$  is the maximal compact subalgebra.

A special feature of all the quiver groups and Lie algebras is that  $\mathbb{F}_\Gamma$  and  $\mathbb{K}_\Gamma$  have the same real dimension

$|\Gamma| - 1$  and one can choose a basis of Hermitian generators  $T^I$  such that:

$$\begin{aligned} \forall \Phi \in \mathbb{F}_\Gamma & : \Phi = i \times \sum_{I=1}^{|\Gamma|-1} c_I T^I ; c_I \in \mathbb{R} \\ \forall \mathbf{K} \in \mathbb{K}_\Gamma & : \mathbf{K} = \sum_{I=1}^{|\Gamma|-1} b_I T^I ; b_I \in \mathbb{R} \end{aligned} \quad (2.22)$$

Correspondingly a generic element  $g \in \mathcal{G}_{\mathbb{Z}_4}$  can be split as follows:

$$\forall g \in \mathcal{G}_{\mathbb{Z}_4} : g = \mathcal{U} \mathcal{H} ; \mathcal{U} \in \mathcal{F}_{\mathbb{Z}_4} ; \mathcal{H} \in \exp[\mathbb{K}_{\mathbb{Z}_4}] \quad (2.23)$$

Using the above property we arrive at the following parametrization of the space  $\mathbb{V}_6$

$$\mathbb{V}_6 = \mathcal{F}_{\mathbb{Z}_4} \cdot (\exp[\mathbb{K}_{\mathbb{Z}_4}] \cdot L_{\mathbb{Z}_4}) \quad (2.24)$$

where, by definition, we have set:

$$\begin{aligned} p \in \exp[\mathbb{K}_{\mathbb{Z}_4}] \cdot L_{\mathbb{Z}_4} & \Rightarrow p = \{\exp[-\mathbf{K}] A_0 \exp[\mathbf{K}], \exp[-\mathbf{K}] B_0 \exp[\mathbf{K}], \exp[-\mathbf{K}] C_0 \exp[\mathbf{K}]\} \\ \{A_0, B_0, C_0\} & \in L_{\mathbb{Z}_4} \\ \mathbf{K} & \in \mathbb{K}_{\mathbb{Z}_4} \end{aligned} \quad (2.25)$$

In our case the three generators  $T^I$  of the real subspace  $\mathbb{K}_{\mathbb{Z}_4}$  have been chosen as follows:

$$\begin{aligned} T^1 & = \begin{pmatrix} 1 & 0 & 0 & 0 \\ 0 & -1 & 0 & 0 \\ 0 & 0 & 0 & 0 \\ 0 & 0 & 0 & 0 \end{pmatrix} ; T^2 = \begin{pmatrix} 0 & 0 & 0 & 0 \\ 0 & 1 & 0 & 0 \\ 0 & 0 & -1 & 0 \\ 0 & 0 & 0 & 0 \end{pmatrix} \\ T^3 & = \begin{pmatrix} 0 & 0 & 0 & 0 \\ 0 & 0 & 0 & 0 \\ 0 & 0 & 1 & 0 \\ 0 & 0 & 0 & -1 \end{pmatrix} \end{aligned} \quad (2.26)$$

So that the relevant real group element takes the following form:

$$\exp[\mathbf{K}] = \begin{pmatrix} \mathfrak{H}_1 & 0 & 0 & 0 \\ 0 & \frac{\mathfrak{H}_2}{\mathfrak{H}_1} & 0 & 0 \\ 0 & 0 & \frac{\mathfrak{H}_3}{\mathfrak{H}_2} & 0 \\ 0 & 0 & 0 & \frac{1}{\mathfrak{H}_3} \end{pmatrix} \quad (2.27)$$

where  $\mathfrak{H}_I$  are, by definition, real. Relying on this, in the Kähler quotient we can invert the order of the operations. First we quotient the action of the compact gauge group  $\mathcal{F}_{\mathbb{Z}_4}$  and then we implement the moment map constraints. We have:

$$\mathbb{V}_6 // \mathcal{F}_{\mathbb{Z}_4} = (\exp[\mathbb{K}_{\mathbb{Z}_4}] \cdot L_{\mathbb{Z}_4}) / \mathbb{Z}_4, \quad (2.28)$$

where  $\mathbb{Z}_4$  acts on  $L_{\mathbb{Z}_4}$  via the action induced by that of the stabiliser of  $L_{\mathbb{Z}_4}$  in  $\mathcal{F}_{\mathbb{Z}_4}$ . The explicit form of the

triple of matrices mentioned in eq. (2.25) is easily calculated on the basis of eqs. (2.17) and (2.27)

$$p = \begin{pmatrix} A \\ B \\ C \end{pmatrix} \equiv \begin{pmatrix} \exp[-\mathbf{K}]A_0 \exp[\mathbf{K}] \\ \exp[-\mathbf{K}]B_0 \exp[\mathbf{K}] \\ \exp[-\mathbf{K}]C_0 \exp[\mathbf{K}] \end{pmatrix} \quad (2.29)$$

The moment map is given by:

$$\begin{aligned} \mu(p) &= \{\mathfrak{P}_1, \mathfrak{P}_2, \mathfrak{P}_3\} \\ \mathfrak{P}_I &= \text{Tr} [T_I ([A, A^\dagger] + [B, B^\dagger] + [C, C^\dagger])] \end{aligned} \quad (2.30)$$

Imposing the moment map constraint we find:

$$\mu^{-1}(\zeta) // \mathcal{F}_{\mathbb{Z}_4} = \{p \in \exp[\mathbb{K}_{\mathbb{Z}_4}] \cdot L_{\mathbb{Z}_4} \mid \mathfrak{P}_I(p) = \zeta_I\} / \mathbb{Z}_4. \quad (2.31)$$

Eq. (2.31) provides an explicit algorithm to calculate the Kähler potential of the final resolved manifold if we are able to solve the constraints for  $\mathfrak{H}_I$  in terms of the triple of complex coordinates  $Z^i$  ( $i = 1, 2, 3$ ). Indeed we recall that the Kähler potential  $\mathcal{H}_{\mathcal{M}_\zeta}$  of the resolved variety  $\mathcal{M}_\zeta = \mathcal{N}_\zeta / \mathcal{F}_{\mathbb{Z}_4}$ , where  $\mathcal{N}_\zeta = \mu^{-1}(\zeta) \subset \mathcal{S}_\Gamma$ , is given by the celebrated formula (see [39, eq. (3.58)] and also [13])

$$\mathcal{H}_{\mathcal{M}_\zeta} = \mathcal{H}_{\mathcal{N}_\zeta} + \zeta_I \mathfrak{C}^{IJ} \log \mathfrak{H}_J^{2\alpha_{\zeta_J}}. \quad (2.32)$$

Here  $\mathcal{H}_{\mathcal{N}_\zeta}$  is the restriction to  $\mathcal{N}_\zeta$  of the Kähler potential of the flat Kähler metric on  $\mathcal{S}_\Gamma$ , which is  $\mathcal{F}_{\mathbb{Z}_4}$ -invariant and therefore can be regarded as a function on  $\mathcal{M}_\zeta$ . The positive rational constants  $\alpha_\zeta$  are to be chosen so that the functions  $\mathfrak{H}_J^{2\alpha_{\zeta_J}}$  are hermitian fiber metrics on the three tautological bundles; these constants are completely determined by the geometry, but it will be easier to fix them later on, using the fact that Chern characters of the tautological line bundles are a basis of the cohomology ring of  $M_\zeta$  [23]. Moreover,

$$\mathfrak{C}^{IJ} = \text{Tr}(T^I T^J) = \begin{pmatrix} 2 & -1 & 0 \\ -1 & 2 & -1 \\ 0 & -1 & 2 \end{pmatrix} \quad (2.33)$$

is the matrix of scalar products of the gauge group generators.

The final outcome of this calculation was already presented in Section 9 of [18]. As it was done there, it is convenient to consider the following linear combinations:

$$\begin{pmatrix} 1 & 0 & -1 \\ 1 & -1 & 1 \\ 0 & 1 & 0 \end{pmatrix} \begin{pmatrix} \mathfrak{P}_1 - \zeta_1 \\ \mathfrak{P}_2 - \zeta_2 \\ \mathfrak{P}_3 - \zeta_3 \end{pmatrix} = 0 \quad (2.34)$$

In this way we obtain:

$$\begin{pmatrix} -\frac{(X_1^2 - X_3^2)(X_1 X_3 (\Delta_1^2 + \Delta_2^2) + (1 + X_2^2)\Delta_3^2)}{X_1 X_2 X_3} \\ \frac{(X_2 + X_2^3 - X_1 X_3 (X_1^2 + X_3^2))(\Delta_1^2 + \Delta_2^2)}{X_1 X_2 X_3} \\ -\frac{(-1 + X_2^2)(X_2 (\Delta_1^2 + \Delta_2^2) + (X_1^2 + X_3^2)\Delta_3^2)}{X_1 X_2 X_3} \end{pmatrix} = \begin{pmatrix} \zeta_1 - \zeta_3 \\ \zeta_1 - \zeta_2 + \zeta_3 \\ \zeta_2 \end{pmatrix} \quad (2.35)$$

where  $\Delta_i = |Z^i|$  are the moduli of the three complex coordinates  $Z^i$ , and  $X_J = \mathfrak{H}_J^2$  for  $J = 1, 2, 3$ .

Applying the general framework developed in [18] we have

$$\mathcal{H} \equiv \begin{pmatrix} \mathfrak{H}_1 & 0 & 0 \\ 0 & \mathfrak{H}_2 & 0 \\ 0 & 0 & \mathfrak{H}_3 \end{pmatrix} \quad (2.36)$$

and the positive definite hermitian matrix  $\mathcal{H}^{2\alpha_{\zeta_j}}$  is the fiber metric on the direct sum:

$$\mathcal{R} = \bigoplus_{I=1}^r \mathcal{R}_I \quad (2.37)$$

of the  $r = 3$  tautological bundles that, by construction, are holomorphic vector bundles with rank equal to the dimensions of the three nontrivial irreducible representations of  $\Gamma$ , which in this case is always one:

$$\mathcal{R}_I \xrightarrow{\pi} \mathcal{M}_\zeta \quad ; \quad \forall p \in \mathcal{M}_\zeta \quad : \quad \pi^{-1}(p) \approx \mathbb{C}^{n_I} \quad (2.38)$$

The compatible connection<sup>7</sup> on the holomorphic vector bundle  $\mathcal{R} = \bigoplus_I \mathcal{R}_I$  is given by  $\vartheta = \bigoplus_I \vartheta_I$ , where

$$\vartheta_I = \alpha_{\zeta_I} \partial \log X_I = \mathcal{H}^{-2\alpha_{\zeta_I}} \partial \mathcal{H}^{2\alpha_{\zeta_I}} \quad (2.39)$$

which is a 1-form with values in  $\mathbb{C}$ , the Lie algebra of the structural group  $\mathbb{C}^*$  of the  $I$ -th tautological vector bundle. The natural connection of the  $\mathcal{F}_{\mathbb{Z}_4}$  principal bundle, mentioned in eq. (2.15) is just, according to the universal scheme, the imaginary part of the connection  $\vartheta$ .

In order to solve the system of equations (2.35) it is convenient to change variables and write:

$$\Sigma = \Delta_1^2 + \Delta_2^2 \quad ; \quad U = \Delta_3^2 \quad (2.40)$$

In this way we obtain:

$$\begin{cases} -UX_2^2X_1^2 - UX_1^2 + UX_2^2X_3^2 + UX_3^2 - \zeta_1X_2X_3X_1 + \zeta_3X_2X_3X_1 - \Sigma X_3X_1^3 + \Sigma X_3^3X_1 & = 0 \\ -\zeta_1X_2X_3X_1 + \zeta_2X_2X_3X_1 - \zeta_3X_2X_3X_1 - \Sigma X_3X_1^3 - \Sigma X_3^3X_1 + \Sigma X_2^3 + \Sigma X_2 & = 0 \\ -UX_1^2X_2^2 - UX_3^2X_2^2 + UX_1^2 + UX_3^2 - \zeta_2X_1X_3X_2 - \Sigma X_2^3 + \Sigma X_2 & = 0 \end{cases} \quad (2.41)$$

This is the fundamental algebraic system encoding all information about the singularity resolution.

### 3 Properties of the moment map algebraic system and chamber structure

The resolubility of the system (2.41), viewed as a set of algebraic equations of higher order has some very peculiar properties that actually encode the topology and analytic structure of the resolved manifold  $Y$  and of its possible degenerations. The most relevant property of (2.41) is that for generic values  $U > 0, \Sigma > 0$  it has always one and only one root where all  $X_i > 0$  are real positive. This is of course expected from the general theory, as we know there are a well-defined quotient, and a Kähler metric on the quotient, for every generic choice of the *level parameters*  $\zeta$  (these are called *Fayet-Iliopoulos parameters* in gauge theory, while in algebraic geometry

<sup>7</sup>Following standard mathematical nomenclature, we call compatible connection on a holomorphic vector bundle, one whose  $(0, 1)$  part is the Cauchy-Riemann operator of the bundle.

they correspond to the so-called *stability parameters*); but it has also been verified numerically at an arbitrary large collection of random points  $\zeta \in \mathbb{R}^3$  and for an arbitrary large collection of points  $\{U, \Sigma\} \in \mathbb{R}_+^2$ .

**The special surface  $\mathcal{S}_2$ .** Although it is not a wall there is in the  $\zeta$  space a planar surface defined by the following conditions

$$\mathcal{S}_2 \equiv \{\zeta_1 = \zeta_3 = a, \quad \zeta_2 = b \neq 2a\} \quad (3.1)$$

where the algebraic system (2.41) acquires a more manageable form without losing generality. The strong simplification is encoded in the following condition:

$$X_1 = X_2 \quad (3.2)$$

Thanks to eq.(3.2), on the plane  $\mathcal{S}_2$  the moment map system reduces to a system of two rather than three equations. To understand eq.(3.2) we need to recall some results already obtained in [18]. Considering the system (2.41), it was there observed that one of the three functions  $X_i$  can always be algebraically solved in terms of the other two. Indeed we can write:

$$X_3 = X_1 \sqrt{\frac{\zeta_2 + \zeta_3 (X_2^2 - 1)}{\zeta_2 + \zeta_1 (X_2^2 - 1)}} \quad (3.3)$$

This relation is the algebraic counterpart, in the moment map equations of the topological result that the homology and cohomology of the resolved variety  $Y$  has dimension 2. If, inspired by eq.(3.3) we consider the case where all parameters  $\zeta_i$  are different from zero but two of them, namely  $\zeta_1$  and  $\zeta_3$  are equal among themselves, i.e. we localize our calculations on the surface  $\mathcal{S}_2$ , then eq.(3.2) follows, yielding a reduced system of moment map equations:

$$\begin{pmatrix} -2aX_2X_1^2 + bX_2X_1^2 - 2\Sigma X_1^4 + \Sigma X_2^3 + \Sigma X_2 \\ -bX_1^2X_2 - 2UX_1^2X_2^2 + 2UX_1^2 - \Sigma X_2^3 + \Sigma X_2 \end{pmatrix} = \begin{pmatrix} 0 \\ 0 \end{pmatrix} \quad (3.4)$$

### 3.1 Generalities on the chamber structure

In general, the space of parameters  $\zeta$  (which are closely related to the stability parameters of the GIT quotient construction)<sup>8</sup> has a chamber structure. Let  $C$  be a chamber in that space, and  $\mathcal{W}$  a wall of  $C$ ; denote by  $\mathcal{M}_C$  the resolution corresponding to a generic  $\zeta$  in  $C$  (they are all isomorphic), and by  $\mathcal{M}_{\mathcal{W}}$  the resolution corresponding to a generic  $\zeta$  in  $\mathcal{W}$ . There is a well-defined morphism  $\gamma_{\mathcal{W}}: \mathcal{M}_C \rightarrow \mathcal{M}_{\mathcal{W}}$  (actually one should take the normalization of the second space, but we skip such details). In general, the morphism  $\gamma_{\mathcal{W}}$  contracts curves or divisors; in [23] the walls are classified according to the nature of the contractions performed by  $\gamma_{\mathcal{W}}$ . One says that  $\mathcal{W}$  is of

1. type 0 if  $\gamma_{\mathcal{W}}$  is an isomorphism;
2. type I if  $\gamma_{\mathcal{W}}$  contracts a curve to a point;
3. type III if  $\gamma_{\mathcal{W}}$  contracts a divisor to a curve.

Walls of type II, that should contract a divisor to a point, do not actually exist, as shown in [23].

<sup>8</sup>Geometric invariant theory, usually shortened into GIT, is the standard way of taking quotients in algebraic geometry [49, 50]. The relation between the GIT approach and the Kähler quotient à la Kronheimer in the problem at hand is explored in [24].

The chamber structure pertaining to our example is analyzed and reconstructed in detail in Section 5. A guide to the localization of walls and chambers is provided by the existence of some lines in  $\zeta$  space where the system (2.41) becomes solvable by radicals or reduces to a single algebraic equation. These lines either turn out to be edges of the convex chambers occurring at intersections of walls, or just belong to walls. We begin by analyzing such solvable lines.

### 3.2 The solvable lines located in $\zeta$ space

In the  $\zeta$  moduli space there are few subcases where the solution of the algebraic system (2.41) can be reduced to finding the roots of a single algebraic equation whose order is equal or less than 6. As anticipated these solvable cases are located on walls of the chamber and in most case occur at the intersection of two walls.

**A) Case Cardano I,**  $\zeta_1 = 0, \zeta_2 = \zeta_3 = s$ . With this choice the general solution of the system (2.41) is provided by setting the ansatz displayed below and by solving the quartic equation for  $X$  contained in the next line:

$$\begin{aligned} X_1 &= 1, & X_2 &= X, & X_3 &= X \\ sX^2 - UX^4 + U - \Sigma X^3 + \Sigma X &= 0 \end{aligned} \quad (3.5)$$

Obviously we need to choose a branch of the solution such that  $X$  is real and positive. As we discuss later on, this is always possible for all values of  $U$  and  $\Sigma$  and the required branch is unique.

To this effect a simple, but very crucial observation is the following. The arithmetic square root  $\sqrt{|s|}$  of the level parameter  $s$  can be used as length scale of the considered space by rescaling the coordinates as follows:  $Z^i \rightarrow \sqrt{|s|} \tilde{Z}^i$  so that equation (3.5) can be rewritten as follows

$$-\tilde{U}X^4 + U - \tilde{\Sigma}X^3 + \mathfrak{s}X^2 + \tilde{\Sigma}X = 0 \quad (3.6)$$

where  $\mathfrak{s}$  denotes the sign of the moment map level. This implies that we have only three cases to be studied, namely:

$$\mathfrak{s} = \begin{cases} 1 \\ 0 \\ -1 \end{cases} \quad (3.7)$$

The second case corresponds to the original singular orbifold while the first and the third yield one instance of what we name the Cardano manifold. We will see that it corresponds to one of the possible degenerations of the full resolution  $Y$ . In the following we disregard the tildas and we simply write:

$$-UX^4 + U - \Sigma X^3 \pm X^2 + \Sigma X = 0 \quad (3.8)$$

**B) Case Cardano II**  $\zeta_3 = 0, \zeta_1 = \zeta_2 = s$ . With this choice the general solution of the system (2.41) is provided by setting the ansatz displayed below and by solving the quartic equation for  $X$  contained in the next line:

$$\begin{aligned} X_1 &= X, & X_2 &= X, & X_3 &= 1 \\ -sX^2 - UX^4 + U - \Sigma X^3 + \Sigma X &= 0 \end{aligned} \quad (3.9)$$

As one sees eq. (3.9) can be reduced to the form (3.8) by means of a rescaling similar to that utilized in the previous case. All previous conclusions apply to this case upon the exchange of  $X_1$  and  $X_3$ .

**C) Case Eguchi-Hanson**  $\zeta_2 = 0, \zeta_1 = \zeta_3 = s$ . With this choice the general solution of the system (2.41) is provided by setting the ansatz displayed below and by solving the quartic equation for  $X$  contained in the next line:

$$\begin{aligned} X_1 = X, \quad X_2 = 1 \quad X_3 = X \\ -2sX^2 + 2\Sigma - 2\Sigma X^4 = 0 \end{aligned} \quad (3.10)$$

The unique real positive branch of the solution to eq. (3.10) is given below:

$$X \rightarrow \frac{\sqrt{\frac{\sqrt{s^2+4\Sigma^2} - s}{\Sigma}}}{\sqrt{2}} \quad (3.11)$$

We will see in a later Section that eq.(3.11) leads to a complex three-dimensional manifold that is the tensor product  $\text{EH} \times \mathbb{C}$ , having denoted by EH the Eguchi-Hanson hyperkähler manifold.

**D) Case Kampé**  $\zeta_2 = 2s, \zeta_1 = \zeta_3 = s$ . With this choice the general solution of the system (2.41) is provided by setting the ansatz displayed below and by solving the sextic equation for  $X$  contained in the next line:

$$\begin{aligned} X_1 = \frac{\sqrt[4]{Z^3+Z}}{\sqrt[4]{2}}, \quad X_2 = Z, \quad X_3 = \frac{\sqrt[4]{Z^3+Z}}{\sqrt[4]{2}} \\ 2(Z^2+1)(sZ - UZ^2 + U)^2 - \Sigma^2 Z(Z^2-1)^2 = 0 \end{aligned} \quad (3.12)$$

As in other cases the root of the sextic equation must be chosen real and positive. Furthermore the absolute value of the parameter  $s$  can be disposed off by means of a rescaling.

### 3.3 The Kähler potential of the quotient manifolds

Before discussing the chamber structure guided by the discovery of the above mentioned solvable edges  $A, B, C, D$  it is useful to complete the determination of the Kähler manifolds singled out by such edges. This requires considering the explicit form of the Kähler potential for the quotient manifolds. Following the general rules of the Kähler quotient resolution à la Kronheimer, as developed in [18], the restriction of the Kähler potential of the linear space  $\mathcal{S}_\Gamma = \text{Hom}_\Gamma(R, \mathcal{D} \otimes R)$  to the algebraic locus  $\mathcal{D}(L_\Gamma)$  and then to the level surface  $\mathcal{N}_\zeta$  is, for the case under consideration, the following one:

$$\mathcal{H}_0|_{\mathcal{N}_\zeta} = \frac{U(X_2^2+1)(X_1^2+X_3^2) + \Sigma(X_2^3+X_2+X_1X_3(X_1^2+X_3^2))}{X_1X_2X_3} \quad (3.13)$$

The complete Kähler potential of the resolved variety is given by:

$$\mathcal{H}_{\mathcal{M}_\zeta} = \mathcal{H}_0|_{\mathcal{N}_\zeta} + \alpha_\zeta \zeta_I \mathfrak{e}^{IJ} \log[X_J] \quad (3.14)$$

The main point we need to stress is that, depending on the choices of the moduli  $\zeta_I$  (up to rescalings) we can obtain substantially different manifolds, both topologically and metrically.

The generic case which captures the entire algebraic structure of the resolved variety, to be discussed in later sections by means of toric geometry, is provided by

$$\zeta_1 \neq 0 \quad , \quad \zeta_2 \neq 0 \quad , \quad \zeta_3 \neq 0 \quad (3.15)$$

We name the corresponding Kähler manifold  $Y$ . The explicit calculation of the Kähler geometry of the manifold  $Y$  is discussed in the later Section 7, relying on the particular case  $\zeta_1 = \zeta_3 = \frac{1}{2}$ ,  $\zeta_2 = 2$ .

For the solvable edges of *moduli space* which we have classified in the previous Section we have instead the following results

**A) Cardano case  $\mathcal{M}_{0,1,1}$ .** We name *Cardano manifold* the one emerging from the choice  $\zeta_1 = 0$ ,  $\zeta_2 = 1$ ,  $\zeta_3 = 1$  where the solution of the moment map equations is reduced to the solution of the quartic algebraic equation (3.8). Choosing the sign plus in that equation and performing the substitution  $X_1 = 1$ ,  $X_2 = X$ ,  $X_3 = X$  the Kähler potential of the Cardano manifold  $\mathcal{M}_{0,1,1}$  takes the form:

$$\mathcal{H}_{\mathcal{M}_{0,1,1}} = 2\alpha_\zeta \log X + \frac{(X^2 + 1)(U(X^2 + 1) + 2\Sigma X)}{X^2} \quad (3.16)$$

where, depending on the  $\Sigma, U$  region,  $X$  is the positive real root of the quartic equation

$$-UX^4 + U - \Sigma X^3 + X^2 + \Sigma X = 0 \quad (3.17)$$

We already argued that this exists and is unique in all regions of the  $\Sigma, U$  plane.

**B) Cardano case  $\mathcal{M}_{1,1,0}$ .** This turns out to be an identical copy of the previous Cardano manifold. It emerges from the choice  $\zeta_1 = 1$ ,  $\zeta_2 = 1$ ,  $\zeta_3 = 0$  for which the solution of the moment map equations are also reduced to the solution of the quartic algebraic equation (3.8). Performing the substitution  $X_1 = X$ ,  $X_2 = X$ ,  $X_3 = 1$  the Kähler potential of the Cardano manifold  $\mathcal{M}_{1,1,0}$  takes the form:

$$\mathcal{H}_{\mathcal{M}_{1,1,0}} = 2\alpha_\zeta \log(X) + \frac{(X^2 + 1)(UX^2 + U + 2\Sigma X)}{X^2} \quad (3.18)$$

which is identical with eq. (3.16) and  $X$  is once again the positive real root of the quartic equation (3.17).

Let us name  $B_i(\Sigma, U)$  the four roots of eq.(3.17) enumerated in the order chosen by MATHEMATICA to implement Cardano's formula. For all the points  $\Sigma > 0, U > 0$  the fourth branch  $B_4(\Sigma, U)$  is the unique real positive one. This property is visualized in fig. 2. Hence let us consider the Kähler potential of eq. (3.16) where  $X \rightarrow \mathfrak{X}(\varpi, \mathfrak{U})$  is the positive real root of the quartic equation (3.17).

We write the positive real solution to the quartic equation (3.17) in terms of two new variables defined below:

$$U = \sqrt{\mathfrak{U}} \quad ; \quad \Sigma = \sqrt{\varpi} \sqrt[4]{\mathfrak{U}} \quad (3.19)$$

As the reader will appreciate later on, these variables are specially prepared to perform the limit to the compact exceptional divisor and are justified by the toric analysis of Section 4.

The explicit form of  $\mathfrak{X}(\varpi, \mathfrak{U})$  (plotted in fig.2) is the following one:

$$\begin{aligned} \mathfrak{X} = & \frac{1}{12\mathfrak{U}^{1/4}} \left( \sqrt{6} \sqrt{\frac{3\sqrt{3}\mathcal{C}}{\sqrt{\frac{4\sqrt[3]{2}\mathcal{A}}{\sqrt[3]{\mathcal{D}}} + 2 \cdot 2^{2/3} \sqrt[3]{\mathcal{D}} + 3\varpi - 8}} - \frac{2\sqrt[3]{2}\mathcal{A}}{\sqrt[3]{\mathcal{D}}} - 2^{2/3} \sqrt[3]{\mathcal{D}} + 3\varpi - 8}} \right. \\ & \left. + \sqrt{3} \sqrt{\frac{4\sqrt[3]{2}\mathcal{A}}{\sqrt[3]{\mathcal{D}}} + 2 \cdot 2^{2/3} \sqrt[3]{\mathcal{D}} + 3\varpi - 8 - 3\sqrt{\varpi}} \right) \quad (3.20) \end{aligned}$$

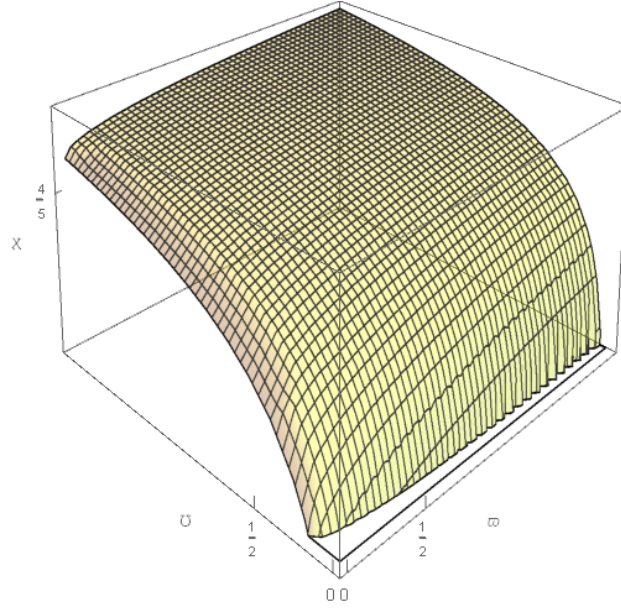


Figure 2: Plot of the 4th branch of the solution to the quartic equation (3.6). This branch is the unique real positive one. The surface is plotted with respect to the new variables  $\varpi$  and  $\bar{U}$  defined in eq. (3.19)

The symbols  $\mathcal{A}, \mathcal{B}, \mathcal{C}, \mathcal{D}$  utilized in (3.20) are just shorthands for certain combinations of the parameters  $(\varpi, \bar{U})$  that we mention below.

$$\begin{aligned}
 \mathcal{A} &= 3\varpi\sqrt{\bar{U}} - 12\bar{U} + 1 \\
 \mathcal{B} &= 9\varpi\sqrt{\bar{U}} + 72\bar{U} + 2 \\
 \mathcal{C} &= \varpi - 8\sqrt{\bar{U}} - 4 \\
 \mathcal{D} &= \sqrt{\mathcal{B}^2 - 4\mathcal{A}^3} + \mathcal{B}
 \end{aligned} \tag{3.21}$$

**C) Eguchi Hanson case  $\mathcal{M}_{s,0,s}$ .** When we choose  $\zeta_1 = s, \zeta_2 = 0, \zeta_3 = s$  the moment map system reduces to eqs. (3.10). Performing the substitution  $X_1 = X, X_2 = 1, X_3 = X$  and using eq. (3.11) the Kähler potential of the manifold  $\mathcal{M}_{s,0,s}$  takes the form:

$$\mathcal{H}_{\mathcal{M}_{s,0,s}} = \underbrace{4\alpha s \log[X] + 2\Sigma X^2 + \frac{2\Sigma}{X^2}}_{\mathcal{H}_2} + 4U \tag{3.22}$$

What we immediately observe from eq. (3.22) is that the Kähler potential is of the form:

$$\mathcal{H}_{\mathcal{M}_{s,0,s}} = \underbrace{\mathcal{H}_2(Z_1, Z_2, \bar{Z}_1, \bar{Z}_2)}_{\text{Kähler potential of a two-fold}} + 4 \times |Z_3|^2 \tag{3.23}$$

Hence the manifold  $\mathcal{M}_{s,0,s}$  is a direct product:

$$\mathcal{M}_{s,0,s} = \mathcal{M}_2 \times \mathbb{C} \tag{3.24}$$

It is not difficult to realize that the manifold  $\mathcal{M}_2$  is just the Eguchi-Hanson space  $EH \equiv ALE_{\mathbb{Z}_2}$ . To this effect it suffices to set  $s = \frac{\ell}{2}$  and rescale the coordinates  $Z^{1,2} \rightarrow \frac{\check{Z}^{1,2}}{2}$ . This implies  $\Sigma = \frac{1}{4}|\check{\mathbf{Z}}|^2$  and the

Kähler potential  $\mathcal{K}_2(Z_1, Z_2, \check{Z}_1, \check{Z}_2)$  turns out to be

$$\mathcal{K}_2 = \sqrt{\ell^2 + |\check{\mathbf{Z}}|^4} + \alpha_\zeta \ell \log \left[ \frac{-\ell + \sqrt{\ell^2 + |\check{\mathbf{Z}}|^4}}{|\check{\mathbf{Z}}|^2} \right] \quad (3.25)$$

which is essentially equivalent to the form of the Eguchi-Hanson Kähler potential given in eq. (7.22) of [18]. This might be already conclusive, yet for later purposes it is convenient to consider the further development of the result (3.25) since the known and fully computable case of the Eguchi-Hanson space allows us to calibrate the general formula for the Kähler potential (2.32) fixing the value of the so far unknown parameter  $\alpha_\zeta$  that, in this case, turns out to be  $\alpha_\zeta = 1$ . To this effect recalling the topological structure of the Eguchi-Hanson space that is the total space of the line bundle  $\mathcal{O}_{\mathbb{P}^1}(-2)$  we perform the change of variables:

$$\check{Z}_1 = u\sqrt{v} \quad ; \quad \check{Z}_2 = \sqrt{v} \quad (3.26)$$

where  $u$  is the complex coordinate of the compact base  $\mathbb{P}^1$ , while  $v$  is the complex coordinate spanning the non-compact fiber. Upon such a change the Kähler potential (3.25) becomes:

$$\mathcal{K}_2 = \sqrt{|v|^2(|u|^2 + 1)^2 + \ell^2} + \alpha_\zeta \ell \log \left( \frac{\sqrt{|v|^2(|u|^2 + 1)^2 + \ell^2} - \ell}{(|u|^2 + 1)\sqrt{|v|^2}} \right) \quad (3.27)$$

A further important information can be extracted from the present case. Setting  $v = 0$  we perform the reduction to the exceptional divisor of this partial resolution which is just the base manifold  $\mathbb{P}^1$  of Eguchi-Hanson space. The reduction of the Kähler 2-form to this divisor is very simple and it is the following one:

$$\mathbb{K}|_{\mathbb{P}^1} = \frac{\rho\sqrt{\ell^2}d\rho \wedge d\theta}{\pi(\rho^2 + 1)^2} \quad (3.28)$$

where we have set  $u = \rho \exp[i\theta]$ . It follows that the period integral of the Kähler 2-form on the unique homology cycle  $C_1$  of the partial resolution  $\text{EH} \times \mathbb{C}$  which is the above mentioned  $\mathbb{P}^1$  is:

$$\int_{C_1} \mathbb{K} = 2\pi \int_0^\infty \frac{\rho\sqrt{\ell^2}d\rho}{\pi(\rho^2 + 1)^2} = \sqrt{\ell^2} \quad (3.29)$$

Equation (3.29) sends us two important messages:

- Whether the level parameter  $s = \ell/2$  is positive or negative does not matter.
- The absolute value  $|s|$  encodes the size of the homology cycle in the exceptional divisor. When it vanishes the homology cycle shrinks to a point and we have a further degeneration.

**D) Sextic case or the *Kampé manifold*<sup>9</sup>  $\mathcal{M}_{s,2s,s}$ .** When we choose  $\zeta_1 = s$ ,  $\zeta_2 = 2s$ ,  $\zeta_3 = s$  the moment map system reduces to eqs. (3.12). With the same positions used there, the Kähler potential of the  $\mathcal{M}_{s,2s,s}$ -manifold turns out to be the following one:

$$\mathcal{H}_{\mathcal{M}_{1,2,1}} = 2s \log(Z) + \frac{\sqrt{2}\sqrt{Z^3 + \bar{Z}} \left( \sqrt{2}U\sqrt{Z^3 + \bar{Z}} + 2\Sigma Z \right)}{Z^2} \quad (3.30)$$

<sup>9</sup>Since it is generally stated that the roots of a general sextic equation can be written in terms of Kampé de Fériet functions, although explicit generic formulae are difficult to be found, we have decided to call  $\mathcal{M}_{s,2s,s}$  the *Kampé manifold* with the same logic that led us to name  $\mathcal{M}_{0,s,s}$  the Cardano manifold.

where the function  $Z(\Sigma, U)$  of the complex coordinates is the positive real root, depending on the  $\Sigma, U$  region of the sextic equation:

$$2(Z^2 + 1)(sZ - UZ^2 + U)^2 - \Sigma^2 Z(Z^2 - 1)^2 = 0 \quad (3.31)$$

In the next Section we discuss the geometry of the crepant resolution of the singularity  $\frac{\mathbb{C}^3}{\mathbb{Z}_4}$  utilizing toric geometry. Then we return to the formulae for the Kähler potential displayed in the present Section in order to see how the Kähler geometry of the entire space and in particular of the various components of the exceptional divisor is realized in the various corners of the moduli-space. This will allow us to discuss the Chamber Structure of this particular instance of Kähler quotient resolution à la Kronheimer.

As we are going to see, all the four cases analyzed in the present Section, the two Cardano cases, the Eguchi-Hanson case and the Kampé case correspond to partial resolutions of the orbifold singularity and indeed they are located on walls or even on edges where some homology cycles shrink to zero. The Kähler geometry of the full resolution will be analyzed in Section 7.

## 4 Toric geometry description of the crepant resolution

As announced above in the present Section we study the full and partial resolutions of the singularity  $\mathbb{C}^3/\mathbb{Z}_4$  in terms of toric geometry. Both resolutions turn to be the total space of the canonical line bundle over an algebraic surface, the second Hirzebruch surface  $\mathbb{F}_2$  and the weighted projective plane  $\mathbb{P}[1, 1, 2]$ . The main output of this study is provided by two informations:

1. The identification as algebraic varieties of the irreducible components of the exceptional divisor  $\mathcal{D}_E$  introduced by the resolution.
2. The explicit form of the atlas of coordinate patches that describe the resolved manifold and the coordinate transformation from the original  $Z_i$  to the new  $u, v, w$  (appropriate to each patch) that constitute the blowup of the singularities.

The second information of the above list and in particular the equation of the exceptional divisor in each patch is the main tool that allows to connect the Kähler quotient description outlined in the previous Section with the algebraic description. In particular by this token we arrive at the determination of the Kähler metric of the exceptional divisor components induced by the Kronheimer construction.

### 4.1 An initial cautionary remark

Let  $\Gamma$  be a finite subgroup of  $\mathrm{SL}(3, \mathbb{C})$ , and let let  $X_0 = (\mathbb{C}^3)^{ss} //_0 \Gamma$ .<sup>10</sup> By general theory (see e.g. [38]) for every generic value of the stability parameter  $\theta$  there is a morphism  $\mathbb{C}^3 //_{\theta} \Gamma \rightarrow X_0$ . Sardo Infriri [54, Thm. 4.4 and Rmk. 4.5] and Craw-Ishii [23, Prop. 2.2] notice that there always is a closed embedding  $\mathbb{C}^3/\Gamma \rightarrow X_0$  (this makes  $\mathbb{C}^3/\Gamma$  into an irreducible component of  $X_0$ ), and that this is an isomorphism if and only if  $\Gamma$  acts freely away from 0. This happens for  $\mathbb{C}^2/\mathbb{Z}_n$  both for the standard  $\mathrm{SU}(2)$  and  $\mathrm{U}(2)$  actions, and for the  $\mathbb{C}^3/\mathbb{Z}_3$  case treated in [18], but not for the present  $\mathbb{C}^3/\mathbb{Z}_4$  case, where each point of the  $z$  axis has a  $\mathbb{Z}_2$  isotropy subgroup.

<sup>10</sup>For an affine scheme, the GIT quotient is constructed as the spectrum of the  $\Gamma$ -invariant subring of the coordinate ring of the affine scheme. In the non-affine case the GIT quotient is obtained by glueing local affine quotients. It is a *categorical* quotient of the open subscheme of  $\theta$ -semistable points and is denoted by the symbol  $X^{ss} //_{\theta} \Gamma$ , after choosing a stability parameter  $\theta$ . See e.g. [49, 50].

On the other hand, one can show the existence of at least one stability chamber such that for generic values of  $\theta$  in that chamber,  $\mathbb{C}^3 //_{\theta} \Gamma$  is a resolution of singularities of  $\mathbb{C}^3 / \Gamma$  [23]. So in that case one has a commutative diagram

$$\begin{array}{ccc} \mathbb{C}^3 //_{\theta} \Gamma & & \\ \downarrow & \searrow & \\ \mathbb{C}^3 / \Gamma & \hookrightarrow & X_0 \end{array}$$

Actually we shall see in Sections 5 and 6 that in the present  $\mathbb{C}^3 / \mathbb{Z}_4$  case *all* stability chambers correspond to the full resolution of singularities.

## 4.2 The singular variety $Y_0 = \mathbb{C}^3 / \mathbb{Z}_4$

We shall denote by  $(x, y, z)$  the coordinates of  $\mathbb{C}^3$ , by  $\{\mathbf{e}_i\}$  the standard basis of  $\mathbb{R}^3$  and by  $\{\varepsilon^i\}$  the dual basis. The action of  $\mathbb{Z}_4$  is given by

$$(x, y, z) \mapsto (\omega x, \omega y, \omega^2 z)$$

with  $\omega^4 = 1$ . It is easy to find a basis for the space of invariant Laurent polynomials:

$$\mathcal{I}_1 = xy^{-1}, \quad \mathcal{I}_2 = y^2 z^{-1}, \quad \mathcal{I}_3 = z^2 \quad (4.1)$$

so that the three vectors

$$\mathbf{u}^1 = \varepsilon^1 - \varepsilon^2, \quad \mathbf{u}^2 = 2\varepsilon^2 - \varepsilon^3, \quad \mathbf{u}^3 = 2\varepsilon^3$$

generate the lattice  $M$  of invariants, which is a sublattice of the standard (dual) lattice  $M_0$ . The lattice  $N$  dual to  $M$  is a superlattice of the standard lattice  $N_0$ , and is generated by the vectors

$$\mathbf{w}_1 = \mathbf{e}_1, \quad \mathbf{w}_2 = \frac{1}{2}\mathbf{e}_1 + \frac{1}{2}\mathbf{e}_2, \quad \mathbf{w}_3 = \frac{1}{4}\mathbf{e}_1 + \frac{1}{4}\mathbf{e}_2 + \frac{1}{2}\mathbf{e}_3. \quad (4.2)$$

The generators of the rays giving the cone associated with the variety  $Y_0$  are obtained by inverting these relations, i.e.,

$$\mathbf{v}_1 = \mathbf{w}_1, \quad \mathbf{v}_2 = 2\mathbf{w}_2 - \mathbf{w}_1, \quad \mathbf{v}_3 = -\mathbf{w}_2 + 2\mathbf{w}_3.$$

From now on, unless differently stated, coordinate expressions will always refer to this basis  $\{\mathbf{w}_i\}$  of  $N$ . So the rays of the fan  $\Sigma_0$  of  $Y_0$  are

$$\mathbf{v}_1 = (1, 0, 0), \quad \mathbf{v}_2 = (-1, 2, 0), \quad \mathbf{v}_3 = (0, -1, 2)$$

They do not form a basis of  $N$ , according to the fact that  $Y_0$  is singular (note indeed that  $N / \sum_i \mathbb{Z}\mathbf{v}_i = \mathbb{Z}_4$ ).

## 4.3 The full resolution $Y$ of $Y_0 = \mathbb{C}^3 / \mathbb{Z}_4$

In this Section we study the full (smooth) resolution  $Y$  of the singular quotient  $Y_0$ , describing its torus-invariant divisors and curves and the natural coordinate systems on its affine patches.

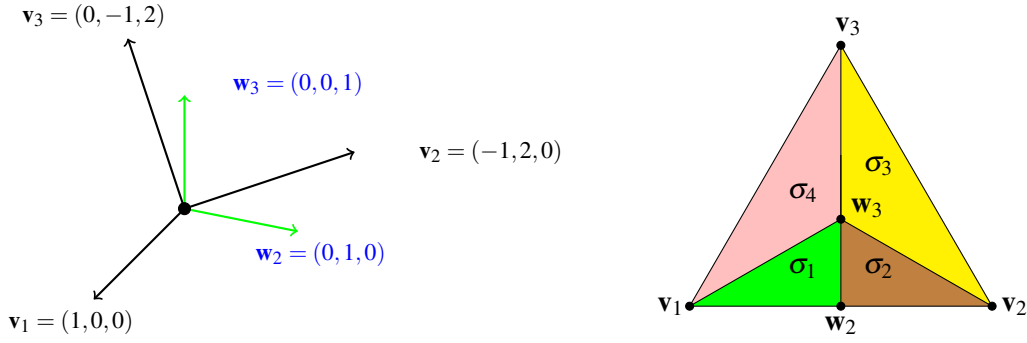


Figure 3: The fan  $\Sigma_Y$  of the resolution  $Y$  and the associated planar graph

### 4.3.1 The fan

The fan of  $Y$  is obtained by adding to the fan  $\Sigma_0$  the rays generated by the lattice points lying on the triangle with vertices  $\{v_i\}$ . These are

$$\mathbf{w}_2 = (0, 1, 0), \quad \mathbf{w}_3 = (0, 0, 1).$$

The torus invariant divisors corresponding to the two new rays of the fan are the components of the exceptional divisor. Since  $\mathbf{w}_3$  is in the interior of the triangle, the corresponding component of the exceptional divisor is compact, while the component corresponding to  $\mathbf{w}_2$ , which lies on the border, is noncompact. Note indeed that, according to the equations (4.2),  $\mathbf{w}_2$  and  $\mathbf{w}_3$  correspond to the junior classes  $\frac{1}{2}(1, 1, 0)$  (noncompact) and  $\frac{1}{4}(1, 1, 2)$  (compact) associated with the given representation of  $\mathbb{Z}_4$ .

We shall denote by  $Y$  this resolution of singularities. Figure 3 shows the fan of  $Y$  and the associated planar graph. The planar graph is obtained by projecting the generators of the rays onto the triangle formed by the three original vertices; this is shown in a 3-dimensional perspective in Figure 4.

One can explicitly check that all cones of  $\Sigma_Y$  are smooth, so that  $Y$  is indeed smooth. Note that all cones of  $\Sigma_Y$  are contained in the cones of  $\Sigma_0$ , which corresponds to the existence of a morphism  $Y \rightarrow Y_0$ .

If we first make the blowup corresponding to the ray  $\mathbf{w}_3$ , i.e., to the junior class  $\frac{1}{4}(1, 1, 2)$ , according to the general theory the exceptional divisor is a copy of the weighted projective plane  $\mathbb{P}[1, 1, 2]$ . When we make the second blowup, i.e. we blow up the  $z$  axis, we also blowup  $\mathbb{P}[1, 1, 2]$  at its singular point, so that the compact component of the exceptional divisor of the resolution of  $Y_0$  is a copy of the second Hirzebruch surface  $\mathbb{F}_2$ . Moreover, the noncompact component of the exceptional divisor is isomorphic to  $\mathbb{P}^1 \times \mathbb{C}$  (which, by the way, turns out to be the weighted projective space  $\mathbb{P}[1, 1, 0]$ ). This will be shown in more detail in the next sections (in particular, the compact exceptional divisor will be characterized as the Hirzebruch surface  $\mathbb{F}_2$  by computing its fan).

By general theory [40] (see also [18]) we know

$$h_2(Y, \mathbb{Q}) = 2, \quad h^2(Y, \mathbb{Q}) = 2, \quad h_c^2(Y, \mathbb{Q}) = 1, \quad h^4(Y, \mathbb{Q}) = 1.$$

### 4.3.2 Divisors

We analyze the toric divisors of  $Y$ ; they are summarized in Table 1. Each of these is associated with a ray of the fan  $\Sigma_Y$ . The divisors corresponding to  $\mathbf{w}_3, \mathbf{w}_2, \mathbf{v}_1, \mathbf{v}_3, \mathbf{v}_2$  will be denoted  $D_c, D_{nc}, D_{EH}, D_4, D'_{EH}$  respectively.

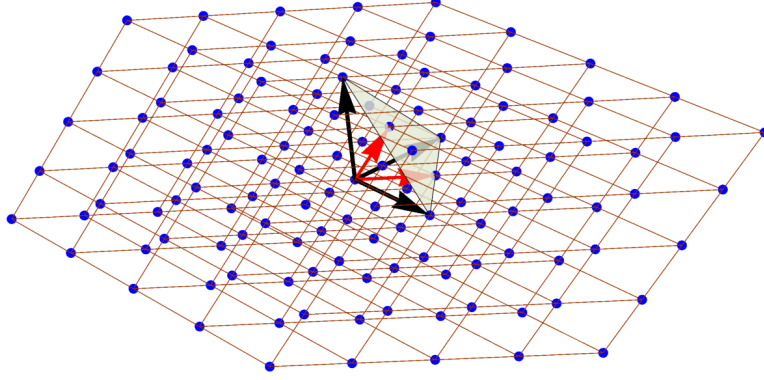


Figure 4: The figure displays a finite portion of the lattice  $N$  dual to the lattice  $M$  of  $\mathbb{Z}_4$ -invariants and the generators of the cone  $\sigma$  describing the singular quotient  $\mathbb{C}^3/\mathbb{Z}_4$  marked as fat dark arrows. The extremal points of the three generators single out a triangle, which intersects the lattice  $N$  in two additional points, namely the extremal points of the vector  $\mathbf{w}_3$  and of the vector  $\mathbf{w}_2$ , marked as lighter arrows in the figure. These vectors have to be added to the fan and divide the original cone into four maximal cones, corresponding to as many open charts of the resolved smooth toric variety.

Since  $Y$  is smooth all of them are Cartier. Table 1 shows the fans of these divisors and what variety they are as intrinsic varieties. The fans are depicted in Figure 5.<sup>11</sup> The fan of  $D_c$  is generated by the rays  $\mathbf{v}_2, \mathbf{w}_2, \mathbf{v}_1, \mathbf{v}_3$ , which shows that  $D_c$  is the second Hirzebruch surface  $\mathbb{F}_2$ . The corresponding curves in  $D_c$  have been denoted  $E_1, E_2, E_3, E_4$  respectively. From the self-intersections of these curves (in  $D_c$ )

$$E_1^2 = 0, \quad E_2^2 = -2, \quad E_3^2 = 0, \quad E_4^2 = 2$$

(see [20, Example 6.4.6]) we see that  $E_2$  is the section of  $\mathbb{F}_2 \rightarrow \mathbb{P}^1$  which squares to  $-2$ , i.e., the exceptional divisor of the blowup  $\mathbb{F}_2 \rightarrow \mathbb{P}[1, 1, 2]$ , while  $E_4$  is the section that squares to 2, and  $E_1, E_3$  are the toric fibers of  $\mathbb{F}_2 \rightarrow \mathbb{P}^1$ .

Table 1: Toric Divisors in  $Y$ . The last column shows the components of the divisor class on the basis given by  $(D_{nc}, D_c)$ . The variety  $\text{ALE}_{A_1}$  is the Eguchi-Hanson space, the crepant resolution of the singular space  $\mathbb{C}^2/\mathbb{Z}_2$ .

Ray	Divisor	Fan	Variety	Components
$\mathbf{w}_3$	$D_c$	$(1, 0), (-1, 2), (0, -1), (0, 1)$	$\mathbb{F}_2$	$(0, 1)$
$\mathbf{w}_2$	$D_{nc}$	$(1, 0), (-1, 0), (0, 1)$	$\mathbb{P}^1 \times \mathbb{C}$	$(1, 0)$
$\mathbf{v}_1$	$D_{EH}$	$(1, 0), (-1, 2), (0, 1)$	$\text{ALE}_{A_1}$	$(-\frac{1}{2}, -\frac{1}{4})$
$\mathbf{v}_3$	$D_4$	$(1, 0), (-1, 4), (0, 1)$	$\text{tot}(\mathcal{O}(-4) \rightarrow \mathbb{P}^1)$	$(0, -\frac{1}{2})$
$\mathbf{v}_2$	$D'_{EH}$	$(1, 0), (-1, 2), (0, 1)$	$\text{ALE}_{A_1}$	$(-\frac{1}{2}, -\frac{1}{4})$

Among the 5 divisors only 2 are independent in cohomology. We consider the exact sequence [20, Thm. 4.2.1]

$$0 \rightarrow M \xrightarrow{A} \text{Div}_{\mathbb{T}}(Y) \xrightarrow{B} \text{Pic}(Y) \rightarrow 0 \quad (4.3)$$

<sup>11</sup>In the cases when the ray associated to the divisor is not a coordinate axis we made a change of basis.

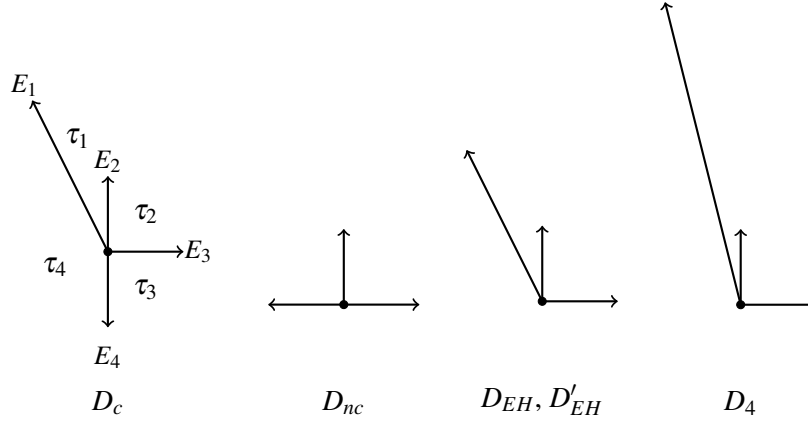


Figure 5: The fans of the 5 toric divisors of  $Y$ . In the fan of  $D_c$  we have labelled the rays with the names of the corresponding divisors; the  $\tau_i$ 's are the maximal cones.

where  $M$  is the dual lattice,  $\text{Div}_{\mathbb{T}}(Y)$  is the group of torus-invariant divisors, and  $\text{Pic}(Y)$  is the Picard group<sup>12</sup> of the full resolution  $Y$ . The morphism  $B$  simply takes the class of a divisor in the Picard group, while for every  $m \in M$ ,  $A(m)$  is the divisor associated with the rational function defined by  $m$ . Moreover we know that the classes of the divisors  $D_{nc}$  and  $D_c$  generate  $\text{Pic}(Y)$  over  $\mathbb{Q}$  [40]. With that choice of basis in  $\text{Pic}(Y) \otimes \mathbb{Q}$ , with the basis given by the 5 divisors in  $\text{Div}_{\mathbb{T}}(Y) \otimes \mathbb{Q}$ , and the basis in  $M \otimes \mathbb{Q}$  given by the duals of the  $\{\mathbf{w}_i\}$ , the morphisms  $A$  and  $B$  are represented over the rationals by the matrices

$$A = \begin{pmatrix} 1 & 0 & 0 \\ -1 & 2 & 0 \\ 0 & -1 & 2 \\ 0 & 1 & 0 \\ 0 & 0 & 1 \end{pmatrix}, \quad B = \begin{pmatrix} -\frac{1}{2} & -\frac{1}{2} & 0 & 1 & 0 \\ -\frac{1}{4} & -\frac{1}{4} & -\frac{1}{2} & 0 & 1 \end{pmatrix}$$

We deduce that the relations among the classes of the 5 toric divisors in the Picard group are<sup>13</sup>

$$[D_{EH}] = [D'_{EH}] = -\frac{1}{2}[D_{nc}] - \frac{1}{4}[D_c] \quad (4.4)$$

$$[D_4] = -\frac{1}{2}[D_c] \quad (4.5)$$

Since the canonical divisor can be written as minus the sum of the torus-invariant divisors, one has

$$[K_Y] = -[D_{nc}] - [D_c] - [D_{EH}] - [D'_{EH}] - [D_4] = 0$$

consistently with the fact that the resolution  $Y \rightarrow Y_0$  is crepant. (Note that  $\text{Pic}(Y)$  is free over  $\mathbb{Z}$  [20, Prop. 4.2.5], so that the equality  $[K_Y] = 0$  in  $\text{Pic}(Y) \otimes \mathbb{Q}$  also implies that  $[K_Y] = 0$  in  $\text{Pic}(Y)$ ).

The matrix  $B$  can also be chosen as

$$B = \begin{pmatrix} 1 & 1 & 0 & -2 & 0 \\ 0 & 0 & 1 & 1 & -2 \end{pmatrix}$$

<sup>12</sup>The Picard group  $\text{Pic}(X)$  of a complex variety  $X$  is the group of isomorphism classes of holomorphic line bundles on  $X$ . Using Čech cohomology it can be represented as the cohomology group  $H^1(X, \mathcal{O}_X^*)$ , where  $\mathcal{O}_X^*$  is the sheaf of nowhere vanishing holomorphic functions on  $X$ .

<sup>13</sup>The notation  $[D]$  means the class in the Picard group of the line bundle  $\mathcal{O}_X(D)$ .

which corresponds to taking the classes of  $D_{EH}$  and  $D_4$  as basis of the Picard group. In this way the matrix  $B$  is integral, which means that  $D_{EH}$  and  $D_4$  generate  $\text{Pic}(Y)$  over the integers.

### 4.3.3 Toric curves and intersections

The planar graph in Figure 3 shows that  $Y$  has 4 compact toric curves, corresponding to the inner edges of the graph. The intersection between a smooth irreducible curve  $C$  and a Cartier divisor  $D$  is defined as

$$C \cdot D = \deg(f^* \mathcal{O}_Y(D))$$

where  $f: C \rightarrow Y$  is the embedding, and  $\mathcal{O}_Y(D)$  is the line bundle associated to the divisor<sup>14</sup> (we shall use this definition in Section 6 to compute the periods of the tautological line bundles). Inspection of the fan allows one to detect when the intersection is transversal (in which case the intersection number is 1), empty (intersection number 0), or the curve is inside the divisor. The intersections are shown in Table 2.

Table 2: Intersections among the toric curves and divisors in the full resolution  $Y$ . For the curves that are inside  $D_c$  the last two columns also show the identifications with the curves corresponding to the rays in the fan of  $D_c$  of Figure 5, and what they are inside the second Hirzebruch surface. Note that  $C_1$  is the intersection between the two components of the exceptional divisor. The basis of the fibration  $D_c \rightarrow \mathbb{P}^1$  may be identified with  $C_1$ , while  $C_2, C_4$  are the fibers over two toric points, which correspond to the cones  $\sigma_1$  and  $\sigma_2$ .

Edge/face	Curve	$D_c$	$D_{nc}$	$D_{EH}$	$D'_{EH}$	$D_4$	Inside $D_c$	
$(\mathbf{w}_2 \mathbf{w}_3)$	$C_1$	0	-2	1	1	0	$E_2$	-2-section
$(\mathbf{v}_1 \mathbf{w}_3)$	$C_2$	-2	1	0	0	1	$E_3$	fiber
$(\mathbf{v}_2 \mathbf{w}_3)$	$C_4$	-2	1	0	0	1	$E_1$	fiber
$(\mathbf{v}_3 \mathbf{w}_3)$	$C_5$	-4	0	1	1	2	$E_4$	2-section
$(\mathbf{v}_1 \mathbf{w}_2)$	$C_3$	1	0	0	0	0		

The intersection numbers of  $D_{EH}$  and  $D_4$  with  $C_1, C_2$  show that the latter are a basis of  $H_2(Y, \mathbb{Z})$  dual to  $\{[D_4], [D_{EH}]\}$ .

### 4.3.4 Coordinate systems and curves

The four 3-dimensional cones in the fan of  $Y$  correspond to four affine open varieties, and since all cones are smooth (basic), they are copies of  $\mathbb{C}^2$ . The variables attached to the rays generating a cone provide a coordinate system on the corresponding affine set. A face between two 3-dimensional cones corresponds to the intersection between the two open sets. Note that all charts have a common intersection, as they all contain the 3-dimensional torus corresponding to the origin of the fan. Table 3 shows the association among cones, rays, coordinates and coordinate expressions of toric curves. Below we provide a list of coordinate systems, with all transition functions between them, and the expressions of the toric curves in the coordinate systems of the charts they belong to. Table 4 displays the coordinate transformations among the four coordinate systems. We have denoted  $C_i, i = 1 \dots 5$  as before, and moreover  $C_6, C_7, C_8$  are the noncompact toric curves in the charts

<sup>14</sup>This also allows one to compute the intersection between a curve  $C$  and a Weil divisor  $D$ . Indeed simplicial toric varieties are  $\mathbb{Q}$ -factorial, i.e., every Weil divisor has a multiple that is Cartier. So if  $mD$  is Cartier, one defines

$$C \cdot D = \frac{1}{m} C \cdot (mD).$$

This may be a rational number.

2, 3 and 4 (analogously,  $C_3$  was the noncompact curve in the chart 1). The column ‘‘Dual gen.’’ displays the generators of the dual cone.

In each chart, the coordinates  $(u, v, w)$  are related to the invariants (4.1) as follows:

$$\begin{aligned}
\{u, v, w\}_1 &= \left\{ \frac{x}{y}, \frac{y^2}{z}, z^2 \right\} \\
\{u, v, w\}_2 &= \left\{ \frac{y}{x}, \frac{x^2}{z}, z^2 \right\} \\
\{u, v, w\}_3 &= \left\{ \frac{y}{x}, \frac{z}{x^2}, x^4 \right\} \\
\{u, v, w\}_4 &= \left\{ \frac{x}{y}, y^4, \frac{z}{y^2} \right\}
\end{aligned} \tag{4.6}$$

Eqs. (4.6) can be easily inverted and one obtains:

$$\begin{aligned}
\text{Chart } X_{\sigma_1} \quad x &\rightarrow u\sqrt{v}\sqrt[4]{w} \quad , \quad y \rightarrow \sqrt{v}\sqrt[4]{w} \quad , \quad z \rightarrow \sqrt{w} \\
\text{Chart } X_{\sigma_2} \quad x &\rightarrow \sqrt{v}\sqrt[4]{w} \quad , \quad y \rightarrow u\sqrt{v}\sqrt[4]{w} \quad , \quad z \rightarrow \sqrt{w} \\
\text{Chart } X_{\sigma_3} \quad x &\rightarrow \sqrt[4]{w} \quad , \quad y \rightarrow u\sqrt[4]{w} \quad , \quad z \rightarrow v\sqrt{w} \\
\text{Chart } X_{\sigma_4} \quad x &\rightarrow u\sqrt[4]{v} \quad , \quad y \rightarrow \sqrt[4]{v} \quad , \quad z \rightarrow \sqrt{vw}
\end{aligned} \tag{4.7}$$

The irrational coordinate transformations (4.7) derived from the toric construction are the essential tool to relate the results of the Kähler quotient construction with the geometry of the exceptional divisor as identified by the toric resolution of the singularity.

The coordinates  $x, y, z$  in the above equation are to be identified with the  $Z^{1,2,3}$  that parameterize the locus  $L_{\mathbb{Z}_4}$  composed by the matrices  $A_0, B_0, C_0$  of eq. (2.17). As we know this locus is lifted to the resolved variety  $Y$  by the action of the quiver group element  $\exp[\Phi]$ , whose corresponding Lie algebra element  $\Phi$  satisfies the moment map equations (2.35).

Table 3: For each cone the table assigns a name to the coordinates associated to the rays. The third column lists the generators of the dual cones. The  $\varepsilon$ 's here are the dual basis to the  $\mathbf{w}$ . We also write the equations of the toric curves in these coordinates.

Cone	Rays	Dual gen.	Coordinates	Curves
$\sigma_1$	$\mathbf{v}_1 \mathbf{w}_2 \mathbf{w}_3$	$\varepsilon_1, \varepsilon_2, \varepsilon_3$	$u_1, v_1, w_1$	$C_1 : v_1 = w_1 = 0, C_2 : u_1 = w_1 = 0, C_3 : u_1 = v_1 = 0$
$\sigma_2$	$\mathbf{v}_2 \mathbf{w}_2 \mathbf{w}_3$	$-\varepsilon_1, \varepsilon_2 + 2\varepsilon_1, \varepsilon_3$	$u_2, v_2, w_2$	$C_1 : v_2 = w_2 = 0, C_4 : u_2 = v_2 = 0, C_6 : u_2 = w_2 = 0$
$\sigma_3$	$\mathbf{v}_2 \mathbf{v}_3 \mathbf{w}_3$	$-\varepsilon_1, -2\varepsilon_1 - \varepsilon_2, \varepsilon_3 + 2\varepsilon_2 + 4\varepsilon_1$	$u_3, v_3, w_3$	$C_4 : u_3 = w_3 = 0, C_5 : v_3 = w_3 = 0, C_7 : u_3 = v_3 = 0$
$\sigma_4$	$\mathbf{v}_1 \mathbf{v}_3 \mathbf{w}_3$	$\varepsilon_1, 2\varepsilon_2 + \varepsilon_3, -\varepsilon_2$	$u_4, v_4, w_4$	$C_2 : u_4 = w_4 = 0, C_5 : v_4 = w_4 = 0, C_8 : u_4 = v_4 = 0$

Table 4: Coordinate changes among the charts described in Table 3

	$\sigma_1$	$\sigma_2$	$\sigma_3$	$\sigma_4$
$\sigma_1$	id	$u_2 = \frac{1}{u_1}, v_2 = u_1^2 v_1, w_2 = w_1$	$u_3 = \frac{1}{u_1}, v_3 = \frac{1}{u_1^2}, w_3 = u_1 v_1^2 w_1$	$u_4 = u_1, v_4 = v_1^2 w_1, w_4 = \frac{1}{v_1}$
$\sigma_2$	$u_1 = \frac{1}{u_2}, v_1 = u_2^2 v_2, w_1 = w_2$	id	$u_3 = u_2, v_3 = \frac{1}{v_2}, w_3 = v_2^2 w_2$	$u_4 = \frac{1}{u_2}, v_4 = u_2^4 v_2^2 w_2, w_4 = \frac{1}{u_2^2 v_2}$
$\sigma_3$	$u_1 = \frac{1}{u_3}, v_1 = \frac{u_3^2}{v_3}, w_1 = v_3^2 w_3$	$u_2 = u_3, v_2 = \frac{1}{v_3}, w_2 = v_3^2 w_3$	id	$u_4 = \frac{1}{u_3}, v_4 = u_3^4 w_3, w_4 = \frac{v_3}{u_3^2}$
$\sigma_4$	$u_1 = u_4, v_1 = \frac{1}{w_4}, w_1 = v_4 w_4^2$	$u_2 = \frac{1}{u_4}, v_2 = \frac{u_4^2}{w_4}, w_2 = v_4 w_4^2$	$u_3 = \frac{1}{u_4}, v_3 = \frac{w_4}{u_4^2}, w_3 = u_4^4 v_4$	id

### 4.3.5 $Y$ as a line bundle on $\mathbb{F}_2$

The full resolution  $Y$  is the total space of the canonical bundle of the second Hirzebruch surface  $\mathbb{F}_2$ ; this is quite clear from the blowup procedure (cf. Section 2.3 in [40]) and was explicitly noted in [17]. Following [20, §7.3]

we give a toric description of this fact. The canonical bundle of  $\mathbb{F}_2$  is the line bundle  $\mathcal{O}_{\mathbb{F}_2}(-2H)$ , where  $H$  is the section of  $\mathbb{F}_2 \rightarrow \mathbb{P}^1$  squaring to 2. We regard  $H$  as the toric divisor  $E_4$ , see Figure 5. To each of the cones  $\tau_i$  of the fan of  $\mathbb{F}_2$  one associates a 3-dimensional cone  $\tilde{\sigma}_i$ , obtaining

$$\begin{aligned}\tilde{\sigma}_1 &= \text{Cone}((0,0,1), (0,1,0), (1,0,0)) \\ \tilde{\sigma}_2 &= \text{Cone}((0,0,1), (-1,2,0), (0,1,0)) \\ \tilde{\sigma}_3 &= \text{Cone}((0,0,1), (0,-1,2), (-1,2,0)) \\ \tilde{\sigma}_4 &= \text{Cone}((0,0,1), (1,0,0), (0,-1,2))\end{aligned}$$

This is the fan of  $Y$ . So,  $\text{tot}(\mathcal{O}_{\mathbb{F}_2}(-2H)) \simeq Y$ , i.e.,  $Y$  is the total space of the canonical bundle of  $\mathbb{F}_2$ . Thus, the canonical bundle of  $Y$  is trivial.<sup>15</sup> This will be the key to the computations of the Kähler potential of  $Y$ , of its Kähler metric, and of the Kähler 2-form integrals on the homology cycles that we shall perform in Section 7.

## 4.4 The partial resolution $Y_3$

The full resolution  $Y$  is obtained by adding two rays to the fan of  $Y_0 = \mathbb{C}^3/\mathbb{Z}_4$ . If we add just one we obtain a partial resolution. Here we examine the partial resolution that will occur in correspondence of some walls of the stability parameters space.

### 4.4.1 The fan

We consider the toric 3-fold  $Y_3$  whose fan  $\Sigma_3$  is generated by the 4 rays  $\mathbf{v}_1, \mathbf{v}_2, \mathbf{v}_3, \mathbf{w}_3$ , which is a partial resolution of  $Y_0$ . This will appear as the partial desingularization occurring at some of the walls of the  $\zeta$  parameter space (space of stability conditions). The fan and the associated planar graph are shown in Figure 6. The cone  $\sigma_1$  is singular, while  $\sigma_2$  and  $\sigma_3$  are smooth, i.e.,  $Y_3$  has one singular toric point. By general theory we know that

$$h_2(Y_3, \mathbb{Q}) = 2, \quad h^2(Y_3, \mathbb{Q}) = h_c^2(Y_3, \mathbb{Q}) = h^4(Y_3, \mathbb{Q}) = h^2(Y_3, \mathbb{Q}) = 1.$$

### 4.4.2 Divisors

The divisors corresponding to  $\mathbf{w}_3, \mathbf{v}_1, \mathbf{v}_3, \mathbf{v}_2$  will be denoted  $D_c, D_{EH}, D'_{EH}, D_4$ , respectively. They are described in Table 5. The corresponding fans are shown in Figure 7.

For the variety  $Y_3$ , which is not smooth, the Picard group in the sequence (4.3) must be replaced by the class group  $\text{Cl}(Y_3)$ , however after tensoring by the rationals the two groups coincide, so that we may ignore this fact.

<sup>15</sup>Let  $L$  be the total space of  $\mathcal{O}_{\mathbb{F}_2}(-2E)$ , with projection  $\pi: L \rightarrow \mathbb{F}_2$ . Then we have an exact sequence

$$0 \rightarrow \pi^* \Omega_{\mathbb{F}_2}^1 \rightarrow \Omega_L^1 \rightarrow \Omega_{L/\mathbb{F}_2}^1 \rightarrow 0.$$

The bundle of relative differentials  $\Omega_{L/\mathbb{F}_2}^1$  is isomorphic to  $\pi^* L^*$ . As a result,

$$K_L = \det(\Omega_L^1) \simeq \pi^* K_{\mathbb{F}_2} \otimes \pi^* L^* \simeq \pi^* \mathcal{O}_{\mathbb{F}_2}(-2H) \otimes \pi^* \mathcal{O}_{\mathbb{F}_2}(2H) \simeq \mathcal{O}_L.$$

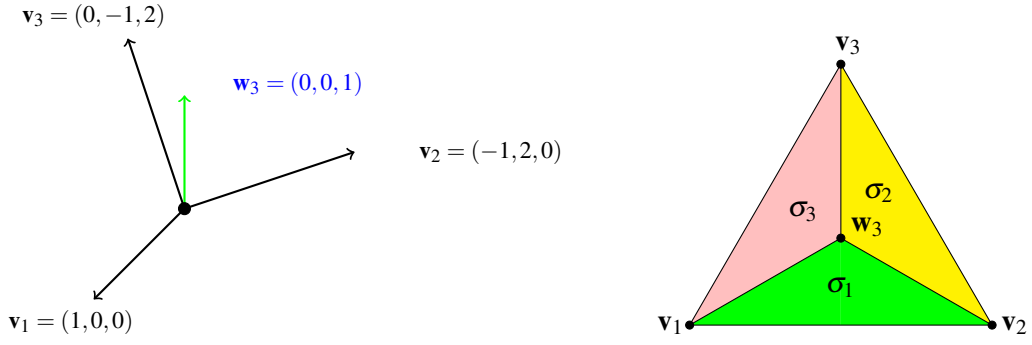


Figure 6: The fan  $\Sigma_3$  of the partial resolution  $Y_3$  and the associated planar graph

The group  $\text{Pic}(Y_3) \otimes \mathbb{Q}$  is generated by the class of  $D_c$ . The matrices  $A$  and  $B$  are now

$$A = \begin{pmatrix} 1 & 0 & 0 \\ -1 & 2 & 0 \\ 0 & -1 & 2 \\ 0 & 0 & 1 \end{pmatrix}, \quad B = \begin{pmatrix} -\frac{1}{4} & -\frac{1}{4} & -\frac{1}{2} & 1 \end{pmatrix}$$

(the order of the toric divisors is  $D_{EH}, D'_{EH}, D_4, D_c$ ). The relations we get among the divisor classes are

$$[D_{EH}] = [D'_{EH}] = -\frac{1}{4}[D_c], \quad [D_4] = -\frac{1}{2}[D_c].$$

Again, this implies  $[K_{Y_3}] = 0$ .

The integral generator of  $\text{Pic}(Y_3)$  is  $D_4$ .  $D_{EH}$  and  $D'_{EH}$  are linearly equivalent, and both generate the class group.

Table 5: Toric Divisors in  $Y_3$

Ray	Divisor	Fan	Variety	Type	Component
$\mathbf{w}_3$	$D_c$	$(1, 0), (-1, 2), (0, -1)$	$\mathbb{P}[1, 1, 2]$	Cartier	1
$\mathbf{v}_1$	$D_{EH}$	$(1, 0), (-1, 2), (0, 1)$	$\text{ALE}_{A_1}$	Weil	$-\frac{1}{4}$
$\mathbf{v}_2$	$D'_{EH}$	$(1, 0), (-1, 2), (0, 1)$	$\text{ALE}_{A_1}$	Weil	$-\frac{1}{4}$
$\mathbf{v}_3$	$D_4$	$(1, 0), (-1, 4), (0, 1)$	$\text{tot}(\mathcal{O}(-4) \rightarrow \mathbb{P}^1)$	Cartier	$-\frac{1}{2}$

#### 4.4.3 Toric curves and intersections

Inspection of the planar graph in Figure 6 shows that  $Y_3$  has 3 toric compact curves, however we know that there is only one independent class in  $H_2(Y_3, \mathbb{Q})$ . The intersection numbers of the curves with the 4 toric divisors are shown in Table 6. The curves  $C_1, C_2, C_4$  are the 3 compact curves.  $C_3$  is a noncompact curve.

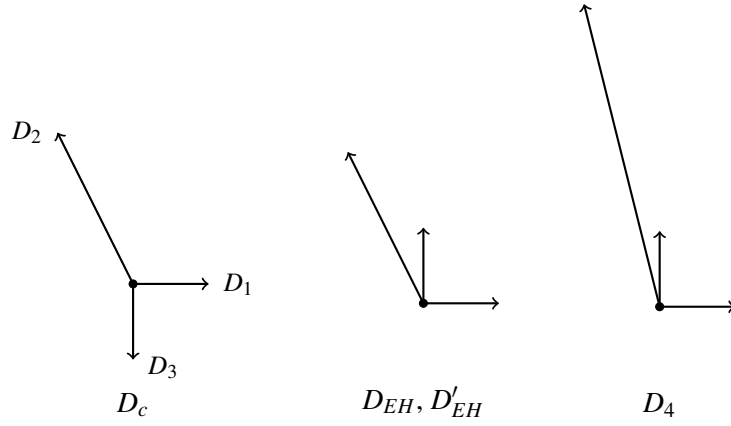


Figure 7: The fans of the 4 toric divisors of  $Y_3$

Table 6: Intersections among the toric curves and divisors in  $Y_3$ . The toric curves are images of curves in  $Y$  via the natural map  $Y \rightarrow Y_3$ , and we have used the same notation for a curve in  $Y$  and its image in  $Y_3$ . The curve  $C_8$  is singular (it is actually the only singular curve among the 6 toric curves of  $Y_3$ ). Note that  $C_8$  is indeed the strict transform of the  $z$  axis, whose points have nontrivial isotropy, and  $Y_3$  does not resolve this singularity as  $D_{nc}$  has been shrunk onto  $C_8$ . The curve  $C_1$  of  $Y$  has shrunk to a point. This will be explicitly checked in Section 8 by noting that the period of the Kähler form on  $C_1$  goes to zero under the blow-down morphism  $Y \rightarrow Y_3$ .

Face	Curve	$D_c$	$D_{EH}$	$D'_{EH}$	$D_4$
$(\mathbf{v}_1 \mathbf{w}_3)$	$C_2$	$-2$	$\frac{1}{2}$	$\frac{1}{2}$	$1$
$(\mathbf{v}_2 \mathbf{w}_3)$	$C_4$	$-2$	$\frac{1}{2}$	$\frac{1}{2}$	$1$
$(\mathbf{v}_1 \mathbf{v}_2)$	$C_8$	$1$			$0$
$(\mathbf{v}_3 \mathbf{w}_3)$	$C_5$	$-4$	$1$	$1$	$2$

#### 4.4.4 The class group

The class group enters the exact sequence

$$0 \rightarrow M \xrightarrow{A} \text{Div } \mathbb{T}(Y_3) \rightarrow \text{Cl}(Y_3) \rightarrow 0.$$

So the problem is that of computing the quotient of two free abelian groups; it may have torsion. The matrix  $A$  can be put into a normal form called the Smith normal form [56]. This is diagonal, and the diagonal entries determine the class group: a diagonal block equal to the identity corresponds to a free summand of the appropriate rank, and if a value  $m$  appears, there is a summand  $\mathbb{Z}_m$ . For  $Y_3$  the Smith normal form of the matrix  $A$  is the identity matrix, so that the quotient is  $\mathbb{Z}$ , i.e.,

$$\text{Cl}(Y_3) = \mathbb{Z}.$$

Comparing with Table 5 we see that the morphism  $\text{Pic}(Y_3) \rightarrow \text{Cl}(Y_3)$  is the multiplication by 2 (indeed,  $2[D'_{EH}] = [D_4]$ ).

#### 4.4.5 $Y_3$ as a line bundle over $\mathbb{P}[1, 1, 2]$

Also  $Y_3$  is the total space of a line bundle, in this case over  $\mathbb{P}[1, 1, 2]$ . The fan of  $\mathbb{P}[1, 1, 2]$  is depicted on the left in Figure 7; it is generated by the vectors  $(1, 0)$ ,  $(-1, 2)$ ,  $(0, -1)$ , corresponding respectively to the divisors  $D_1$ ,  $D_2$ ,  $D_3$ . The divisors  $D_1$  and  $D_2$  are Weil, while  $D_3$  is Cartier. In the class group, which is  $\mathbb{Z}$ , they are related by

$$[D_3] = 2[D_2] = 2[D_1].$$

Each of  $D_1$  and  $D_2$  generates the class group, and  $D_3$  generates the Picard group.

We study the line bundle  $\mathcal{O}_{\mathbb{P}[1,1,2]}(-2D_3) = \mathcal{O}_{\mathbb{P}[1,1,2]}(-4)$ . By applying the algorithm in [20, §7.3] we see that its fan is that of  $Y_3$ , i.e.,  $Y_3 = \text{tot}(\mathcal{O}_{\mathbb{P}[1,1,2]}(-4))$ . Again, since  $-2D_3$  is a canonical divisor of  $Y_3$ ,  $K_{Y_3}$  is trivial. Again the toric divisors of  $Y_3$  may be obtained from this description:  $D_{EH}$  and  $D'_{EH}$  are the inverse images of  $D_1$  and  $D_2$ , while  $D_4$  is the inverse image of  $D_3$ ; since  $D_3 \cdot D_3 = 2$ , then  $D_4$  is the total space of  $\mathcal{O}(-4)$  on  $\mathbb{P}^1$ . Moreover,  $D_c$  is the image of the zero section. Note that  $Y_3$  is obtained by shrinking  $D_{nc}$  to a  $\mathbb{P}^1$ ; actually  $D_{nc}$  is the total space of the trivial line bundle on the divisor  $E$  in  $\mathbb{F}_2$ , and  $\mathbb{P}[1, 1, 2]$  is indeed obtained by shrinking that divisor to a point.

In Section 8 using the generalized Kronheimer construction we shall calculate the Kähler potential, Kähler metric and Kähler form of  $Y_3$ , verifying that the base of the bundle is indeed singular, as the periods of the Kähler form on the cycle  $C_1$  vanish. This means that  $C_1$  shrinks to a point, and since  $C_1$  inside the compact exceptional divisor  $\mathbb{F}_2$  is the exceptional divisor of the blow-down  $\mathbb{F}_2 \rightarrow \mathbb{P}[1, 1, 2]$ , the base variety becomes singular.

### 4.5 The degeneration $Y_{EH}$

Another degeneration occurring on some edges of the space of stability parameters is the product  $Y_{EH} = \text{ALE}_{A_1} \times \mathbb{C}$ .

#### 4.5.1 The fan

We consider the toric 3-fold whose fan is generated by the rays  $\mathbf{v}_1, \mathbf{w}_2, \mathbf{v}_3, \mathbf{w}_3$ . The three rays  $\mathbf{w}_2, \mathbf{w}_3, \mathbf{v}_3$  generate the fan of the ALE space  $\text{ALE}_{A_1}$  and are orthogonal to  $\mathbf{v}_1$ , so that this is indeed a product manifold  $Y_{EH} = \text{ALE}_{A_1} \times \mathbb{C}$ . Its fan and planar graph are shown in Figure 8. All cones are contained in the cones of  $\Sigma_Y$  (this is easily visualized by noting that the planar graph is a subgraph of that of  $Y$ ), so that there is a morphism  $Y_{EH} \rightarrow Y$ ; on the contrary, there does not seem to be morphism  $Y \rightarrow Y_{EH}$ , so that  $Y_{EH}$  does not appear to be a degeneration of  $Y$ , and  $Y_{EH}$  is not a desingularization of  $Y_0$ .

*Remark 4.1.* The fans generated by collections of rays  $\mathbf{v}_2, \mathbf{w}_2, \mathbf{v}_3, \mathbf{w}_3$ , and  $\mathbf{v}_1, \mathbf{w}_2, \mathbf{v}_2, \mathbf{w}_3$  describe the same variety. △

The cohomology of this variety is

$$h_2(Y_{EH}, \mathbb{Q}) = 1, \quad h_c^2(Y_{EH}, \mathbb{Q}) = 0, \quad h^2(Y_{EH}, \mathbb{Q}) = 1, \quad h_c^4(Y_{EH}, \mathbb{Q}) = 1, \quad h^4(Y_{EH}, \mathbb{Q}) = 0$$

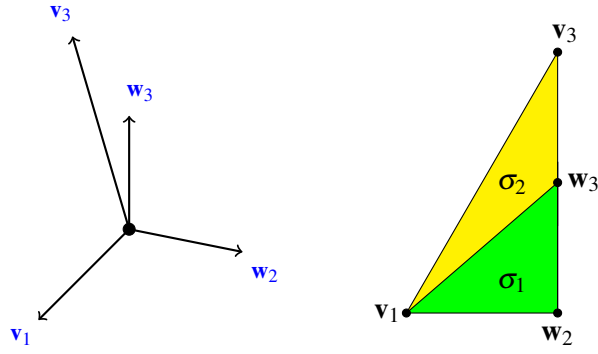


Figure 8: The fan  $\Sigma_{EH}$  of the product variety  $Y_{EH}$  and the associated planar graph

#### 4.5.2 Divisors

The 4 toric divisors corresponding to the rays generated by  $\mathbf{v}_1, \mathbf{w}_3, \mathbf{v}_2, \mathbf{v}_3$  will be denoted  $D_{EH}, D_3, D_0, D_4$  respectively. They are described in Table 7. They are all Cartier as  $Y_{EH}$  is smooth. Their fans are depicted in Figure 9. The matrices  $A, B$  in this case are

$$A = \begin{pmatrix} 1 & 0 & 0 \\ 0 & 1 & 0 \\ 0 & -1 & 2 \\ 0 & 0 & 1 \end{pmatrix}, \quad B = \begin{pmatrix} 0 & -\frac{1}{2} & -\frac{1}{2} & 1 \end{pmatrix}$$

with the divisors ordered as  $D_{EH}, D_0, D_4, D_3$ . The relations among the divisor classes are

$$[D_{EH}] = 0, \quad [D_0] = [D_4] = -\frac{1}{2}[D_3].$$

Again,  $[K_{Y_{EH}}] = 0$ . The fact that  $D_{EH}$  is cohomologous to zero is consistent with  $\text{Pic}(Y_{EH}) \simeq p_1^* \text{Pic}(\text{ALE}_{A_1})$ , with  $p_1: Y_{EH} \rightarrow \text{ALE}_{A_1}$  the projection onto the first factor.

Table 7: Toric Divisors in  $Y_{EH}$

Ray	Divisor	Fan	Variety	Component
$\mathbf{w}_2$	$D_0$	$(1,0), (0,1)$	$\mathbb{C}^2$	$-\frac{1}{2}$
$\mathbf{v}_1$	$D_{EH}$	$(1,0), (-1,2), (0,1)$	$\text{ALE}_{A_1}$	0
$\mathbf{w}_3$	$D_3$	$(1,0), (-1,0), (0,1)$	$\mathbb{P}^1 \times \mathbb{C}$	1
$\mathbf{v}_3$	$D_4$	$(1,0), (-1,4), (0,1)$	$\text{tot}(\mathcal{O}(-4) \rightarrow \mathbb{P}^1)$	$-\frac{1}{2}$

#### 4.5.3 Toric curves and intersections

There is one compact toric curve, corresponding to the face  $(\mathbf{v}_1 \mathbf{w}_3)$ . It lies in  $D_{EH}$  and  $D_3$ . The intersection numbers are shown in Table 8.

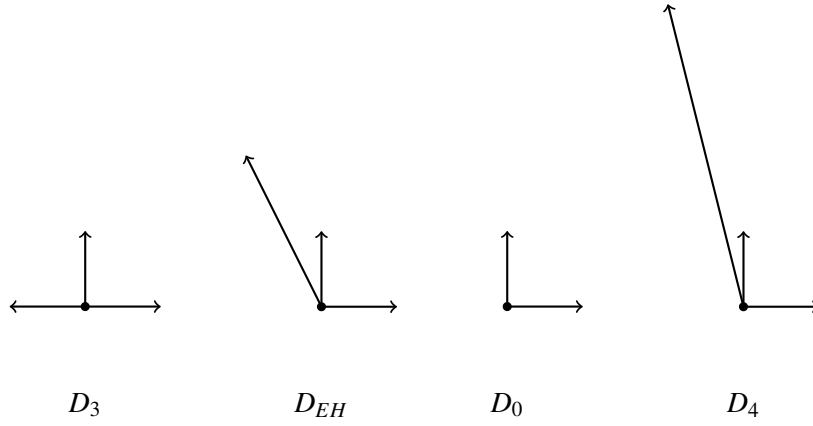


Figure 9: The fans of the 4 toric divisors of  $Y_{EH}$

Table 8: Intersections among the toric curves and divisors in  $Y_{EH}$

	$D_0$	$D_{EH}$	$D_3$	$D_4$
$C$	1	0	-2	1

#### 4.5.4 A relation with the full resolution

Let  $g = (\omega, \omega, \omega^2)$  be the generator of the action of  $\mathbb{Z}_4$ . The square  $g^2$  leaves every point of the  $z$  axis fixed, so that

$$\mathbb{C}^3 / \langle g^2 \rangle \simeq \mathbb{C}^2 / \mathbb{Z}_2 \times \mathbb{C}.$$

Blowing up we get  $Y_{EH}$ . Now  $g$  still acts on  $Y_{EH}$  producing a quotient which is singular along a  $\mathbb{P}^1$ . Blowing up we get  $Y$ ; the corresponding exceptional divisor is  $D_C$ , the second Hirzebruch surface. So  $Y_{EH}$  is the desingularization of a partial quotient of  $\mathbb{C}^3$ , and by a further quotient and subsequent desingularization it produces  $Y$ . The following diagram depicts this situation.

$$\begin{array}{ccc}
 & & Y \\
 & & \downarrow \\
 Y_{EH} & \longrightarrow & Y_{EH} / \mathbb{Z}_2 \\
 \downarrow & & \downarrow \\
 \mathbb{C}^3 / \mathbb{Z}_2 & \longrightarrow & \mathbb{C}^3 / \mathbb{Z}_4
 \end{array} \tag{4.8}$$

Note that  $Y_{EH} / \mathbb{Z}_2$  is therefore a partial desingularization of  $\mathbb{C}^3 / \mathbb{Z}_4$ , and indeed it corresponds to the fan obtained by adding the ray  $\mathbf{w}_2$  to the fan of  $\mathbb{C}^3 / \mathbb{Z}_4$ . Note also that the composed map  $Y_{EH} \rightarrow \mathbb{C}^3 / \mathbb{Z}_4$  in diagram (4.8) is not a resolution of singularities as it is 2:1.

#### 4.5.5 $Y_{EH}$ as a fibration

As it happens also for  $Y$  and  $Y_3$ ,  $Y_{EH}$  is the total space of a vector bundle, actually in two different way. In particular it is the pullback of the line bundle  $\mathcal{O}(-2)$  on  $\mathbb{P}^1$  via the projection  $\mathbb{P}^1 \times \mathbb{C} \rightarrow \mathbb{P}^1$  (namely, the total space of the canonical bundle of  $\mathbb{P}^1 \times \mathbb{C}$ ).

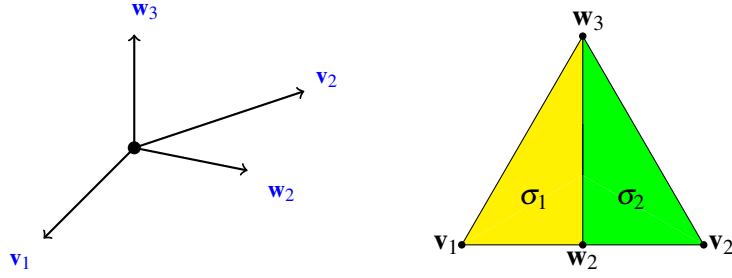


Figure 10: The fan of the second realization of  $Y_{EH}$  and the associated planar graph

#### 4.6 Summary: the exceptional divisor, curves and homology 2-cycles

Some of the main upshots of the discussion and computations made in this Section are the following.

- The general theory encoded in the Ito-Reid theorem [40], confirmed by the explicit toric constructions, tells us that the quotient  $\mathbb{C}^3/\mathbb{Z}_4$  has a crepant resolution of singularities  $Y$ . This may be computed using toric geometry. The exceptional divisor has a compact component,  $D_c$ , isomorphic to the second Hirzebruch surface  $\mathbb{F}_2$ , and a noncompact component  $D_{nc}$ , isomorphic to  $\mathbb{C} \times \mathbb{P}^1$ . This agrees with the age computations which show that the groups  $H_c^{1,1}(Y)$  and  $H^{2,2}(Y)$  are both one-dimensional.

- Let  $\pi: Y \rightarrow \mathbb{C}^3/\mathbb{Z}_4$  be the blow-down morphism. The compact exceptional divisor  $D_c$  is the inverse image  $\pi^{-1}(0)$  of the fixed point  $0 \in \mathbb{C}^3$ , while the noncompact component  $D_{nc}$  is the preimage of the fixed line  $\{x = y = 0\}$ .

- Using this information it is immediate to identify the equation of the compact exceptional divisor in the open chart associated with the cone  $\sigma_1$  as

$$w = 0. \quad (4.9)$$

This, together with the substitutions (4.7), is all what we need to compute the periods of the first Chern classes of the tautological bundles represented by the following closed  $(1, 1)$ -forms:

$$\omega_{1,2,3}^{(1,1)} = \frac{i}{2\pi} \partial \bar{\partial} \log [X_{1,2,3}]^{\alpha_{1,2,3}} \quad (4.10)$$

As we explain further on, although we are not able to compute the forms  $\omega_{1,2,3}^{(1,1)}$  for the general case, yet we succeed in calculating their periods on the basis of the homology cycles by restricting the moment map equations to the latter, using to this purpose the equations of such loci as derived from the toric description.

Again in the chart corresponding to the cone  $\sigma_1$ , the noncompact component  $D_{nc}$  of the exceptional divisor has equation

$$v = 0. \quad (4.11)$$

The two components intersect along the curve

$$C_1 = \{u, v, w \mid w = 0, v = 0\}. \quad (4.12)$$

- Finally, we consider the curve

$$C_2 = \{u, v, w \mid w = 0, u = 0\}. \quad (4.13)$$

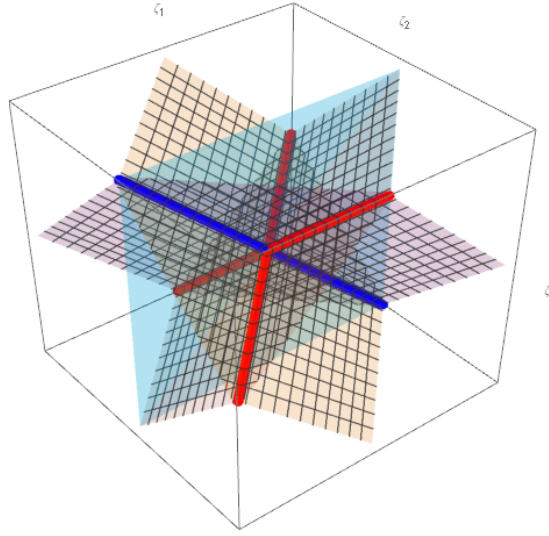


Figure 11: The structure of the stability chambers. The space  $\mathbb{R}^3$  where the moment map equations always admit real nonnegative solutions is divided in two halves by the presence of a wall of type 0, named  $\mathcal{W}_0$  which is defined by the equation  $\zeta_2 = 0$  and is marked in the figure as a cyan transparent surface without meshing. In addition there are other three walls, respectively described by  $\mathcal{W}_1 \Leftrightarrow \zeta = \{x+y, x, y\}$ ,  $\mathcal{W}_2 \Leftrightarrow \zeta = \{x, x+y, y\}$  and  $\mathcal{W}_3 \Leftrightarrow \zeta = \{x, y, x+y\}$ , where  $x, y \in \mathbb{R}$ . The planes  $\mathcal{W}_{1,3}$  are of type 0, while  $\mathcal{W}_2$  is of type 1. These three infinite planes provide the partition of  $\mathbb{R}^3$  into eight disjoint chambers that are described in the main text. The three planes  $\mathcal{W}_{1,2,3}$  are marked in the figure as meshed surfaces of three different colors. On the three intersections of two of these planes we find the already discussed lines where the moment map equations can be solved by radicals, corresponding to the Eguchi-Hanson degeneration  $Y_{EH} \times \mathbb{C}$  (blue line) and to the two Cardano degenerations (red lines).

i.e., the intersection between  $D_{EH}$  and  $D_c$ . It corresponds to the face  $xz$  of the fan of  $Y$ . As a curve in  $\mathbb{F}_2$ , it corresponds to the ray generated by  $(1,0)$ , squares to  $-2$ , and is the exceptional divisor of the blowup  $\mathbb{F}_2 \rightarrow \mathbb{P}^2/\mathbb{Z}_2$ , and a section of the fibration  $\mathbb{F}_2 \rightarrow \mathbb{P}^1$  (and of course it is a copy of  $\mathbb{P}^1$ ). It intersects  $D_{nc}$  again in the point  $u = v = w = 0$ , which corresponds to the cone generated by  $(1,0)$  and  $(0,1)$  in the fan of  $D_{nc}$ . This is the  $\mathbb{P}^1$  which generates the Picard group of the Eguchi-Hanson space  $D_{EH}$ .

- Note that  $\dim H_2(Y) = 2$ , and indeed the curves  $C_1$  and  $C_2$  provide a basis for  $H_2(Y, \mathbb{Z})$ .

## 5 Chamber Structure and the tautological bundles

We can now compare the analytical results obtained from the Kähler quotient à la Kronheimer with the general predictions of the resolution of the singularity provided by toric geometry. This provides a concrete example of how the chamber structure of the  $\zeta$  parameter space controls the topology of the resolutions of the singularity [23]. In the following we evaluate the periods of the differential forms arising from the Kronheimer construction on the cycles given by the curves  $C_1, C_2$  that both are contained in  $D_c$ , namely in the compact component of the exceptional divisor (actually we are pulling back the differential forms from  $\mathcal{M}_{a,b,c}$  to  $Y$  via the relevant contraction morphism  $\gamma: Y \rightarrow \mathcal{M}_{a,b,c}$ , and we use the fact that the pullback is injective in cohomology; however we shall understand that pullback in the notation). We succeed evaluating the differential form periods on the considered curves by restricting the moment map equations to the relevant exceptional divisor  $D_c$  and then to its relevant sub-loci.

According to the general theory of the Kronheimer-like construction presented in [18], there are three

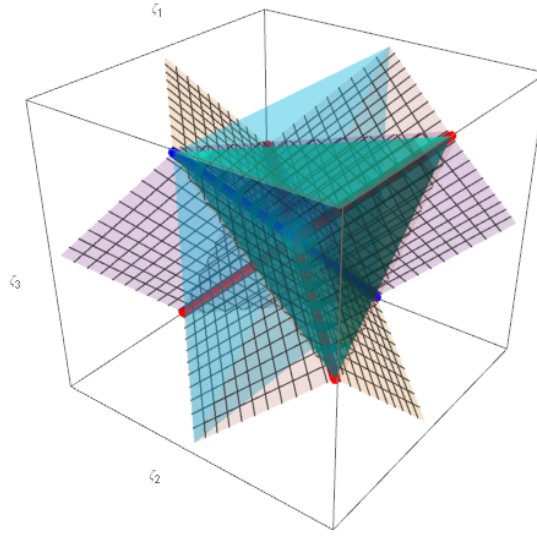


Figure 12: In fig.11 we displayed only the walls defining the chamber structure. In the present picture besides the walls we show also one of the eight chambers, namely Chamber 1. It is marked as a transparent greenish-blue colored portion of three dimensional space. It is a convex cone delimited by the aforementioned walls.

tautological bundles; their first Chern classes are encoded in the triple of (1,1)-forms given in eq. (4.10).

## 5.1 The stability chambers

The result of the various calculations presented in subsequent sections singles out the structure of the stability chambers which is summarized in figs. 11 and 12. Let us illustrate this structure in detail. Understanding the geometry of these pictures is a very useful guide through the subsequent computations. The original data from which we start are the following ones. To begin with we know that the entire  $\zeta$  space is just  $\mathbb{R}^3$ .

In figs. 11 and 12 we have drawn 3 lines. These lines correspond to the following 4 instances of degenerate spaces where the algebraic system of the moment map equations becomes solvable or partially solvable:

### 1) Eguchi-Hanson case

$$\zeta_1 = s \quad ; \quad \zeta_2 = 0 \quad ; \quad \zeta_3 = s \quad (5.1)$$

In pictures 11, 12 this line is fat and drawn in blue color:

### 2) Cardano 1

$$\zeta_1 = s \quad ; \quad \zeta_2 = s \quad ; \quad \zeta_3 = 0 \quad (5.2)$$

In pictures 11, 12 this line is solid fat and drawn in red color. We remind the reader that the name Cardano is due to the fact that the solution of the entire moment map equation system reduces to the solution of a single algebraic equation of the fourth order (see eq. (3.6)).

### 3) Cardano 2

$$\zeta_1 = 0 \quad ; \quad \zeta_2 = s \quad ; \quad \zeta_3 = s \quad (5.3)$$

In pictures 11, 12 this line is solid fat and drawn in red color.

In addition we have a 4th line that we have not drawn in fig. 11 and 12. This line entirely lies on one of the walls to be described below.

#### 4) Kampé

$$\zeta_1 = s \quad ; \quad \zeta_2 = 2s \quad ; \quad \zeta_3 = s \quad (5.4)$$

In fig. 13 this line is dashed fat and drawn in black color. We remind again the reader that the manifold was named Kampé because the solution of the moment map equations reduces to finding the roots of a single algebraic equation of the sixth order.

In all these cases  $s$  is a nonzero real number.

Since the exceptional solvable cases must lie on some walls we have tried to conjecture which planar cones might partition the infinite cube into chambers so that the exceptional lines could lie on such planar cones and possibly be edges at some of their intersections.

With some ingenuity we introduced the following four planar walls (here  $x, y$  are real parameters)

$$\mathcal{W}_1 : \quad \{x + y, x, y\} \quad (5.5)$$

$$\mathcal{W}_2 : \quad \{x, x + y, y\} \quad (5.6)$$

$$\mathcal{W}_3 : \quad \{x, y, x + y\} \quad (5.7)$$

$$\mathcal{W}_0 : \quad \{x, 0, y\} \quad (5.8)$$

that were depicted in fig. 11, 12. and split the space  $\mathbb{R}^3$  into eight convex three-dimensional cones. The list of the eight convex cones that provide as many stability chambers is obtained through the following argument. The three planes  $\mathcal{W}_{1,2,3}$  are respectively orthogonal to the following three vectors:

$$\mathbf{n}_1 = \{-1, 1, 1\} \quad (5.9)$$

$$\mathbf{n}_2 = \{1, -1, 1\} \quad (5.10)$$

$$\mathbf{n}_3 = \{1, 1, -1\}. \quad (5.11)$$

The eight convex regions are defined by choosing the signs of the projections  $\mathbf{n}_{1,2,3} \cdot \zeta$  in all possible ways. In this way we obtain:

$$\begin{aligned} \text{Chamber I} &\equiv \{\zeta_1 - \zeta_2 - \zeta_3 > 0 \quad , \quad -\zeta_1 + \zeta_2 - \zeta_3 > 0 \quad , \quad -\zeta_1 - \zeta_2 + \zeta_3 > 0\} \\ \text{Chamber II} &\equiv \{\zeta_1 - \zeta_2 - \zeta_3 > 0 \quad , \quad -\zeta_1 + \zeta_2 - \zeta_3 > 0 \quad , \quad -\zeta_1 - \zeta_2 + \zeta_3 < 0\} \\ \text{Chamber III} &\equiv \{\zeta_1 - \zeta_2 - \zeta_3 > 0 \quad , \quad -\zeta_1 + \zeta_2 - \zeta_3 < 0 \quad , \quad -\zeta_1 - \zeta_2 + \zeta_3 > 0\} \\ \text{Chamber IV} &\equiv \{\zeta_1 - \zeta_2 - \zeta_3 < 0 \quad , \quad -\zeta_1 + \zeta_2 - \zeta_3 > 0 \quad , \quad -\zeta_1 - \zeta_2 + \zeta_3 > 0\} \\ \text{Chamber V} &\equiv \{\zeta_1 - \zeta_2 - \zeta_3 < 0 \quad , \quad -\zeta_1 + \zeta_2 - \zeta_3 < 0 \quad , \quad -\zeta_1 - \zeta_2 + \zeta_3 > 0\} \\ \text{Chamber VI} &\equiv \{\zeta_1 - \zeta_2 - \zeta_3 < 0 \quad , \quad -\zeta_1 + \zeta_2 - \zeta_3 > 0 \quad , \quad -\zeta_1 - \zeta_2 + \zeta_3 < 0\} \\ \text{Chamber VII} &\equiv \{\zeta_1 - \zeta_2 - \zeta_3 > 0 \quad , \quad -\zeta_1 + \zeta_2 - \zeta_3 < 0 \quad , \quad -\zeta_1 - \zeta_2 + \zeta_3 < 0\} \\ \text{Chamber VIII} &\equiv \{\zeta_1 - \zeta_2 - \zeta_3 < 0 \quad , \quad -\zeta_1 + \zeta_2 - \zeta_3 < 0 \quad , \quad -\zeta_1 - \zeta_2 + \zeta_3 < 0\} \end{aligned} \quad (5.12)$$

Four of the above eight chambers are displayed in fig. 14.

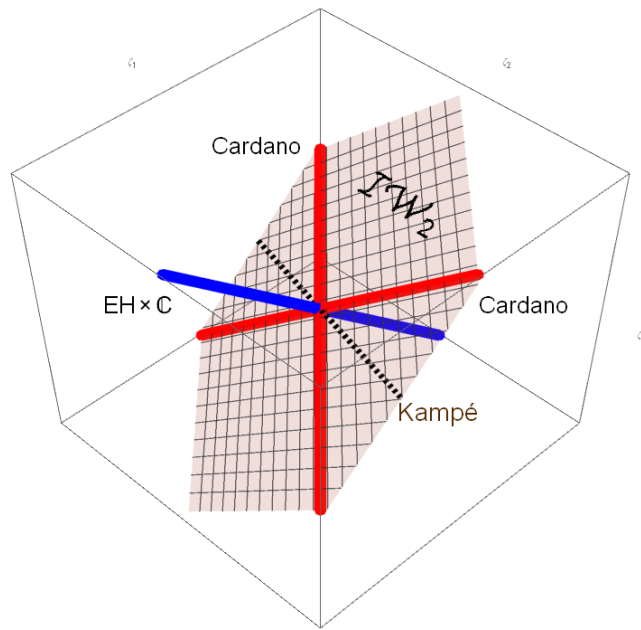


Figure 13: This picture shows the type I plane  $\mathcal{W}_2$ . The two Cardano manifolds (red lines) and the Kampé manifold (dashed black line) lay all in this plane, whose generic point corresponds, as we are going to see, to the degeneration  $Y_3$ . The Eguchi-Hanson degeneration (blue line) is instead out of this plane and intersects it only in the origin.

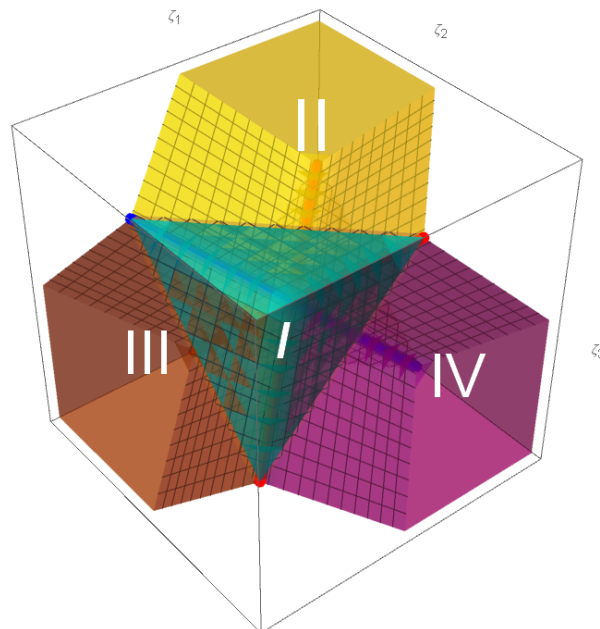


Figure 14: The partition of  $\mathbb{R}^3$  into 8 convex cones. In the picture, out of the eight regions, we show only four, marking them in different transparent colors.

## 5.2 Edges

The special solvable cases that we have found all sit at the intersection of two of the three walls  $\mathscr{W}_{1,2,3}$ . In particular the Cardano manifolds are edges at the intersection of the following walls:

$$\text{Cardano 1} = \mathscr{W}_1 \cap \mathscr{W}_2 \quad ; \quad \text{Cardano 2} = \mathscr{W}_2 \cap \mathscr{W}_3 \quad (5.13)$$

while the Eguchi-Hanson case is the intersection:

$$Y_{EH} = \mathscr{W}_1 \cap \mathscr{W}_3 \quad (5.14)$$

Note also that this edge lays entirely on the wall  $\mathscr{W}_0$ . From this point of view the Eguchi-Hanson case is similar to the Kampé case, that lays entirely on the wall  $\mathscr{W}_2$ . The difference however is that, as we advocate below, the wall  $\mathscr{W}_0$  is of type 0 while  $\mathscr{W}_2$  is of type 1. In the first case the Eguchi-Hanson line is the only degeneracy pertaining to the wall  $\mathscr{W}_0$ , while in the second case the Kampé line yields an instance of the degeneracy  $Y_3$  as any other point of the same wall. Actually also the Cardano cases that lay on the same wall correspond to a different realization of  $Y_3$ .

## 6 Periods of the Chern classes of the tautological bundles

The most appropriate instrument to verify the degeneracy/non-degeneracy of the singularity resolutions provided by the Kähler quotient with given  $\zeta$  parameters is provided by the calculation of the period matrix:

$$\mathbf{\Pi} \equiv \Pi_{i,J} = \int_{C_i} \omega_J \quad ; \quad i = (1,2), \quad J = (1,2,3) \quad (6.1)$$

where  $\omega_J$  are the first Chern classes of the tautological bundles and the curves  $C_i$  provide a basis of homology 2-cycles. In particular the combination:

$$\mathbf{Vol}_i = \zeta_I \mathfrak{e}^{IJ} \int_{C_i} \omega_J = \frac{i}{2\pi} \zeta_I \mathfrak{e}^{IJ} \int_{C_i} \partial \bar{\partial} \log(X_J)^{\alpha_{\zeta}} = \int_{C_i} \mathbb{K}_{\zeta} \quad (6.2)$$

is the volume of the cycle  $C_i$  in the resolution identified by the level parameters  $\zeta$ , having denoted by  $\mathbb{K}_{\zeta}$  the corresponding Kähler 2-form.<sup>16</sup> If the volume of the two homology cycles yielding the homology basis is nonzero there is no degeneration. Instead in case of degenerations at least one of such volumes vanishes. This is precisely what happens on the walls of type III, while in the interior of all chambers no degeneration appears.

Through the calculations detailed in the following subsections we have been able to compute the periods of the first Chern forms  $\omega_{1,2,3}^{(1,1)}$  on the basis of homology cycles  $C_{1,2}$  both for the interior points of all the chambers and for all the walls. As far as the interior chamber case is concerned our results are summarized in Table 9. For the walls the results are instead summarized in Table 10, while for the edges they are given in Table 11.

Let us discuss the results in Table 9. The three leftmost columns display the degrees of the tautological line bundles  $\mathscr{B}_I$  restricted to the curves  $C_1, C_2$ ; as the classes of the latter provide a basis of  $H_2(Y, \mathbb{Z})$ , these numbers give the first Chern classes of the line bundles over the integral basis of the Picard group  $\text{Pic}(Y)$  given by the

<sup>16</sup>Let us remark that in agreement with eq. (3.14) the contribution  $\partial \bar{\partial} \mathscr{K}_0$  to the Kähler 2-form is an exact form, whose integral on homology cycles therefore vanishes. Hence the volume of the homology cycles is provided the linear combination of periods specified in eq. (6.2). We also remark that, as the volume of a nonzero cycle is always positive, this is consistent with the positivity of the so-called Hodge line bundle  $\otimes_{j=1}^3 L_j^{\Theta(\mathscr{B}_j)}$ .

Chamber 1	cycle	$f \omega_1$	$f \omega_2$	$f \omega_3$
	$C_1$	1	0	1
	$C_2$	1	1	1
Chamber 2	cycle	$f \omega_1$	$f \omega_2$	$f \omega_3$
	$C_1$	1	0	1
	$C_2$	1	1	1
Chamber 3	cycle	$f \omega_1$	$f \omega_2$	$f \omega_3$
	$C_1$	1	0	1
	$C_2$	0	-1	0
Chamber 4	cycle	$f \omega_1$	$f \omega_2$	$f \omega_3$
	$C_1$	1	0	1
	$C_2$	1	1	1
Chamber 5	cycle	$f \omega_1$	$f \omega_2$	$f \omega_3$
	$C_1$	1	0	1
	$C_2$	0	-1	0
Chamber 6	cycle	$f \omega_1$	$f \omega_2$	$f \omega_3$
	$C_1$	1	0	1
	$C_2$	-1	-1	-1
Chamber 7	cycle	$f \omega_1$	$f \omega_2$	$f \omega_3$
	$C_1$	1	0	1
	$C_2$	0	-1	0
Chamber 8	cycle	$f \omega_1$	$f \omega_2$	$f \omega_3$
	$C_1$	1	0	1
	$C_2$	0	-1	0

Table 9: The periods of the tautological bundle first Chern classes on the basis of homological cycles calculated in the interior points of all the chambers.

Wall $\mathscr{W}_0$	cycle	$f \omega_1$	$f \omega_2$	$f \omega_3$
	$C_1$	3	0	3
	$C_2$	2	0	-2
Wall $\mathscr{W}_1$	cycle	$f \omega_1$	$f \omega_2$	$f \omega_3$
	$C_1$	1	0	1
	$C_2$	0	-2	0
Wall $\mathscr{W}_2$	cycle	$f \omega_1$	$f \omega_2$	$f \omega_3$
	$C_1$	0	0	0
	$C_2$	1	4	1
Wall $\mathscr{W}_3$	cycle	$f \omega_1$	$f \omega_2$	$f \omega_3$
	$C_1$	1	0	1
	$C_2$	0	-2	0

Table 10: The periods of the tautological bundle first Chern Classes on the basis of homological cycles calculated on the 4 walls. For the walls  $\mathscr{W}_0$  and  $\mathscr{W}_2$  we have chosen  $\alpha = 4$  instead of  $\alpha = 2$  to get integer values for the periods.

Cardano $\zeta = \{0, s, s\}$	cycle	$f \omega_1$	$f \omega_2$	$f \omega_3$
	$C_1$	0	0	0
	$C_2$	-1	-1	0
Cardano $\zeta = \{s, s, 0\}$	cycle	$f \omega_1$	$f \omega_2$	$f \omega_3$
	$C_1$	0	0	0
	$C_2$	0	-1	-1
Eguchi-Hanson $\zeta = \{s, 0, s\}$	cycle	$f \omega_1$	$f \omega_2$	$f \omega_3$
	$C_1$	-1	0	1
	$C_2$	0	0	0

Table 11: The periods of the tautological bundle first Chern Classes on the basis of homological cycles calculated on the edges. Again, on the Eguchi-Hanson edge we have taken  $\alpha = 4$ .

divisors  $D_{EH}, D_4$ , dual to the previously mentioned basis of  $H_2(Y, \mathbb{Z})$ . Note that the three columns correspond to the compact junior conjugacy class, the noncompact junior class, and the senior class respectively, and the Poincaré duality between  $H_c^2(Y)$  and  $H^4(Y)$  explains why in all chambers  $\mathcal{R}_1$  and  $\mathcal{R}_3$  have the same Chern classes, and are therefore isomorphic.

We know from the McKay correspondence that the cohomology of  $Y$  is generated by algebraic classes which are in a one-to-one correspondence with the elements of  $\mathbb{Z}_4$ . One issue is how these classes are expressible in terms of the Chern characters of the tautological bundles. In general, this correspondence is highly nontrivial and is governed by a complicated combinatorics [22, 51]. This is indeed exemplified by our calculations. For instance, one can check that in the chambers 1, 2 and 4 one has

$$\langle \text{ch}_2(\mathcal{R}_1), w \rangle = \langle \text{ch}_2(\mathcal{R}_3), w \rangle = 1, \quad \langle \text{ch}_2(\mathcal{R}_2), w \rangle = 0, \quad (6.3)$$

(the triangular brackets are the pairing between cohomology and homology in dimension 4),<sup>17</sup> where  $w$  is the generator of  $H_4(Y, \mathbb{Z})$  given by the divisor  $D_4$ . So the second Chern character of  $\mathcal{R}_1 \simeq \mathcal{R}_3$  does provide a  $\mathbb{Z}$ -basis for  $H^4(Y, \mathbb{Z})$ , and similar in chamber 6 with  $-1$  instead of 1. On the other hand in the chambers 3, 5, 7 and 8 all line bundles have zero second Chern character, and one needs to take a suitable combination of them to get a generator.

In order to illustrate the procedure which leads to the results presented in the mentioned tables there are several steps one has to take that are explained in the following subsections.

## 6.1 The fundamental algebraic system and a dense toric chart covering the variety

The main difficulty with any explicit calculation within the framework of the Kähler quotient à la Kronheimer is that, for this case as for the majority of all cases, the moment map equation system is algebraic of higher order and explicit analytic solutions are mostly out of reach.

However, in the case under consideration and similarly in most of the other cases, the homology cycles on which we would like to integrate our differential forms are entirely contained in the compact component of the exceptional divisor  $D_c$ . This is not too surprising since all the homology is produced by the resolution and disappears in the original orbifold case. Hence the first step in a strategy that leads to the calculation of the period matrix (6.1) necessarily foresees a reduction of the moment map algebraic system (2.41) to the exceptional divisor in the hope that there it becomes of lower effective degree and therefore manageable.

In view of the above observation we consider the transcription of the algebraic system (2.41) in terms of toric coordinates that expose the presence of the exceptional divisor. There are 4 toric charts (see eq. (4.7)), yet from the point of view of the algebraic system of moment map equations there are only two distinguishable charts, namely the chart  $X_{\sigma_1}$  and  $X_{\sigma_4}$ . Indeed, at this level, chart  $X_{\sigma_2}$  is identical with chart  $X_{\sigma_1}$  and chart  $X_{\sigma_3}$  is identical with chart  $X_{\sigma_4}$ . We choose chart  $X_{\sigma_1}$  since, as it is evident from the planar diagram in Fig. 3, the charts 1 and 2 are the only ones that contain both curves  $C_1$  and  $C_2$ .

<sup>17</sup>In general, homology and cohomology are not dual to each other, but are rather related by the exact sequence

$$0 \rightarrow \text{Ext}_{\mathbb{Z}}^1(H_{n-1}(Y, \mathbb{Z}), \mathbb{Z}) \rightarrow H^n(Y, \mathbb{Z}) \rightarrow H_n(X, \mathbb{Z})^\vee \rightarrow 0.$$

However in our case the Ext groups are zero as the homology groups are free over  $\mathbb{Z}$  (see e.g. [37, Thm. 3.2]).

### 6.1.1 Chart $X_{\sigma_1}$

In order to perform our calculations we find it convenient to introduce the following notation. With reference to the coordinates  $u_1, v_1, w_1$  we set:

$$\lambda = \sqrt{|w_1|} \quad ; \quad \sigma = |v_1| \quad ; \quad \delta = (1 + |u_1|^2) \quad (6.4)$$

which yields

$$\Sigma = \delta \lambda \sigma \quad ; \quad U = \lambda^2 \quad (6.5)$$

The next point in the algorithm leading to the calculation of the period matrix on the compact exceptional divisor consists of the replacement of the variables  $X_{1,2,3}$  with new ones  $T_{1,2,3}$  related to the previous ones in the following way:

$$X_1 = \frac{\sqrt{\lambda} T_1}{\sqrt{\sigma}} \quad ; \quad X_2 = \lambda^2 T_2 \quad ; \quad X_3 = \frac{\sqrt{\lambda} T_3}{\sqrt{\sigma}} \quad (6.6)$$

The rationale of the transformation (6.6) is as follows. The reduction to the compact exceptional divisor consists of setting  $w_1 = 0$  and hence  $\lambda \rightarrow 0$ . From the point of view of the (1,1)-forms  $\omega_I$  defined in eq. (4.10), multiplication of  $X_I$  by any power of the modulus square of any complex coordinate is uneffective because of the logarithm. In other words, instead of eq. (4.10) we can write equally well:

$$\omega_I^{(1,1)} = \frac{i}{2\pi} \partial \bar{\partial} \log [T_I]^{\alpha_I} \quad (6.7)$$

The specific choice of powers of  $\lambda$  and  $\sigma$  utilized in (6.6) is the result of a search of the appropriate values that lead to a finite algebraic system with nontrivial solutions in the two limits  $\lambda \rightarrow 0$  and  $\sigma \rightarrow 0$ , corresponding respectively to the compact and noncompact exceptional divisor.

After these replacements in eqs. (2.35), the final form of the system of the moment map equations is turned into the following one:

$$\begin{pmatrix} -T_1^2 (1 + \lambda^4 T_2^2) - \delta T_1^3 T_3 + (1 + \lambda^4 T_2^2) T_3^2 + T_1 T_3 (\delta T_3^2 + T_2 (-\zeta_1 + \zeta_3)) \\ \delta \lambda^4 \sigma^2 T_2^3 - \delta T_1 T_3 (T_1^2 + T_3^2) + T_2 (\delta \sigma^2 - T_1 T_3 (\zeta_1 - \zeta_2 + \zeta_3)) \\ -(-1 + \lambda^4 T_2^2) (T_1^2 + \delta \sigma^2 T_2 + T_3^2) - T_1 T_2 T_3 \zeta_2 \end{pmatrix} = \begin{pmatrix} 0 \\ 0 \\ 0 \end{pmatrix} \quad (6.8)$$

### 6.1.2 Equations of the two homology cycles

In order to calculate the periods of the differential forms (6.7) on the basis of the homology curves  $C_1$  and  $C_2$  we need the equations of such loci in the coordinates  $\lambda, \sigma, \delta$  defined in equation (6.4). We have

$$\begin{aligned} \text{Curve } C_1 & : \quad \sigma = 0 \quad ; \quad \lambda \rightarrow 0 \quad ; \quad \delta = (1 + \Delta) \\ \text{Curve } C_2 & : \quad \sigma = \sqrt{\Delta} \quad ; \quad \lambda \rightarrow 0 \quad ; \quad \delta = 1 \end{aligned} \quad (6.9)$$

Conventionally, we denote  $\Delta = |t|^2$  the modulus squared of the complex coordinate  $t$  spanning the curve, whatever it might be. In the case  $C_1$  we have  $\Delta = |u|^2$ , while in the case  $C_2$  we have  $\Delta = |v|^2$ .

In the sequel we use also polar coordinates, setting:

$$\begin{aligned}\rho &\equiv \sqrt{|u|^2} & ; & \quad r \equiv \sqrt{|v|^2} \\ u &= \rho \exp[i\theta] & ; & \quad v = r \exp[i\psi]\end{aligned}$$

### 6.1.3 Reduction to the compact exceptional divisor

Furthermore it is convenient to introduce the following variables, already utilized in eq. (3.19):

$$\varpi \equiv \delta^2 \sigma^2 \quad ; \quad \mathcal{U} \equiv \lambda^4 \tag{6.10}$$

and the following relation between the unknowns  $T_{1,2,3}$  which follows from linear combinations of the equations in the system (6.8)

$$T_3 = T_1 \sqrt{\frac{\zeta_2 + \zeta_3 (T_2^2 \mathcal{U} - 1)}{\zeta_2 + \zeta_1 (T_2^2 \mathcal{U} - 1)}} \tag{6.11}$$

We see that in the limit  $\mathcal{U} \rightarrow 0$ , which is the equation of the compact exceptional divisor  $D_c$ , the expression for  $T_3$  is proportional to that for  $T_1$  in any point of  $\zeta$  space. This has the nontrivial consequence, that the periods of  $\omega_1$  and  $\omega_3$  are always equal. In other words the first Chern classes of the first and third tautological bundles are always cohomologous.

Inserting eqs. (6.11), (6.10) into (6.8) and performing the limit  $\mathcal{U} \rightarrow 0$  we obtain the new system:

$$\left( \begin{array}{c} \frac{(\zeta_1 - \zeta_3) T_1^2 \left( \delta \sqrt{\frac{\zeta_3 - \zeta_2}{\zeta_1 - \zeta_2}} T_1^2 + (\zeta_1 - \zeta_2) \sqrt{\frac{\zeta_3 - \zeta_2}{\zeta_1 - \zeta_2}} T_2 + 1 \right)}{\zeta_1 - \zeta_2} \\ T_2 \left( \varpi - \sqrt{\frac{\zeta_3 - \zeta_2}{\zeta_1 - \zeta_2}} (\zeta_1 - \zeta_2 + \zeta_3) T_1^2 \right) - \frac{\delta (\zeta_1 - 2\zeta_2 + \zeta_3) \sqrt{\frac{\zeta_3 - \zeta_2}{\zeta_1 - \zeta_2}} T_1^4}{\zeta_1 - \zeta_2} \\ \frac{(\zeta_2 - \zeta_3) T_1^2}{\zeta_2 - \zeta_1} - \zeta_2 \sqrt{\frac{\zeta_3 - \zeta_2}{\zeta_1 - \zeta_2}} T_2 T_1^2 + T_2 \varpi + T_1^2 \end{array} \right) = \begin{pmatrix} 0 \\ 0 \\ 0 \end{pmatrix} \tag{6.12}$$

which is the appropriate reduction to the exceptional divisor  $D_c$  of the moment map equations. By construction the three equations in (6.12) are linear dependent and can be solved for the two unknowns  $T_{1,2}$  in terms of the variables  $\delta, \varpi$ . Indeed they are quadratic, cubic, or quartic and can be solved by radicals.

## 6.2 Periods inside the chambers.

Let us begin with the periods in the interior points of the chambers, the result of whose calculation was summarized in Table 9. We found it convenient to choose eight rational points as representatives of the eight chambers.

Explicitly we utilize the following ones:

Chamber 1	$\zeta_1 \rightarrow -\frac{1}{2}$	$\zeta_2 \rightarrow -\frac{3}{4}$	$\zeta_3 \rightarrow -\frac{1}{2}$
Chamber 2	$\zeta_1 \rightarrow -\frac{1}{16}$	$\zeta_2 \rightarrow -\frac{3}{16}$	$\zeta_3 \rightarrow -\frac{3}{4}$
Chamber 3	$\zeta_1 \rightarrow -\frac{1}{16}$	$\zeta_2 \rightarrow -\frac{3}{4}$	$\zeta_3 \rightarrow -\frac{3}{16}$
Chamber 4	$\zeta_1 \rightarrow -\frac{3}{4}$	$\zeta_2 \rightarrow -\frac{1}{16}$	$\zeta_3 \rightarrow -\frac{3}{16}$
Chamber 5	$\zeta_1 \rightarrow -\frac{1}{4}$	$\zeta_2 \rightarrow -\frac{1}{2}$	$\zeta_3 \rightarrow \frac{1}{2}$
Chamber 6	$\zeta_1 \rightarrow -\frac{1}{4}$	$\zeta_2 \rightarrow \frac{1}{2}$	$\zeta_3 \rightarrow -\frac{1}{2}$
Chamber 7	$\zeta_1 \rightarrow \frac{3}{4}$	$\zeta_2 \rightarrow -\frac{1}{4}$	$\zeta_3 \rightarrow -\frac{1}{2}$
Chamber 8	$\zeta_1 \rightarrow \frac{3}{4}$	$\zeta_2 \rightarrow \frac{1}{2}$	$\zeta_3 \rightarrow \frac{3}{4}$

(6.13)

Inserting the values (6.13) into the system (6.12) we obtain eight algebraic systems that we specialize to either the  $C_1$  or the  $C_2$  cycle by setting:

$C_1$	$\varpi = 0$ ; $\delta = (1 + \rho^2)$
$C_2$	$\varpi = r^2$ ; $\delta = 1$

(6.14)

The 16 linear systems obtained in this way can be solved for  $T_1, T_2$ , and thanks to the relation (6.11), each solution for  $T_{1,2}$  yields also a solution for  $T_3$ . Excluding the spurious solutions  $T_1 \rightarrow 0, T_2 \rightarrow 0$  and  $T_1 \rightarrow 0$  in the case of the  $C_1$  systems we find 2 branches, while in the case of the  $C_2$  systems we find 4 branches. We know that in each case only one branch is the limit on the considered curve of the unique positive real solution of the full system (6.8) yet in absence of the analytic form of the solution of (6.8) we do not know which is the right branch. We circumvent this difficulty in the following way. First we remark that in the case of a form:

$$\Omega = \frac{i}{2\pi} \partial \bar{\partial} J(t, \bar{t}) \quad (6.15)$$

where  $t = \tau e^{i\xi}$  is the complex coordinate written in polar form, of a  $\mathbb{P}^1$ , when  $J(t, \bar{t})$  is a function only of the modulus  $\tau$

$$J(t, \bar{t}) = J(\tau) \quad (6.16)$$

we have:

$$\Omega = \frac{1}{4\pi} \left( \frac{dJ(\tau)}{d\tau} + \tau \frac{d^2J(\tau)}{d\tau^2} \right) d\tau \wedge d\xi \quad (6.17)$$

Correspondingly for the integral of  $\Omega$  on the supporting space we find:

$$\int_{\mathbb{P}^1} \Omega = \frac{1}{2} \int_0^\infty \left( \frac{dJ(\tau)}{d\tau} + \tau \frac{d^2J(\tau)}{d\tau^2} \right) d\tau = \tau \frac{dJ(\tau)}{d\tau} \Big|_0^\infty \quad (6.18)$$

Utilizing this idea we calculate  $\rho \frac{dJ_{1,2,3}(\rho)}{d\rho}$  in the case when

$$J_{1,2,3}(u, \bar{u}) = \log[T_{1,2,3}(\rho)] |_{C_1} \quad (6.19)$$

is defined in term of a solution  $T_{1,2,3}(\rho)$  of the moment map equations reduced to  $C_1$ , and  $r \frac{dJ_{1,2,3}(r)}{dr}$  in the case when

$$J_{1,2,3}(v, \bar{v}) = \log[T_{1,2,3}(r)] |_{C_2} \quad (6.20)$$

is defined in term of a solution  $T_{1,2,3}(r)$  of the moment map equations reduced to  $C_2$ . In both cases we used all the available nontrivial branches.

**Cycle  $C_1$ .** In this case the result is very simple and uniform. For all chambers and for all branches we always have:

$$\rho \frac{dJ_{1,3}(\rho)}{d\rho} = -\frac{1}{(\rho^2+1)} \quad ; \quad \rho \frac{dJ_2(\rho)}{d\rho} = 0 \quad (6.21)$$

This implies that in all chambers we have the periods:

$$\int_{C_1} \omega_1 = 1 \quad ; \quad \int_{C_1} \omega_2 = 0 \quad ; \quad \int_{C_1} \omega_3 = 1 \quad (6.22)$$

which is the result shown in Table 9. There is however an implication of this universal result on the factor  $\alpha_\zeta$ . Utilizing (6.22) in eq.(6.2) we obtain that the volume of the cycle  $C_1$  is given by

$$\mathbf{Vol}_1|_{\text{Chamber } k} = \alpha_k (\zeta_1 - \zeta_2 + \zeta_3) = \alpha_k \mathbf{n}_2 \cdot \zeta \quad (6.23)$$

Hence in order for the volume of the cycle  $C_1$  to be positive in every chamber the factor  $\alpha_k$  has to change sign so as to compensate the negative sign of  $\mathbf{n}_2 \cdot \zeta$  when this occurs. Specifically we have:

Ch. I	Ch. II	Ch. III	Ch. IV	Ch. V	Ch. VI	Ch. VII	Ch. VIII	(6.24)
$\alpha_1 < 0$	$\alpha_2 < 0$	$\alpha_3 > 0$	$\alpha_4 < 0$	$\alpha_5 > 0$	$\alpha_6 < 0$	$\alpha_7 > 0$	$\alpha_8 > 0$	

As we have previously mentioned, in the interiors of the chambers we always take  $|\alpha| = 2$ , while on some walls we have taken  $|\alpha| = 4$ .

**Cycle  $C_2$ .** In the case of the second cycle, the result is more complex since, as we already mentioned, we have four branches. The explicit analytic forms of  $rJ'_{1,2,3}(r)$  for all the branches and in all the chambers is displayed in Table 12. Utilizing eq. (6.18) and the results of Table 12 we obtain the candidate values of the periods that are displayed in Table 13. As one sees from that table, in every chamber there is only the ambiguity of an overall sign. In view of the result (6.24) for the factor  $\alpha_k$  relative to the various chambers, in each of them we choose the overall sign for the  $C_2$  periods that leads to a positive value for the volume of that cycle, according to equation (6.2). Performing such a choice, one finally arrives at the result displayed in Table 9.

### 6.3 Periods on the walls and on the edges

Utilizing the same algorithm as in the case of the interior of the chambers, we have calculated the periods also on the walls and on the edges obtaining the results displayed in Tables 10 and 11. We skip the details for the type 0 walls  $\mathscr{W}_{1,3}$ , since these calculations are identical with those presented in the previous subsection, simply with different values of the  $\zeta$  parameters. For the case of the wall  $\mathscr{W}_2$  the detailed calculation of the Kampé case presented in section 8 produces the periods displayed in Table 10. Additional care is instead required while treating the case of the type 0 wall  $\mathscr{W}_0$  and the Cardano edges.

		$-rJ'_1(r)$	$-rJ'_2(r)$	$-rJ'_3(r)$
Chamber 1	br. 1	$\frac{4r^2-1}{4\sqrt{16r^4-40r^2+1}}$	$\frac{4r^2}{\sqrt{16r^4-40r^2+1}}$	$\frac{4r^2-1}{4\sqrt{16r^4-40r^2+1}}$
	br. 2	$\frac{4r^2-1}{4\sqrt{16r^4-40r^2+1}}$	$\frac{4r^2}{\sqrt{16r^4-40r^2+1}}$	$\frac{4r^2-1}{4\sqrt{16r^4-40r^2+1}}$
	br. 3	$\frac{1-4r^2}{4\sqrt{16r^4-40r^2+1}}$	$-\frac{4r^2}{\sqrt{16r^4-40r^2+1}}$	$\frac{1-4r^2}{4\sqrt{16r^4-40r^2+1}}$
	br. 4	$\frac{1-4r^2}{4\sqrt{16r^4-40r^2+1}}$	$-\frac{4r^2}{\sqrt{16r^4-40r^2+1}}$	$\frac{1-4r^2}{4\sqrt{16r^4-40r^2+1}}$
Chamber 2	br. 1	$\frac{5-8r^2}{4\sqrt{64r^4+32r^2+25}}$	$-\frac{8r^2}{\sqrt{64r^4+32r^2+25}}$	$\frac{5-8r^2}{4\sqrt{64r^4+32r^2+25}}$
	br. 2	$\frac{5-8r^2}{4\sqrt{64r^4+32r^2+25}}$	$-\frac{8r^2}{\sqrt{64r^4+32r^2+25}}$	$\frac{5-8r^2}{4\sqrt{64r^4+32r^2+25}}$
	br. 3	$\frac{8r^2-5}{4\sqrt{64r^4+32r^2+25}}$	$\frac{8r^2}{\sqrt{64r^4+32r^2+25}}$	$\frac{8r^2-5}{4\sqrt{64r^4+32r^2+25}}$
	br. 4	$\frac{8r^2-5}{4\sqrt{64r^4+32r^2+25}}$	$\frac{8r^2}{\sqrt{64r^4+32r^2+25}}$	$\frac{8r^2-5}{4\sqrt{64r^4+32r^2+25}}$
Chamber 3	br. 1	$\frac{2r^2+1}{4\sqrt{4r^4-16r^2+1}}$	$\frac{2r^2}{\sqrt{4r^4-16r^2+1}}$	$\frac{2r^2+1}{4\sqrt{4r^4-16r^2+1}}$
	br. 2	$\frac{2r^2+1}{4\sqrt{4r^4-16r^2+1}}$	$\frac{2r^2}{\sqrt{4r^4-16r^2+1}}$	$\frac{2r^2+1}{4\sqrt{4r^4-16r^2+1}}$
	br. 3	$\frac{-2r^2-1}{4\sqrt{4r^4-16r^2+1}}$	$-\frac{2r^2}{\sqrt{4r^4-16r^2+1}}$	$\frac{-2r^2-1}{4\sqrt{4r^4-16r^2+1}}$
	br. 4	$\frac{-2r^2-1}{4\sqrt{4r^4-16r^2+1}}$	$-\frac{2r^2}{\sqrt{4r^4-16r^2+1}}$	$\frac{-2r^2-1}{4\sqrt{4r^4-16r^2+1}}$
Chamber 4	br. 1	$\frac{7-8r^2}{4\sqrt{64r^4+96r^2+49}}$	$-\frac{8r^2}{\sqrt{64r^4+96r^2+49}}$	$\frac{7-8r^2}{4\sqrt{64r^4+96r^2+49}}$
	br. 2	$\frac{7-8r^2}{4\sqrt{64r^4+96r^2+49}}$	$-\frac{8r^2}{\sqrt{64r^4+96r^2+49}}$	$\frac{7-8r^2}{4\sqrt{64r^4+96r^2+49}}$
	br. 3	$\frac{8r^2-7}{4\sqrt{64r^4+96r^2+49}}$	$\frac{8r^2}{\sqrt{64r^4+96r^2+49}}$	$\frac{8r^2-7}{4\sqrt{64r^4+96r^2+49}}$
	br. 4	$\frac{8r^2-7}{4\sqrt{64r^4+96r^2+49}}$	$\frac{8r^2}{\sqrt{64r^4+96r^2+49}}$	$\frac{8r^2-7}{4\sqrt{64r^4+96r^2+49}}$
Chamber 5	br. 1	$\frac{4r^2+3}{4\sqrt{16r^4-56r^2+9}}$	$\frac{4r^2}{\sqrt{16r^4-56r^2+9}}$	$\frac{4r^2+3}{4\sqrt{16r^4-56r^2+9}}$
	br. 2	$\frac{4r^2+3}{4\sqrt{16r^4-56r^2+9}}$	$\frac{4r^2}{\sqrt{16r^4-56r^2+9}}$	$\frac{4r^2+3}{4\sqrt{16r^4-56r^2+9}}$
	br. 3	$\frac{-4r^2-3}{4\sqrt{16r^4-56r^2+9}}$	$-\frac{4r^2}{\sqrt{16r^4-56r^2+9}}$	$\frac{-4r^2-3}{4\sqrt{16r^4-56r^2+9}}$
	br. 4	$\frac{-4r^2-3}{4\sqrt{16r^4-56r^2+9}}$	$-\frac{4r^2}{\sqrt{16r^4-56r^2+9}}$	$\frac{-4r^2-3}{4\sqrt{16r^4-56r^2+9}}$
Chamber 6	br. 1	$\frac{5-4r^2}{4\sqrt{16r^4+72r^2+25}}$	$-\frac{4r^2}{\sqrt{16r^4+72r^2+25}}$	$\frac{5-4r^2}{4\sqrt{16r^4+72r^2+25}}$
	br. 2	$\frac{5-4r^2}{4\sqrt{16r^4+72r^2+25}}$	$-\frac{4r^2}{\sqrt{16r^4+72r^2+25}}$	$\frac{5-4r^2}{4\sqrt{16r^4+72r^2+25}}$
	br. 3	$\frac{4r^2-5}{4\sqrt{16r^4+72r^2+25}}$	$\frac{4r^2}{\sqrt{16r^4+72r^2+25}}$	$\frac{4r^2-5}{4\sqrt{16r^4+72r^2+25}}$
	br. 4	$\frac{4r^2-5}{4\sqrt{16r^4+72r^2+25}}$	$\frac{4r^2}{\sqrt{16r^4+72r^2+25}}$	$\frac{4r^2-5}{4\sqrt{16r^4+72r^2+25}}$
Chamber 7	br. 1	$\frac{-2r^2-1}{4\sqrt{4r^4-8r^2+1}}$	$-\frac{2r^2}{\sqrt{4r^4-8r^2+1}}$	$\frac{-2r^2-1}{4\sqrt{4r^4-8r^2+1}}$
	br. 2	$\frac{-2r^2-1}{4\sqrt{4r^4-8r^2+1}}$	$-\frac{2r^2}{\sqrt{4r^4-8r^2+1}}$	$\frac{-2r^2-1}{4\sqrt{4r^4-8r^2+1}}$
	br. 3	$\frac{2r^2+1}{4\sqrt{4r^4-8r^2+1}}$	$\frac{2r^2}{\sqrt{4r^4-8r^2+1}}$	$\frac{2r^2+1}{4\sqrt{4r^4-8r^2+1}}$
	br. 4	$\frac{2r^2+1}{4\sqrt{4r^4-8r^2+1}}$	$\frac{2r^2}{\sqrt{4r^4-8r^2+1}}$	$\frac{2r^2+1}{4\sqrt{4r^4-8r^2+1}}$
Chamber 8	br. 1	$\frac{-r^2-1}{4\sqrt{r^4+1}}$	$-\frac{r^2}{\sqrt{r^4+1}}$	$\frac{-r^2-1}{4\sqrt{r^4+1}}$
	br. 2	$\frac{-r^2-1}{4\sqrt{r^4+1}}$	$-\frac{r^2}{\sqrt{r^4+1}}$	$\frac{-r^2-1}{4\sqrt{r^4+1}}$
	br. 3	$\frac{r^2+1}{4\sqrt{r^4+1}}$	$\frac{r^2}{\sqrt{r^4+1}}$	$\frac{r^2+1}{4\sqrt{r^4+1}}$
	br. 4	$\frac{r^2+1}{4\sqrt{r^4+1}}$	$\frac{r^2}{\sqrt{r^4+1}}$	$\frac{r^2+1}{4\sqrt{r^4+1}}$

Table 12: The indefinite integrals for the calculation of periods of the tautological Chern Classes along the cycle  $C_2$ .

Chamber 1		$\int_{C_2} \omega_1$	$\int_{C_2} \omega_2$	$\int_{C_2} \omega_3$
	branch <sub>1</sub>	-1	-2	-1
	branch <sub>2</sub>	-1	-2	-1
	branch <sub>3</sub>	1	2	1
	branch <sub>4</sub>	1	2	1
Chamber 2		$\int_{C_2} \omega_1$	$\int_{C_2} \omega_2$	$\int_{C_2} \omega_3$
	branch <sub>1</sub>	1	2	1
	branch <sub>2</sub>	1	2	1
	branch <sub>3</sub>	-1	-2	-1
	branch <sub>4</sub>	-1	-2	-1
Chamber 3		$\int_{C_2} \omega_1$	$\int_{C_2} \omega_2$	$\int_{C_2} \omega_3$
	branch <sub>1</sub>	0	-2	0
	branch <sub>2</sub>	0	-2	0
	branch <sub>3</sub>	0	2	0
	branch <sub>4</sub>	0	2	0
Chamber 4		$\int_{C_2} \omega_1$	$\int_{C_2} \omega_2$	$\int_{C_2} \omega_3$
	branch <sub>1</sub>	1	2	1
	branch <sub>2</sub>	1	2	1
	branch <sub>3</sub>	-1	-2	-1
	branch <sub>4</sub>	-1	-2	-1
Chamber 5		$\int_{C_2} \omega_1$	$\int_{C_2} \omega_2$	$\int_{C_2} \omega_3$
	branch <sub>1</sub>	0	-2	0
	branch <sub>2</sub>	0	-2	0
	branch <sub>3</sub>	0	2	0
	branch <sub>4</sub>	0	2	0
Chamber 6		$\int_{C_2} \omega_1$	$\int_{C_2} \omega_2$	$\int_{C_2} \omega_3$
	branch <sub>1</sub>	1	2	1
	branch <sub>2</sub>	1	2	1
	branch <sub>3</sub>	-1	-2	-1
	branch <sub>4</sub>	-1	-2	-1
Chamber 7		$\int_{C_2} \omega_1$	$\int_{C_2} \omega_2$	$\int_{C_2} \omega_3$
	branch <sub>1</sub>	0	2	0
	branch <sub>2</sub>	0	2	0
	branch <sub>3</sub>	0	-2	0
	branch <sub>4</sub>	0	-2	0
Chamber 8		$\int_{C_2} \omega_1$	$\int_{C_2} \omega_2$	$\int_{C_2} \omega_3$
	branch <sub>1</sub>	0	2	0
	branch <sub>2</sub>	0	2	0
	branch <sub>3</sub>	0	-2	0
	branch <sub>4</sub>	0	-2	0

Table 13: The candidate period integrals of the tautological Chern classes along the cycle  $C_2$ .

### 6.3.1 The type 0 wall $\mathscr{W}_0$

If we choose:

$$\zeta = \{p, 0, q\} \quad ; \quad p, q \in \mathbb{R} \quad (6.25)$$

we are, by definition, on the wall  $\mathscr{W}_0$ . The main property of this wall is that the moment map algebraic system (2.41) implies

$$X_2 = 1. \quad (6.26)$$

Hence the rescaling ansatz (6.6) is not appropriate on this wall for the reduction of the moment map equations to the exceptional compact divisor  $D_c$ . Another rescaling scheme is required.

Choosing (6.25) and implementing eq. (6.26) the third of eqs. (2.41) is automatically satisfied and we are left with

$$\begin{pmatrix} X_3 X_1 \left( -p + q + X_3^2 \sqrt[4]{\bar{U}} \sqrt{\delta \bar{\omega}} \right) + X_3 X_1^3 \sqrt[4]{\bar{U}} \left( -\sqrt{\delta \bar{\omega}} \right) - 2X_1^2 \sqrt{\bar{U}} + 2X_3^2 \sqrt{\bar{U}} \\ 2\sqrt[4]{\bar{U}} \sqrt{\delta \bar{\omega}} - X_3 X_1 \left( p + q + X_3^2 \sqrt[4]{\bar{U}} \sqrt{\delta \bar{\omega}} \right) + X_3 X_1^3 \sqrt[4]{\bar{U}} \left( -\sqrt{\delta \bar{\omega}} \right) \\ 0 \end{pmatrix} = \begin{pmatrix} 0 \\ 0 \\ 0 \end{pmatrix} \quad (6.27)$$

where we used the same real variables  $\delta, \bar{\omega}, \bar{U}$  utilized in previous sections. Given eq. (6.27), an appropriate rescaling that assures a finite limit  $\bar{U} \rightarrow 0$  is provided by the one below:

$$X_1 = T_1 \bar{U}^{3/8} \quad , \quad X_3 = \frac{T_3}{\sqrt[8]{\bar{U}}} \quad (6.28)$$

Implementing the above substitution in the system (6.27) and factoring out a common factor  $\bar{U}^{1/4}$  we can perform the limit  $\bar{U} \rightarrow 0$  and we get:

$$\begin{pmatrix} T_3 \left( T_1 \left( -p + q + T_3^2 \sqrt{\delta \bar{\omega}} \right) + 2T_3 \right) \\ 2\sqrt{\delta \bar{\omega}} - T_1 T_3 \left( p + q + T_3^2 \sqrt{\delta \bar{\omega}} \right) \\ 0 \end{pmatrix} = \begin{pmatrix} 0 \\ 0 \\ 0 \end{pmatrix} \quad (6.29)$$

The limiting system (6.29) is solvable by radicals and it has four branches that can be treated exactly as in the case of the previous section, calculating the derivatives with respect to the  $\rho$  and  $r$  variables that lead to the evaluation of the Kähler form and of its integrals. An additional care which is required in this case is that one has to calculate first the derivatives and then set either  $r$  or  $\rho$  to zero. Doing the operations in the opposite order one meets undefined limits for either  $T_1$  or  $T_2$ . Just as above we have to choose the right branch in order to get a positive volume for the two homology cycles. Through these steps one arrives at the result displayed for  $\mathscr{W}_0$  in Table 10.

### 6.3.2 Periods of the Cardano manifold

The case of the Cardano manifold was treated in section 3.3. In particular it was shown that the Kähler potential for the two instances of this manifold is given by eq. (3.18), where  $X = \mathfrak{X}(\bar{\omega}, \bar{U})$  is the 4th root of the quartic equation (3.17), explicitly written down in eq. (3.20). At the same time the triplet of (1,1)-forms  $\omega_i$  is defined

as

$$\begin{aligned} \zeta = \{1, 1, 0\} \quad \omega_1 = 0 \quad \omega_2 = \Omega \quad \omega_3 = \Omega \quad ; \quad \Omega &= \frac{i}{2\pi} \partial \bar{\partial} \mathfrak{X}(\varpi, \mathcal{U})^2 \\ \zeta = \{0, 1, 1\} \quad \omega_1 = \Omega \quad \omega_2 = \Omega \quad \omega_3 = 0 \quad ; \quad \Omega &= \frac{i}{2\pi} \partial \bar{\partial} \mathfrak{X}(\varpi, \mathcal{U})^2 \end{aligned} \quad (6.30)$$

Developing the function  $\mathfrak{X}(\varpi, \mathcal{U})$  in power series of the variable  $\mathcal{U}$  we find

$$\mathfrak{X}(\varpi, \mathcal{U}) = \frac{1}{2} \left( \sqrt{\varpi} + \sqrt{\varpi+4} \right) + \frac{1}{12} \left( -\frac{6(\varpi^2+3\varpi)}{\sqrt{\varpi+4}} - 6\sqrt{\varpi}(\varpi+1) \right) \sqrt{\mathcal{U}} + \mathcal{O}(\mathcal{U}). \quad (6.31)$$

In this case the reduction of the forms to the exceptional compact divisor can be performed in complete analytic safety restricting  $\mathfrak{X}(\varpi, \mathcal{U})$  to its zeroth order term in  $\mathcal{U}$ . In this way we obtain the precise expression of the (1,1)-form  $\Omega$  whose integrals are then easily calculated. From eq. (6.31) and from the definition of the variable  $\varpi$  we arrive at the conclusion that

$$\begin{aligned} \Omega &= \frac{i}{2\pi} \partial \bar{\partial} \mathfrak{Q}(\rho, r) \\ \mathfrak{Q}(\rho, r) &= \log \left( \frac{(\rho^2+1)^2 r^2 + \sqrt{(\rho^2+1)^2 r^2 \sqrt{(\rho^2+1)^2 r^2 + 4 + 4}}}{2\sqrt{(\rho^2+1)^2 r^2 + 4}} \right) \end{aligned} \quad (6.32)$$

From the above result it immediately follows that:

$$\Omega|_{C_1} = 0 \quad ; \quad \int_{C_2} \Omega = -1. \quad (6.33)$$

This yields the values of the periods as displayed in Table 11.

It appears that the Cardano manifold is another realization of the  $Y_3$  degeneration of the full resolution  $Y$  just as the Kampé manifold to be discussed in section 8, see in particular subsection 8.3. The same arguments presented there apply here as well and lead to the same conclusion. Hence also the Cardano manifold is a line bundle over the singular weighted projective space  $\mathbb{P}[1, 1, 2]$ .

## 6.4 Summary of the chamber and wall structure

We have 8 chambers and 4 walls.

- All interiors of the 8 chambers correspond to the full resolution  $Y$ . This is consistent with Theorem 1.1 in [23], which states that there exists a chamber where the variety corresponding to the generic point is a resolution of singularities, and with the fact that according to toric geometry there appears to be only one full resolution of singularities.
- Among the four walls  $\mathscr{W}_i$ , only  $\mathscr{W}_2$  is of type III, while the others are type 0. The generic point on  $\mathscr{W}_2$  corresponds to the partial resolution  $Y_3$  (note that  $Y_3$  is obtained from  $Y$  by collapsing the noncompact exceptional divisor to a line).
- The triple intersection  $\mathscr{W}_0 \cap \mathscr{W}_1 \cap \mathscr{W}_3$  is an edge whose generic point corresponds to the smooth variety  $Y_{EH}$ . This is quite interesting as  $Y_{EH}$  is not a resolution of singularities of  $\mathbb{C}^3/\mathbb{Z}_4$ ; a morphism  $Y_{EH} \rightarrow \mathbb{C}^3/\mathbb{Z}_4$  exists, but it is 2:1, as we discussed in Section 4.5.4.

## 7 The resolved variety $Y$

As stressed in the previous Section about the chamber structure, for all points of the  $\zeta$  space that do not lay on walls, the topological and algebraic character of the resolution obtained from the Kähler quotient à la Kronheimer is always the same, namely the variety we named  $Y$ . Hence, in order to describe the Kähler Geometry of the resolved variety  $Y \rightarrow \mathbb{C}^3/\mathbb{Z}_4$ , we can utilize any preferred convenient point in  $\zeta$  space that avoids the walls. Furthermore we utilize the crucial information that  $Y$  is the total space of the canonical line bundle over the second Hirzebruch surface  $\mathbb{F}_2$ .

The strategy that we adopt to find the explicit form of the Kähler geometry of the variety  $Y$  is based on the following steps:

1. We choose the realization of the  $Y$  space provided by the Kronheimer construction in the plane  $\zeta_1 = \zeta_3 = a$  and  $\zeta_2 = b \neq 2a$ . In this case, as we know, two of the tautological fiber bundles are identified having  $X_1 = X_3$  and the moment map equations are simpler.
2. We reduce the moment map equations to the compact exceptional divisor (the second Hirzebruch surface) and we obtain a system solvable by radicals whose explicit solution is particularly simple.
3. We obtain the complete solution for the full variety starting from the solution on the Hirzebruch surface and expressing the required fiber metrics  $T_{1,2}$  in terms of a unique function of two variables that is defined as a particular root of a sextic equation.

### 7.1 The two addends of the Kähler potential

First we write the restriction to the hypersurface  $\mathcal{N}_\zeta$  of the Kähler potential of the flat variety  $\text{Hom}(Q \otimes R, R)^{\mathbb{Z}_4}$ . It is the following object.

$$\mathcal{K}_0 = \frac{U(X_2^2 + 1)(X_1^2 + X_3^2) + \Sigma(X_2^3 + X_2 + X_1 X_3(X_1^2 + X_3^2))}{X_1 X_2 X_3} \quad (7.1)$$

As we know from eq. (3.14) the final Kähler potential of the resolved variety is of the form

$$\mathcal{K} = \mathcal{K}_0 + \mathcal{K}_{\log} \quad (7.2)$$

where

$$\mathcal{K}_{\log} \equiv \sum_{I=1}^3 \sum_{J=1}^3 \zeta_I \mathfrak{e}^{IJ} \log[X_J]^{\alpha_\zeta} \quad (7.3)$$

is the logarithmic part of the Kähler potential that contains the information on the tautological bundle Chern classes. The matrix  $\mathfrak{e}^{IJ}$  is defined by

$$\mathfrak{e}^{IJ} = \text{Tr}(\tau^I \tau^J) = \begin{pmatrix} 2 & -1 & 0 \\ -1 & 2 & -1 \\ 0 & -1 & 2 \end{pmatrix} = \text{Cartan matrix of } \mathfrak{a}_3 \quad (7.4)$$

where  $\tau^I$  are the generators of the  $U(1) \times U(1) \times U(1)$  gauge group  $\mathcal{F}_{\mathbb{Z}_4}$  in the  $4 \times 4$  dimensional representation corresponding to the regular representation of  $\mathbb{Z}_4$  advocated by the Kronheimer construction. Next, according to the general strategy outlined at the beginning of this Section we extract the Kähler geometry induced on the

compact exceptional divisor by the Kronheimer–like crepant resolution of the orbifold singularity.

Explicitly, we derive the Kähler potential of the Hirzebruch surface from the Kähler quotient construction when

$$\zeta_1 = \zeta_3 = a \quad ; \quad \zeta_2 = b \neq 2a. \quad (7.5)$$

### 7.1.1 Reduction to the compact exceptional divisor of the moment map equations

The final form of the moment map equations in the coordinates (6.4) was given above in eq. (6.8). After some experiments we found that a convenient point in chamber number 2 is

$$\zeta_1 = \zeta_3 = \frac{1}{2} \quad ; \quad \zeta_2 = 2. \quad (7.6)$$

If we choose such values for the moment map levels and furthermore if we set  $T_3 = T_1$ , as indeed we must do in this case, the system (6.8) reduces to

$$\begin{pmatrix} 0 \\ -2\delta T_1^4 + T_1^2 T_2 + \delta \sigma^2 T_2 (1 + \lambda^4 T_2^2) \\ -2T_1^2 T_2 - (2T_1^2 + \delta \sigma^2 T_2) (-1 + \lambda^4 T_2^2) \end{pmatrix} = \begin{pmatrix} 0 \\ 0 \\ 0 \end{pmatrix}. \quad (7.7)$$

## 7.2 Exact solution of the moment map equations

Let us consider the following six order algebraic equation for an unknown  $F$ :

$$\begin{aligned} \mathfrak{P}(F) \equiv & 2 + F(-5 - \varpi) + F^2(3 - 2\mathcal{U}) + 2F^6\mathcal{U}^3 + F^3(2\mathcal{U} + 2\varpi\mathcal{U}) \\ & + F^4(\mathcal{U} - 2\mathcal{U}^2) + F^5(3\mathcal{U}^2 - \varpi\mathcal{U}^2) = 0 \end{aligned} \quad (7.8)$$

The coefficients of the above equations are written in terms of the two quantities:

$$\varpi = \delta^2 \sigma^2 = (1 + |u|^2)^2 |v|^2 \quad ; \quad \mathcal{U} = \lambda^4 = |w|^2 \quad (7.9)$$

which depend on the toric coordinates  $u, v, w$  of the variety  $Y$ . Since  $w = 0$  is the equation of the compact component of the exceptional divisor, which is isomorphic to the second Hirzebruch surface  $\mathbb{F}_2$ , it follows that  $u, v$  are coordinates of  $\mathbb{F}_2$ . Furthermore taking into account the fibered structure of  $\mathbb{F}_2 \rightarrow \mathbb{P}_1$  which is a  $\mathbb{P}_1$ -bundle over  $\mathbb{P}_1$ ,  $u$  is a coordinate for the  $\mathbb{P}_1$  basis while  $v$  is a coordinate for the  $\mathbb{P}_1$  fiber.

Equation (7.9) has six roots that implicitly define as many functions of  $\varpi, \mathcal{U}$ . The sextic polynomial  $\mathfrak{P}(F)$  has the important property that for  $\varpi > 0$  and  $\mathcal{U} > 0$  there are always two real roots and two pairs of complex conjugate roots. Hence the largest real root is a unique identification of one of the six roots. We unambiguously define a function  $\mathfrak{F}(\varpi, \mathcal{U})$  by saying that it is the largest real root of equation (4)

$$\mathfrak{F}(\varpi, \mathcal{U}) \equiv \text{largest real root of } \mathfrak{P}(F). \quad (7.10)$$

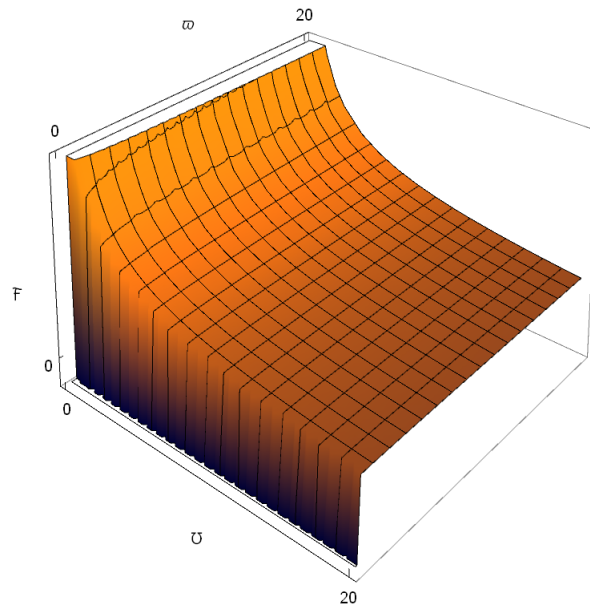


Figure 15: Plot of the function  $\mathfrak{F}(\varpi, \mathcal{U})$

The exact solution of the moment map equations can be written as follows:

$$\begin{aligned}
T_1 &= \sqrt{\frac{\mathfrak{F}}{2\delta}} \left( -\varpi + \mathfrak{F}^2(3+2\varpi)\mathcal{U} + 2\mathfrak{F}^5\mathcal{U}^3 - 2(1+\mathcal{U}) + \mathfrak{F}^4\mathcal{U}^2(3-\varpi+2\mathcal{U}) \right. \\
&\quad \left. + \mathfrak{F}^3\mathcal{U}(1+\mathcal{U}-\varpi\mathcal{U}) + \mathfrak{F}(3+\mathcal{U}+\varpi\mathcal{U}) \right)^{\frac{1}{2}} \\
T_2 &= \mathfrak{F}
\end{aligned} \tag{7.11}$$

where by  $\mathfrak{F}$  we obviously mean  $\mathfrak{F}(\varpi, \mathcal{U})$ .

### 7.2.1 Properties of the function $\mathfrak{F}(\varpi, \mathcal{U})$

The function  $\mathfrak{F}(\varpi, \mathcal{U})$  is well defined and it can be developed in power series of the parameter  $\mathcal{U}$ :

$$\mathfrak{F}(\varpi, \mathcal{U}) = \sum_{n=0}^{\infty} \mathfrak{F}_n(\varpi) \mathcal{U}^n \tag{7.12}$$

We display the first two terms of this development:

$$\begin{aligned}
\mathfrak{F}_0(\varpi) &= \frac{1}{6} \left( 5 + \varpi + \sqrt{1 + 10\varpi + \varpi^2} \right) \\
\mathfrak{F}_1(\varpi) &= - \left( \left( \left( 5 + \varpi + \sqrt{1 + \varpi(10 + \varpi)} \right)^2 \left( 7 + 11\sqrt{1 + \varpi(10 + \varpi)} \right) \right. \right. \\
&\quad \left. \left. + \varpi \left( 46 + 7\varpi + 7\sqrt{1 + \varpi(10 + \varpi)} \right) \right) \right) / \left( 648\sqrt{1 + \varpi(10 + \varpi)} \right)
\end{aligned} \tag{7.13}$$

The function  $\mathfrak{F}(\varpi, \mathcal{U})$  can also be plotted and its behavior is displayed in fig. 15.

### 7.3 Induced Kähler geometry of the exceptional divisor $D_c \sim \mathbb{F}_2$

Next we study the Kähler geometry of the compact exceptional divisor induced by the Kronheimer construction of the Kähler geometry of  $Y$ .

### 7.3.1 Solution of the moment map equations reduced to the compact exceptional divisor

If we perform the limit  $\lambda \rightarrow 0$  in the moment map equations (7.9) we reduce them to compact exceptional divisor, namely to second Hirzebruch surface

$$\begin{pmatrix} 0 \\ -2\delta T_1^4 + (\delta\sigma^2 + T_1^2) T_2 \\ \delta\sigma^2 T_2 - T_1^2 (-2 + 2T_2) \end{pmatrix} = \begin{pmatrix} 0 \\ 0 \\ 0 \end{pmatrix} \quad (7.14)$$

The system (7.14) has five different solutions but the only one that is positive real both for  $T_1$  and  $T_2$  is the following one:

$$\begin{aligned} T_1 &= \frac{1}{2} \sqrt{\frac{1 + \delta^2 \sigma^2 + \sqrt{1 + 10\delta^2 \sigma^2 + \delta^4 \sigma^4}}{\delta}} \\ T_2 &= \frac{1}{6} \left( 5 + \delta^2 \sigma^2 + \sqrt{1 + 10\delta^2 \sigma^2 + \delta^4 \sigma^4} \right) \end{aligned} \quad (7.15)$$

This in terms of the invariants reads as follows:

$$\begin{aligned} T_1|_{\mathbb{F}_2} &= \frac{1}{2} \sqrt{\frac{1 + \varpi + \sqrt{1 + 10\varpi + \varpi^2}}{\delta}}; \\ T_2|_{\mathbb{F}_2} &= \frac{1}{6} \left( 5 + \varpi + \sqrt{1 + 10\varpi + \varpi^2} \right) = \mathfrak{F}_0(\varpi) \end{aligned} \quad (7.16)$$

Comparing with eqs. (7.13) and (7.11) we see that indeed the reduction to the compact exceptional divisor of the solution corresponds to the zero-th order terms in the series expansion in  $\mathcal{U}$ .

### 7.3.2 Derivation of the Kähler potential of $\mathbb{F}_2$ .

In order to study the Kähler geometry we have first to calculate the Kähler potential. Performing the substitutions (6.6) and (6.5) in  $\mathcal{K}_0$  as defined by equation (7.1), substituting the solution (7.11) for  $T_{1,2}$  and performing the limit  $\lambda \rightarrow 0$ , namely  $\mathcal{U} \rightarrow 0$ , we obtain:

$$\mathcal{K}_0|_{\mathbb{F}_2} = \frac{3 + 7\varpi + 3\sqrt{1 + 10\varpi + \varpi^2}}{1 + \varpi + \sqrt{1 + 10\varpi + \varpi^2}}. \quad (7.17)$$

For the logarithmic part of the Kähler potential defined in eq. (7.3) we have instead

$$\mathcal{K}_{\log}|_{\mathbb{F}_2} \equiv \frac{\kappa_1}{2} \log \left[ \frac{1}{2} \sqrt{\frac{1 + \varpi + \sqrt{1 + 10\varpi + \varpi^2}}{\delta}} \right] + \kappa_2 \log \left[ \frac{1}{6} \left( 5 + \varpi + \sqrt{1 + 10\varpi + \varpi^2} \right) \right]. \quad (7.18)$$

The parameters  $\kappa_{1,2}$  have been introduced to keep track of the consequences of the pairing matrix  $\mathfrak{C}_{IJ}$  choice.

**The Kähler potential in polar coordinates.** The final outcome of the above construction is that the Kähler potential of the metric induced on the second Hirzebruch surface is the following one

$$\mathcal{K}_{\mathbb{F}_2} = J(\rho, r, \kappa_1, \kappa_2) \quad (7.19)$$

where  $\rho$  and  $r$ , defined in eq. (6.10) are the norms of the two complex coordinates and the function  $J(\rho, r, \kappa_1, \kappa_2)$  is the following explicit one:

$$\begin{aligned}
J(\rho, r, \kappa_1, \kappa_2) = & \frac{3 + 7r^2(1 + \rho^2)^2 + 3\sqrt{1 + 10r^2(1 + \rho^2)^2 + r^4(1 + \rho^2)^4}}{1 + r^2(1 + \rho^2)^2 + \sqrt{1 + 10r^2(1 + \rho^2)^2 + r^4(1 + \rho^2)^4}} \\
& + \frac{\kappa_1}{2} \log \left[ \frac{1}{2} \sqrt{\frac{1 + r^2(1 + \rho^2)^2 + \sqrt{1 + 10r^2(1 + \rho^2)^2 + r^4(1 + \rho^2)^4}}{1 + \rho^2}} \right] \\
& + \kappa_2 \log \left[ \frac{1}{6} \left( 5 + r^2(1 + \rho^2)^2 + \sqrt{1 + 10r^2(1 + \rho^2)^2 + r^4(1 + \rho^2)^4} \right) \right]
\end{aligned} \tag{7.20}$$

### 7.3.3 Calculation of the Kähler metric and of the Ricci tensor of $\mathbb{F}_2$

From the above data we can calculate the Kähler metric, the Kähler 2-form and also the determinant of the metric which finally yields the Ricci tensor and the Ricci 2-form. We performed this calculation utilizing a MATHEMATICA code and in the following lines we present these results. The best way to display them is in terms of polar coordinates, namely performing the transformation

$$u = \exp[i\theta]\rho \quad ; \quad v = \exp[i\psi]r \tag{7.21}$$

**The Kähler 2-form.** We do not display the explicit form of the Kähler metric since it is too long and messy. As usual it is just given by the derivatives with respect to the original complex coordinates of the Kähler potential:

$$g_{IJ^*} = \partial_i \partial_{j^*} J(\rho, r, \kappa_1, \kappa_2) \quad ; \quad z_i \equiv \{u, v\} \quad ; \quad \bar{z}_{j^*} \equiv \{\bar{u}, \bar{v}\} ; \tag{7.22}$$

once transformed to the polar coordinates  $\rho, r, \theta, \psi$  the Kähler form has the following structure:

$$\begin{aligned}
\mathbb{K} = & \mathbb{K}_{r\theta} dr \wedge d\theta + \mathbb{K}_{r\rho} dr \wedge d\rho - \mathbb{K}_{\psi r} dr \wedge d\psi \\
& + \mathbb{K}_{\theta\rho} d\theta \wedge d\rho - \mathbb{K}_{\psi\theta} d\theta \wedge d\psi + \mathbb{K}_{\rho\psi} d\rho \wedge d\psi
\end{aligned} \tag{7.23}$$

where the explicit form of the components calculated by the MATHEMATICA code are also too long and messy to be displayed.

**The Ricci tensor and the Ricci 2-form** Using the same MATHEMATICA code we have calculated the Ricci tensor of the above metric defined by:

$$R_{ij^*} = \partial_i \partial_{j^*} \log[\text{Det}[g]] \tag{7.24}$$

and the Ricci 2-form defined by

$$\mathbb{R}ic = -\frac{i}{2\pi} R_{ij^*} dz^i \wedge d\bar{z}^{j^*} = \frac{i}{2\pi} \bar{\partial} \partial \log[\text{Det}[g]] \tag{7.25}$$

Once transformed to polar coordinates the Ricci 2-form has the same structure as the Kähler 2-form, namely

$$\begin{aligned}\mathbb{R}ic &= \mathbb{R}ic_{r\theta}dr \wedge d\theta + \mathbb{R}ic_{r\rho}dr \wedge d\rho - \mathbb{R}ic_{\psi r}dr \wedge d\psi + \mathbb{R}ic_{\theta\rho}d\theta \wedge d\rho \\ &- \mathbb{R}ic_{\psi\theta}d\theta \wedge d\psi + \mathbb{R}ic_{\rho\psi}d\rho \wedge d\psi\end{aligned}\quad (7.26)$$

The explicit form of the components of  $\mathbb{R}ic$  is even more massive than those of the Kähler 2-form and cannot be exhibited. An important issue is whether the constructed Kähler metric might be a Kähler-Einstein metric, namely whether the Ricci tensor might be proportional to the metric coefficients. However it is well known that Hirzebruch surfaces cannot carry Kähler-Einstein metrics [4]. An easy way of checking this fact is to note that, since the Ricci form represents the first Chern class of the tangent bundle to the Hirzebruch surface, we have

$$\int_{C_1} \mathbb{R}ic = \int_{C_1} c_1(T_{\mathbb{F}_2}) = 2H \cdot C_1 = 0, \quad (7.27)$$

where  $H$  is the divisor described in Sections 4.3.4 and 4.3.5, while on the other hand the integral of Kähler form on the curve  $C_1$  is of course positive; note that one also must have:

$$\int_{C_2} \mathbb{R}ic = 2H \cdot C_2 = 2. \quad (7.28)$$

To check the robustness of our computations we verified explicitly these equations, as we show below.

**Reduction to the homology cycle  $C_1$ .** The reduction to the homology cycle  $C_1$  is obtained by setting  $r = \psi = 0$  together with the vanishing of their differentials. Applying such a procedure to the Kähler 2-form and to the Ricci 2-form we obtain:

$$\mathbb{K}|_{C_1} = -\kappa_1 \frac{\rho d\rho \wedge d\theta}{4\pi(1+\rho^2)^2} \quad ; \quad \mathbb{R}ic|_{C_1} = 0 \quad (7.29)$$

This confirms eq. (7.27).

**Period of the Kähler two form on  $C_1$ .** Next we can calculate the period of the Kähler form on  $C_1$  and we obtain:

$$\int_{C_1} \mathbb{K} = - \int_0^{2\pi} d\theta \int_0^\infty \frac{\kappa_1 \rho}{4\pi(1+\rho^2)^2} d\rho = -\frac{\kappa_1}{4} \quad (7.30)$$

**Period of the Kähler two form on  $C_2$ .** Here we calculate the restriction of the Kähler 2-form to the homology cycle  $C_2$  and we obtain

$$\mathbb{K}|_{C_2} = - (f_0(r) + \kappa_1 f_1(r) + \kappa_2 f_2(r)) dr \wedge d\psi \quad (7.31)$$

where

$$\begin{aligned}f_0(r) &= \frac{r \left( r^6 - \left( \sqrt{r^4 + 10r^2 + 1} - 15 \right) r^4 + \left( 27 - 10\sqrt{r^4 + 10r^2 + 1} \right) r^2 - \sqrt{r^4 + 10r^2 + 1} + 5 \right)}{2\pi (r^4 + 10r^2 + 1)^{3/2}} \\ f_1(r) &= \frac{3r(r^2 + 1)}{4\pi (r^4 + 10r^2 + 1)^{3/2}} \\ f_2(r) &= \frac{r(5r^2 + 1)}{\pi (r^4 + 10r^2 + 1)^{3/2}}\end{aligned}\quad (7.32)$$

We find

$$\int_0^\infty f_1(r) dr = -\frac{1}{4} \quad ; \quad \int_0^\infty f_2(r) dr = -1 \quad ; \quad \int_0^\infty f_0(r) dr = 0 \quad (7.33)$$

So that the period of the Kähler 2-form on  $C_2$  is the following one:

$$\int_{C_2} \mathbb{K} = \frac{\kappa_1}{4} + \kappa_2. \quad (7.34)$$

Recalling eq. (7.3), and with the present choice of  $\zeta$ , the values of  $\kappa_1$  and  $\kappa_2$  are

$$\kappa_1 = -4\alpha, \quad \kappa_2 = 3\alpha,$$

so that the volumes of  $C_1$  and  $C_2$  are

$$\int_{C_1} \mathbb{K} = \alpha, \quad \int_{C_2} \mathbb{K} = 2\alpha,$$

As we have previously discussed, we choose  $\alpha = 2$  so that the periods of the tautological bundles are all integral.

In a similar way we calculated the period of the Ricci 2-form on  $C_2$  and as it was expected we found:

#### 7.4 The isometry group of the second Hirzebruch surface and of the full resolution $Y$

The Kähler potential is function only of the following combination

$$\varpi = |v|^2 \left( 1 + |u|^2 \right)^2. \quad (7.35)$$

Given an element of  $SU(2)$ , namely a  $2 \times 2$  matrix

$$\gamma = \begin{pmatrix} a & b \\ c & d \end{pmatrix}; \quad ad - bc; \quad \gamma^\dagger = \gamma^{-1}, \quad (7.36)$$

the object  $\varpi$  is invariant under the holomorphic transformation

$$(u, v) \longrightarrow \left( \frac{au + b}{cu + d}, v(cu + d)^2 \right). \quad (7.37)$$

According to the description we give in the Appendix, the coordinate  $(u, t)$  transform as follows:

$$(u, t) \longrightarrow \left( \frac{au + b}{cu + d}, t(cu + d)^{-2} \right). \quad (7.38)$$

Hence we conclude that the coordinate  $t$  spanning the fiber in the Hirzebruch surface is related with the toric coordinate  $v$  by

$$t = \frac{1}{v} \quad (7.39)$$

It is also evident that the complete isometry group of the Kähler metric  $\mathbb{K}$  is  $SU(2) \times U(1)$ , where  $SU(2)$  acts as in eq. (7.37), while  $U(1)$  is simply the phase transformation of  $v$ . This is inherited by the Kähler metric of the full variety  $Y$ . Actually in the case of  $Y$  the isometry group extends by means of an extra  $U(1)$  factor

corresponding to the phase transformation of the coordinate  $w$  spanning the fiber of the line bundle  $Y \longrightarrow \mathbb{F}_2$ :

$$\text{Iso}_Y = \text{SU}(2) \times \text{U}(1) \times \text{U}(1). \quad (7.40)$$

## 7.5 Ricci-flat metrics on $Y$

All smooth resolutions of singularities of  $\mathbb{C}^3/\Gamma$ , where  $\Gamma$  acts as a subgroup of  $\text{SU}(3)$ , carry Ricci-flat Kähler metrics, as proved in [41]. Therefore, the variety  $Y$  carries a Ricci-flat metric — actually, as  $\dim H^2(Y, \mathbb{Q}) = 2$ , it carries a 2-parameter family of such metrics. However *one should not expect* the metric coming from the generalized Kronheimer construction to be one of these metrics; we shall check this point in calculations that will appear in a future publication [5]. Moreover, as the action of  $\mathbb{Z}_4$  on  $\mathbb{C}^3 - \{0\}$  is not free (all points of the  $z$  axis have a  $\mathbb{Z}_2$  isotropy, compare discussion in Section 4.5.4), the Ricci-flat metrics are not ALE; they do have a suitable asymptotically Euclidean behaviour away from the singular locus, but as the latter is not compact, their asymptotics is more complicated than that of an ALE metric (these metrics have been called “QALE” by Joyce).

## 8 The partial resolution $Y_3$ and its Kähler geometry

In this Section we construct the Kähler Geometry of the partial desingularization  $P_3$  of the quotient  $\mathbb{C}^3/\mathbb{Z}_4$  that occurs at some walls of the  $\zeta$  space; the computations suggest that the partial desingularization  $P_3$  is again the total space of a line bundle, this time over a singular variety  $Q_2$ . Actually  $P_3$  is  $Y_3$ , one of the degenerations arising in our toric analysis, and the base variety  $Q_2$  is the weighted projective space  $\mathbb{P}[1,1,2]$ .

The strategy that we adopt is analogous to that utilized for the nondegenerate variety  $Y$  and it goes along the following steps:

1. We choose the partial desingularization space  $P_3$  provided by the Kronheimer construction in the plane  $\zeta_1 = \zeta_3 = a, \zeta_2 = 2a$ .
2. Reducing the moment map equations to the compact exceptional divisor (the singular surface  $Q_2$ ) we obtain a system solvable by radicals and the explicit solution is particularly simple.
3. We obtain the complete solution for the full variety starting from the solution on the  $Q_2$  surface and expressing the sought-for fiber metrics  $T_{1,2}$  as power series in the coordinate  $w$  that represents the section of the line bundle over  $Q_2$ .

### 8.1 Construction of the Kähler geometry of $Q_2$

With the same logic utilized in the case of the full resolution we begin with the analysis of the Kähler Geometry of the singular base manifold  $Q_2$  of the line bundle  $P_3 \longrightarrow Q_2$ . Our main weapon in this analysis is the reduction of the algebraic system of moment map equation to the exceptional divisor by means of the limit  $\lambda \longrightarrow 0$ . We construct the Kähler potential of  $Q_2$  performing the limit  $\lambda \longrightarrow 0$  both on the nonlogarithmic part of the Kähler potential of the resolution and on the logarithmic one.

### 8.1.1 Construction of the Kähler potential

We choose the following special point on the chamber wall  $\mathscr{W}_1$

$$\zeta_1 = 1, \quad \zeta_3 = 1, \quad \zeta_2 = 2 \quad (8.1)$$

so that the system in eq. (6.8) becomes

$$\begin{pmatrix} (-1 - \lambda^4 T_2^2 - \delta T_1 T_3) (T_1^2 - T_3^2) \\ \delta (\sigma^2 T_2 + \lambda^4 \sigma^2 T_2^3 - T_1 T_3 (T_1^2 + T_3^2)) \\ -2T_1 T_2 T_3 - (-1 + \lambda^4 T_2^2) (T_1^2 + \delta \sigma^2 T_2 + T_3^2) \end{pmatrix} = \begin{pmatrix} 0 \\ 0 \\ 0 \end{pmatrix} \quad (8.2)$$

According with what we discussed in Section 6.1 and eq. (3.12) we perform the replacement

$$T_1 = \sqrt{\frac{\sigma}{\lambda}} \frac{\sqrt[4]{Z^3 + Z}}{\sqrt[4]{2}} \quad ; \quad T_2 = \frac{1}{\lambda^2} Z \quad ; \quad T_3 = \sqrt{\frac{\sigma}{\lambda}} \frac{\sqrt[4]{Z^3 + Z}}{\sqrt[4]{2}} \quad (8.3)$$

and introduce the appropriate rescaling

$$Z = \lambda^2 z. \quad (8.4)$$

In this way the system (8.2) becomes

$$\begin{pmatrix} 0 \\ 0 \\ -\sqrt{2} (-1 + z + z^2 \lambda^4) \sqrt{z + z^3 \lambda^4} \sigma + (z \delta - z^3 \delta \lambda^4) \sigma^2 \end{pmatrix} = \begin{pmatrix} 0 \\ 0 \\ 0 \end{pmatrix}. \quad (8.5)$$

Then we reduce the system to the exceptional divisor performing the limit  $\lambda \rightarrow 0$  and we obtain the algebraic equation

$$\sqrt{z} \sigma (\sqrt{2} - \sqrt{2} z + \sqrt{z} \delta \sigma) = 0 \quad (8.6)$$

whose unique everywhere positive real solution is

$$z = \frac{1}{4} \left( 4 + \delta^2 \sigma^2 + \delta \sigma \sqrt{8 + \delta^2 \sigma^2} \right). \quad (8.7)$$

## 8.2 The Kähler potential addends

As in the case of the fully resolved variety  $Y$ , we begin by writing the restriction to the hypersurface  $\mathcal{N}_\zeta$  of the Kähler potential of the flat variety  $\text{Hom}(Q \otimes R, R)^{\mathbb{Z}_4}$ . Inserting the above choices in eq. (7.40) we obtain

$$\mathcal{K}_0 = \frac{2 + 2z^2 \lambda^4 + 2\sqrt{2} \sqrt{z + z^3 \lambda^4} \delta \sigma}{z} \quad (8.8)$$

For the logarithmic part of the Kähler potential we have

$$\mathcal{K}_{\log} \equiv \zeta_I \mathfrak{C}^{IJ} \log [X_J]^{\alpha_{\zeta_J}} \quad (8.9)$$

with the above choices and disregarding addends  $\log[\lambda]$  since  $\lambda$  is a modulus square of a holomorphic function, we find:

$$\mathcal{K}_{\log} = 2\alpha_{\zeta_2} \log [T_2] = 2\alpha_{\zeta_2} \log [z] \quad (8.10)$$

so that

$$\mathcal{H} = \frac{2 + 2z^2\lambda^4 + 2\sqrt{2}\delta\sigma\sqrt{z + z^3\lambda^4}}{z} + 2\alpha_{\zeta_2} \log[z] \quad (8.11)$$

This determines the Kähler geometry of the singular variety  $P_3$ , provided we are able to write the appropriate positive real solution  $z = \hat{\mathfrak{F}}(\lambda, \delta\sigma)$  of the moment map equation (8.5).

### 8.2.1 The Kähler potential of $Q_2$

Performing the limit  $\lambda \rightarrow 0$  and substituting for  $z$  the solution of the reduced moment map equations presented in eq. (8.7) we obtain the Kähler potential of the divisor  $Q_2$ :

$$\begin{aligned} \mathcal{H}|_{Q_2} = & \frac{2 \left( 4 + 2\sqrt{2}\delta\sigma\sqrt{4 + \delta\sigma(\delta\sigma + \sqrt{8 + \delta^2\sigma^2})} \right)}{4 + \delta\sigma(\delta\sigma + \sqrt{8 + \delta^2\sigma^2})} \\ & + 2\alpha_{\zeta_2} \log \left[ \frac{1}{4} \left( 4 + \delta\sigma(\delta\sigma + \sqrt{8 + \delta^2\sigma^2}) \right) \right] \end{aligned} \quad (8.12)$$

Naming

$$T = \delta\sigma = r(1 + \rho^2) \quad ; \quad W = \frac{1}{4} \left( 4 + T \left( T + \sqrt{8 + T^2} \right) \right) \quad (8.13)$$

where, just as before,

$$r = |v| \quad ; \quad \rho = |u| \quad (8.14)$$

the result (8.12) can be rewritten in the following much simpler form:

$$\mathcal{H}|_{Q_2} = 4 - \frac{2}{W} + 2\alpha_{\zeta_2} \log[W] \approx -\frac{2}{W} + 2\alpha_{\zeta_2} \log[W] \quad (8.15)$$

From these data one can compute the Kähler metric; when  $\alpha_{\zeta_2} = 1$  this takes the particularly simple form

$$g_{ij}^* = \begin{pmatrix} \frac{2r \left( r + \frac{2\sqrt{2}}{\sqrt{W}} \right)}{1 + W} & \frac{2\sqrt{2}e^{-i(\theta-\psi)}\rho}{\sqrt{W}(1+W)} \\ \frac{2\sqrt{2}e^{i(\theta-\psi)}\rho}{\sqrt{W}(1+W)} & \frac{2(-1+W)}{r^2(W+W^2)} \end{pmatrix} \quad (8.16)$$

where  $\theta$  and  $\psi$  are the phases of  $u$  and  $v$ , respectively. This is enough for our purposes since the periods we are interested in scale multiplicatively with respect to  $\alpha_{\zeta_2}$ .

### 8.2.2 The determinant of the Kähler metric and the Ricci tensor

Calculating the determinant of  $g_{ij}^*$  we find

$$\det[g] = \frac{4}{W + W^2} \quad (8.17)$$

then calculating the Ricci tensor we obtain:

$$\begin{aligned}
\text{Ric}_{11^*} &= -\frac{(-1+W)W(1+5W)}{r^2(1+W)^4} \\
\text{Ric}_{12^*} &= -\frac{\sqrt{2}e^{i(\theta-\psi)}W^{3/2}(1+5W)\rho}{(1+W)^4} \\
\text{Ric}_{21^*} &= -\frac{\sqrt{2}e^{-i(\theta-\psi)}W^{3/2}(1+5W)\rho}{(1+W)^4} \\
\text{Ric}_{22^*} &= \frac{1}{\sqrt{2}\sqrt{W}(1+W)^5}r(140-4W(70+W(-34+W(6+5W)))) \\
&\quad + \sqrt{2}r\sqrt{W}(140+W(-139+W(4+W-2W^2))) \\
&\quad - 70r^2W(-1+\rho^4)
\end{aligned} \tag{8.18}$$

Again, from here we can see that the constructed metric is not Kähler-Einstein.

Next considering the transformation to polar coordinates

$$u = e^{i\theta}\rho \quad ; \quad v = e^{i\psi}r \tag{8.19}$$

we write out the form of the Kähler 2-form explicitly:

$$\begin{aligned}
\mathbb{K} &= \frac{2\sqrt{2}\rho^2 dr \wedge d\theta}{\pi\sqrt{W}(1+W)} + \frac{2(-1+W)dr \wedge d\psi}{\pi r W(1+W)} \\
&\quad - \frac{2r(2\sqrt{2}+r\sqrt{W})\rho d\theta \wedge d\rho}{\pi\sqrt{W}(1+W)} + \frac{2\sqrt{2}r\rho d\rho \wedge d\psi}{\pi\sqrt{W}(1+W)}
\end{aligned} \tag{8.20}$$

### 8.2.3 Calculations of periods of the Kähler 2-form on homology cycles

Starting from eq. (8.19) we can calculate the periods of the Kähler 2-form on the homology cycles  $C_1$  and  $C_2$ . This allows one to get a clear picture of the degeneration of the  $Y$  variety, showing which cycles in  $Y_3$  shrink to a vanishing volume.

**Cycle  $C_1$ .** Setting  $r = 0$  and  $\psi = 0$  we obtain the reduction of the Kähler 2-form to the cycle  $C_1$ . Expanding in power series of  $r$  around  $r = 0$  we obtain

$$\mathbb{K} = -\frac{2(\sqrt{2}\rho d\theta \wedge dr)r}{\pi} + \mathcal{O}(r^2) \tag{8.21}$$

It follows that for  $r = 0$  (equation of the cycle  $C_1$ ) the Kähler 2-form goes to zero, namely the  $C_1$  cycle shrinks to zero.

**Cycle  $C_2$ .** The reduction to the cycle  $C_2$  is obtained in the limit  $\rho \rightarrow 0$ ,  $\theta \rightarrow 0$ . We obtain

$$\mathbb{K}|_{C_2} = \frac{(4+r^2-r\sqrt{8+r^2})dr \wedge d\psi}{2\pi\sqrt{8+r^2}} \tag{8.22}$$

so that for  $\alpha_{\zeta_j} = 1$  we get

$$\int_{C_2} \mathbb{K} = 2\pi \int_0^\infty \frac{(4+r^2 - r\sqrt{8+r^2})}{2\pi\sqrt{8+r^2}} dr = 2 \quad (8.23)$$

and the result of a generic  $\alpha_{\zeta_j}$  is therefore

$$\mathbb{K}|_{C_2} = 2\alpha_{\zeta_j}.$$

It follows that for  $\rho = 0$  (equation of the cycle  $C_2$ ) the Kähler form has period  $2\alpha_{\zeta_j}$ .

### 8.3 Interpretation

The interpretation of the above results is sufficiently clear. The cycle  $C_1$  is the intersection of the two components of the exceptional divisor  $D_c$  and  $D_{nc}$ , where  $D_c$  is the Hirzebruch surface  $\mathbb{F}_2$  and  $D_{nc} = \mathbb{P}^1 \times \mathbb{C}$ . The vanishing of the cycle  $C_1$  means that the exceptional divisor  $D_{nc}$  has disappeared, while the compact one  $D_c$  remains in the form of the singular variety  $\mathbb{P}[1, 1, 2]$ . This means that  $P_3$  is precisely the partial resolution of the orbifold singularity called  $Y_3$  in Section 4.4.

#### 8.3.1 Periods of the Chern forms $\omega_{1,2,3}$ .

The fiber metrics of the three tautological bundles are for the chosen point of the  $\zeta$  space given by

$$\mathcal{H}_{1,2,3} = \left\{ \alpha_{\zeta_j} \log \left[ \frac{(Z+Z^3)^{1/4}}{2^{1/4}} \right], \alpha_{\zeta_j} \log[Z], \alpha_{\zeta_j} \log \left[ \frac{(Z+Z^3)^{1/4}}{2^{1/4}} \right] \right\} \quad (8.24)$$

substituting  $Z \rightarrow \lambda^2 z$  we obtain:

$$\mathcal{H}_{1,2,3} = \left\{ \frac{1}{4} \alpha_{\zeta_j} \log \left[ \frac{1}{2} (z\lambda^2 + z^3\lambda^6) \right], \alpha_{\zeta_j} \log [z\lambda^2], \frac{1}{4} \alpha_{\zeta_j} \log \left[ \frac{1}{2} (z\lambda^2 + z^3\lambda^6) \right] \right\} \quad (8.25)$$

Performing the reduction to compact exceptional divisor we have;

$$\begin{aligned} \mathcal{H}_{1,2,3} &= \left\{ \alpha_{\zeta_j} \frac{\log[z]}{4}, \alpha_{\zeta_j} \log[z], \alpha_{\zeta_j} \frac{\log[z]}{4} \right\} \\ z &= \frac{1}{4} \left( 4 + r^2 (1 + \rho^2)^2 + r (1 + \rho^2) \sqrt{8 + r^2 (1 + \rho^2)^2} \right). \end{aligned} \quad (8.26)$$

So that for the period integrals, whatever is the supporting cycle, we obtain:

$$\left\{ \int \omega_1, \int \omega_2, \int \omega_3 \right\} = \left\{ \frac{1}{4} \alpha_{\zeta_j} \int \Omega, \alpha_{\zeta_j} \int \Omega, \frac{1}{4} \alpha_{\zeta_j} \int \Omega \right\} \quad ; \quad \Omega = \frac{i}{2\pi} \partial \bar{\partial} \log[z] \quad (8.27)$$

The periods of  $\Omega$  are very easily calculated since in cohomology we have:

$$\alpha_{\zeta_j} [\Omega] = \frac{1}{2} [\mathbb{K}] \quad (8.28)$$

where  $\mathbb{K}$  is the Kähler 2-form. The above equation follows from eq. (8.11) and the observation that the non-logarithmic part of the Kähler potential gives rise to a cohomologically trivial addend in  $\mathbb{K}$ .

Hence we have:

$$\int_{C_1} \Omega = 0 \quad ; \quad \int_{C_2} \Omega = 1 \quad (8.29)$$

In conclusion we have that there is only one independent tautological bundle corresponding to  $\omega_2$  and we have:

$$\int_{C_1} \omega_{1,2,3} = 0 \quad ; \quad \int_{C_2} \omega_2 = \alpha_{\zeta_j} \quad ; \quad \int_{C_2} \omega_{1,3} = \frac{\alpha_{\zeta_j}}{4} \quad ; \quad [\mathbb{K}] = 2[\omega_2]. \quad (8.30)$$

#### 8.4 The Kähler geometry of the singular variety $Y_3$

Let us finally derive the Kähler geometry of the singular threefold  $Y_3$  which is the total space of a line bundle over the singular exceptional divisor  $\mathbb{P}[1,1,2]$ . To this effect let us consider the following sextic equation for an unknown  $F$ , where the coefficients are functions of the same invariants  $\varpi$  and  $\mathcal{U}$  previously defined in eqs. (7.9):

$$\begin{aligned} \mathcal{P}(F) \equiv & 2 + F(-4 - \varpi) + F^2(2 - 2\mathcal{U}) + 2F^3\varpi\mathcal{U} + 2F^6\mathcal{U}^3 + F^4(2\mathcal{U} - 2\mathcal{U}^2) \\ & + F^5(4\mathcal{U}^2 - \varpi\mathcal{U}^2) = 0 \end{aligned} \quad (8.31)$$

Just as in the case of the full variety  $Y$ , the sextic polynomial  $\mathcal{P}(F)$  has the property that, for all positive values of the parameters  $\varpi$  and  $\mathcal{U}$ , it has two positive real roots and four complex roots arranged in two pairs of complex conjugate roots. Hence the largest real root is uniquely identified and singles out a precise function  $\mathfrak{G}(\varpi, \mathcal{U})$  of the parameters:

$$\mathfrak{G}(\varpi, \mathcal{U}) \equiv \text{largest real root of } \mathcal{P}(F). \quad (8.32)$$

The function  $\mathfrak{G}(\varpi, \mathcal{U})$  can be developed in power series of  $\mathcal{U}$  and we have:

$$\begin{aligned} \mathfrak{G}(\varpi, \mathcal{U}) = & \frac{1}{4} \left( 4 + \varpi + \sqrt{\varpi(8 + \varpi)} \right) \\ & \frac{\left( \left( 4 + \varpi + \sqrt{\varpi(8 + \varpi)} \right)^2 \left( 3\varpi^2 + 4\sqrt{\varpi(8 + \varpi)} + \varpi \left( 16 + 3\sqrt{\varpi(8 + \varpi)} \right) \right) \right) \mathcal{U}}{64\sqrt{\varpi(8 + \varpi)}} \\ & + O[\mathcal{U}]^2 \end{aligned} \quad (8.33)$$

In terms of this function and of the above variables the Kähler potential of the complete  $Y_3$  variety takes the form

$$\mathcal{K}_{Y_3} = \frac{2 \left( 1 + \mathfrak{G}^2\mathcal{U} + \sqrt{2}\sqrt{\mathfrak{G}\varpi(1 + \mathfrak{G}^2\mathcal{U})} + \mathfrak{G} \log[\mathfrak{G}] \right)}{\mathfrak{G}} \quad (8.34)$$

The function  $\mathfrak{G}(\varpi, \mathcal{U})$  is displayed in Figure 16.

## 9 Summary of the Chamber Structure Discussion

We can now try to summarize our long and detailed discussion of the chamber structure pertaining to the Kähler quotient resolution à la Kronheimer of the singularity  $\mathbb{C}^3/\mathbb{Z}_4$ .

First of all let us stress that the chamber structure is one of the most relevant aspects of the entire construction from the point of view of any physical application in the context of the gauge/duality correspondence. Indeed the  $\zeta$  parameters are the Fayet-Iliopoulos parameters in the gauge theory side of the correspondence, while they should be retrievable as fluxes of suitable  $p$ -forms on the supergravity side of the correspondence and hence as *parameters of the Ricci flat Kähler metric* existing on the same resolved smooth manifold. Therefore, loosely speaking, the chamber structure is a mathematical synonymous of *Phase Diagram* of the Gauge Theory.

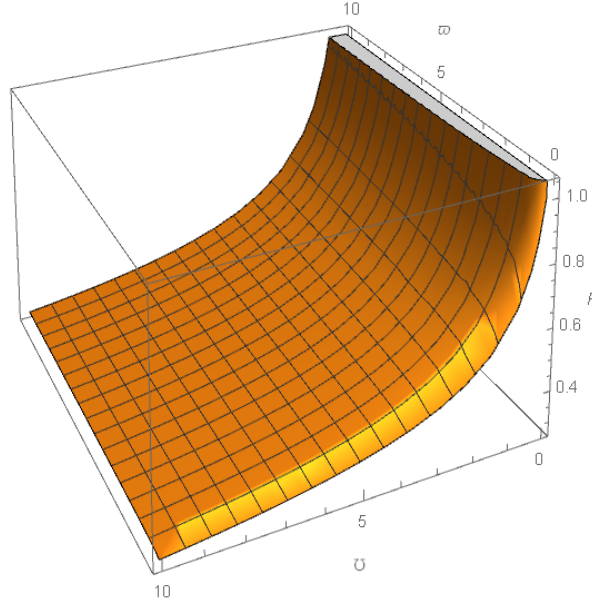


Figure 16: Plot of the function  $\mathfrak{G}(\varpi, \mathcal{U})$ .

Having clarified the physical relevance of the topic, let us state what results we found. The toric analysis of the problem has revealed several possible degenerations of the full resolution  $Y \rightarrow \mathbb{C}^3/\mathbb{Z}_4$ . Only three of such manifolds are realized by the Kähler quotient:

- a) The complete resolution  $Y$ , which happens to be the total space of the canonical line bundle of the compact exceptional divisor  $D_c \simeq \mathbb{F}_2$  where  $\mathbb{F}_2$  is the second Hirzebruch surface. In this case the exceptional divisor has an additional non-compact component  $D_{nc} \simeq \mathbb{P}^1 \times \mathbb{C}$
- b) The partial resolution  $Y_3$  which happens to be the total space of the canonical line bundle over the singular compact exceptional divisor  $D_c \simeq \mathbb{P}[1, 1, 2]$ . In this case the non-compact exceptional divisor  $D_{nc}$  disappears since its compact factor  $\mathbb{P}^1$  shrinks to zero.
- c) The partial resolution  $Y_{EH} = \text{ALE}_{A_1} \times \mathbb{C}$ , which again can be seen as the total space of the canonical line bundle of the noncompact exceptional divisor  $D_{nc}$ . In this case it is the compact exceptional divisor that disappears.

The three aforementioned manifolds are realized in  $\zeta$  space  $\mathbb{R}^3$  in the way we summarize below.

There are four intersecting planar walls  $\mathscr{W}_{0,1,2,3}$  that partition the entire  $\zeta$  space into eight disjoint convex cones (stability chambers).

1. The smooth space  $Y$  is realized in all interior points of all the chambers and in all generic points of the three walls of type 0, namely  $\mathscr{W}_0, \mathscr{W}_1, \mathscr{W}_3$ .
2. The singular space  $Y_3 \rightarrow \mathbb{P}[1, 1, 2]$  is realized in all generic points of the type 1 wall  $\mathscr{W}_2$ . The latter contains the Kampé line and the two Cardano edges that are also realization of  $Y_3$ .
3. The smooth space  $Y_{EH}$  is realized on the homonymous edge, which is the intersection of the wall  $\mathscr{W}_0$  with the wall  $\mathscr{W}_2$ .

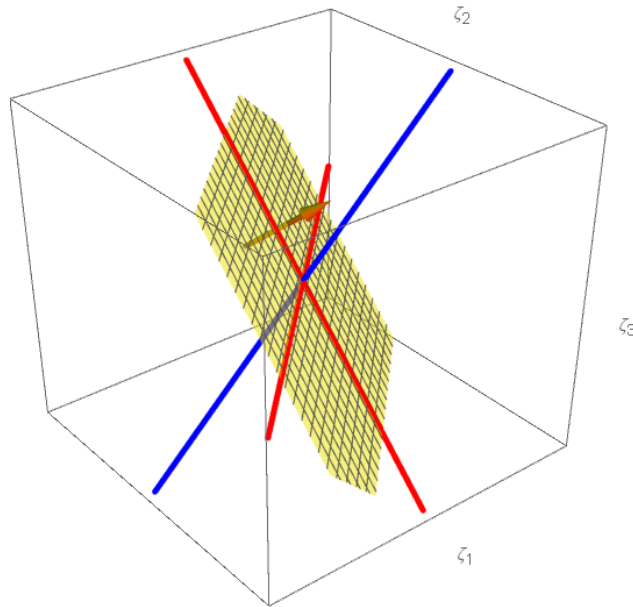


Figure 17: Path crossing the  $\mathscr{W}_2$  wall. The line with an arrowhead shown in this figure is the one we have chosen to create a movie of wall crossing.

**Wall Crossing.** Crossing a wall is the mathematical analog of a physical phase transition. When the wall we cross is of type 0, we simply go from one realization of the  $Y$  manifold to another one. On the two sides of the wall the supporting variety is the same, yet the tautological bundles may be different. On the walls of type 0 we have a third realization of  $Y$ , but the configuration of the tautological line bundles may vary.

Most dramatic is the crossing of a wall of type III. In this case we go from one realization of the  $Y$  manifold to another one passing through a degenerate singular manifold that is located on the wall. There is a simple numerical procedure to visualize such a phenomenon. Let us explain how it works.

Considering the three-dimensional Euclidean space with coordinates  $X_1, X_2, X_3$ , a solution of the moment map system (2.41) defines a two-dimensional surface in this space. This is so because the coefficients of the system depend on the two parameters  $\Sigma, U$ , or alternatively  $\varpi, \upsilon$ . Creating a grid of  $\varpi, \upsilon$ -values we can obtain a picture of the aforementioned two-dimensional surface by interpolating the numerical solutions of the system (2.41) in all points of the grid at fixed  $\zeta$  parameters. Such a picture is like a photograph of a movie. The other photographs of this movie are provided by repeating the same procedure with other  $\zeta$  parameters. The effect of crossing is better visualized when all the photographs are arranged along a line in  $\zeta$  space that crosses the wall and is orthogonal to it.

Let us consider the unique type III wall  $\mathscr{W}_2$  and the line that crosses it orthogonally, displayed in fig.17. Along this line we have numerically constructed a few photographs as previously described. In fig. 18 we display three of them. One before crossing, one on the wall and one after crossing. As it is evident from the figure, just on the wall the surface representing the solution is substituted by a line. This happens because the solution for  $X_1, X_2, X_3$  is expressed in terms of simple functions of single function  $Z(\varpi, \upsilon)$  of the two variables. This obviously yields the parametric equation of a line. We already know this for the Kampé line, where we have eq. (3.12) and the function  $Z$  is defined as a positive real root of the sextic equation (3.31). Actually a similar result applies to all points of the  $\mathscr{W}_2$  plane, namely for:

$$\zeta = \{x, x+y, y\} \tag{9.1}$$

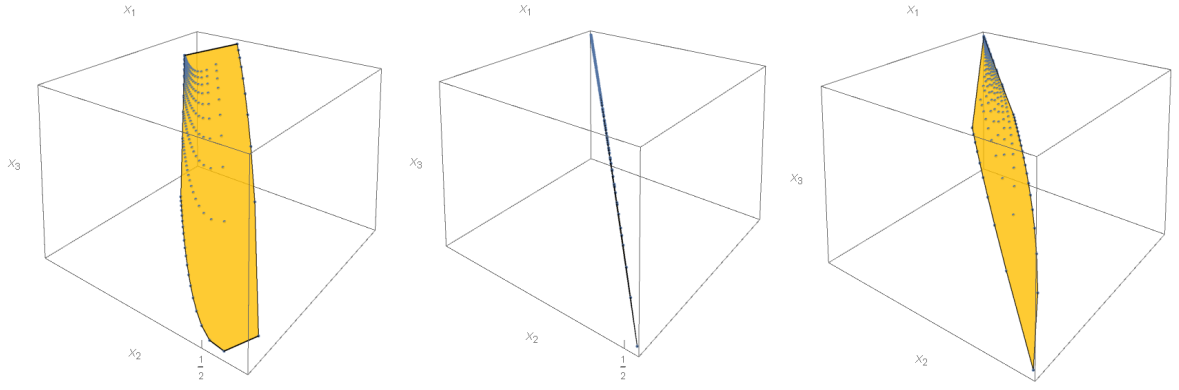


Figure 18: Crossing the  $\mathcal{W}_2$  wall. Before crossing the solution of the algebraic system (2.41) traces a surface in  $\mathbf{X}$  space. After crossing the solution traces another surface. Just on the wall the solution traces a line rather than a surface. This is just the symptom of degeneration of the corresponding manifold.

Indeed we can easily prove by direct substitution that for such a choice of the level parameters the solution of the moment map equations (2.41) can be written as follows:

$$\begin{aligned}
 X_1 &= \sqrt[4]{\frac{Z(xZ^2 + y)^{3/2}}{(x+y)\sqrt{x+yZ^2}}} \\
 X_2 &= Z \\
 X_3 &= \frac{\sqrt[4]{\frac{Z}{x+y}}(x+yZ^2)^{3/8}}{\sqrt[8]{xZ^2 + y}}
 \end{aligned} \tag{9.2}$$

where  $Z$  is, by definition, the real positive solution of the following equation:

$$\frac{U(Z^4 - 1)\sqrt{Z(x+y)}(xZ^2 + y)^{3/4}}{\sqrt[4]{x+yZ^2}} + Z(xZ^2 + y)\left(\sqrt{Z(x+y)}\sqrt[4]{(xZ^2 + y)(x+yZ^2)} + \Sigma(Z^2 - 1)\right) = 0 \tag{9.3}$$

Note that the solution (9.2), (9.3) becomes that of the Kampé manifold (3.12), (3.31) when  $x = y = s$ . Similarly for either  $x = 0$  or  $y = 0$  the solution (9.2), (9.3) degenerates in either version of the solution defining the Cardano manifold. In that case the degree of the equation reduces from six to four allowing for the use of Cardano's formula. This is the conclusive prove that at any point of the type III wall we realize the same manifold  $Y_3$ . Why is it degenerate? The answer is that the very fact that we express all the  $X_I$  in terms of a single function  $Z(\varpi, \bar{v})$  implies that the Chern classes of all the tautological bundles are cohomologous and conversely that the homology group is of dimension 1 rather than two.

## 10 Conclusions

What we have done in this paper was already described at the end of the introductory Section 1 and we do not repeat it here. We rather point out the perspectives opened up by our results and what are the necessary steps that have still to be taken in the development of our program.

As we have advocated, for the sake of the conceivable physical applications in the context of brane theory, of the quotient singularity resolutions, it is quite relevant to understand the explicit analytic structure of the

exceptional divisors and of the homology 2-cycles, having, at the same time, command on the explicit form of the forms  $\omega^{(1,1)}$  representing the first Chern classes of the tautological bundles. In this paper we succeeded in these two tasks because we had two very strong allies:

1. Toric Geometry, applicable to the case of abelian cyclic groups  $\Gamma$ , that allows one to identify the possible full or partial resolutions of the quotient singularity and study in great detail their geometry, determining also the appropriate coordinate transformations leading to the equations of the divisors.
2. The technique of localizing the moment map equations on divisors and curves, which allows for their solutions on these loci.

Furthermore, we were able to clarify the Chamber Structure which, as already stressed, encodes the phase diagram of the corresponding gauge theory.

However it is on the two fronts mentioned above that mathematical work is still needed. Ito-Reid theorem applies in general and in particular to nonabelian groups. An urgent task is the extension of the sort of explicit results obtained in this paper to nonabelian cases. A second urgent task which is equally important for abelian and nonabelian cases is the explicit solution of the moment map equations in cases where the algebraic equation is of degree  $d > 4$ . To this effect a quite valuable help might come from the recent developments in algebraic geometry that represent roots of higher order algebraic equations in terms of theta constants associated with suitable hyperelliptic Riemann surfaces [57]. We plan to study that case.

From the physical side, as we already stated, we plan to utilize the present explicit singularity resolution to study the corresponding supergravity brane solutions and dual gauge theories. In this context the geometrical results obtained here might be the origin of new interesting D3-brane and M2-brane physics. Such applications to the holographic scheme demand the construction of *Ricci flat metrics* on the same manifolds  $Y$  that are derived from the Kronheimer construction and the precise identification of the their deformation parameters with the Fayet-Iliopoulos parameters  $\zeta$ . These questions and issues will be addressed in forthcoming publications [5].

## Acknowledgements

We acknowledge with great pleasure important and illuminating discussions with our colleagues and close friends, Mario Trigiante, Massimo Bianchi, Francisco Morales and Francesco Fucito. U.B. likes to thank CEMPI (Centre Européen pour les Mathématiques, la Physique et leur Interactions) for supporting his visit to Université de Lille in February-March 2019 (Labex CEMPI ANR-11-LABX-0007-01). U.B.'s research is also supported by GNSAGA-INdAM and by the PRIN project “Geometria delle Varietà Algebriche.”

## Appendix: structure of the Hirzebruch surfaces

Let us give some details about the geometry of the second Hirzebruch surface  $\mathbb{F}_2$ , which appears as the compact component of the exceptional divisor of the resolution  $Y \rightarrow \mathbb{C}^3/\mathbb{Z}_4$ .

Let  $(U, V)$  be homogeneous coordinates on  $\mathbb{P}^1$  and  $(X, Y, Z)$  homogeneous coordinates of  $\mathbb{P}^2$ .

**Definition 10.1.** *The  $n$ -th Hirzebruch surface  $\mathbb{F}_n$  is defined as the locus cut out in  $\mathbb{P}^1 \times \mathbb{P}^2$  by the following equation of degree  $n + 1$ :*

$$0 = \mathcal{P}_n(U, V, X, Y, Z) = XU^n - YV^n \quad (10.1)$$

It is convenient to describe the Hirzebruch surface in terms of inhomogeneous coordinates choosing open charts both for  $\mathbb{P}^1$  and for  $\mathbb{P}^2$ . We can cover  $\mathbb{P}^1$  with two charts: that where  $V \neq 0$  and that where  $U \neq 0$ . For  $\mathbb{P}^2$ , we need instead three charts respectively corresponding to  $Z \neq 0, Y \neq 0$  and  $X \neq 0$ . Hence we have a total of six charts.

**Description of  $\mathbb{F}_n$  in the chart  $V \neq 0, Z \neq 0$ .** According with the chosen conditions we set:

$$s = \frac{U}{V} \quad ; \quad v = \frac{X}{Z} \quad ; \quad w = \frac{Y}{Z} \quad (10.2)$$

and from eq. (10.1) we obtain:

$$0 = vs^n - w. \quad (10.3)$$

Introducing a new complex variable  $t$ , a simple parametric description of the locus satisfying the constraint (10.3) is provided by setting:

$$v(u,t) = tu^{-1} \quad ; \quad w(u,t) = tu^{n-1} \quad ; \quad s(u,t) = u \quad (10.4)$$

Hence  $(u,t)$  can be identified with a system of local coordinates on  $\mathbb{F}_n$ . Let us now recall that the group  $SU(2)$  is the isometry group of  $\mathbb{P}^1$  equipped with the Fubini-Study Kähler metric. Given a group element

$$\mathbf{g} = \begin{pmatrix} a & b \\ c & d \end{pmatrix} \in SU(2) \quad (10.5)$$

its action on the coordinate  $u$  (regarded as a coordinate of  $\mathbb{P}^1$ ) is given by the corresponding fractional linear transformation

$$\mathbf{g}(u) = \frac{au+b}{cu+d} \quad (10.6)$$

The action of  $\mathbf{g}$  on the coordinate  $u$  can be extended also to the variable  $t$  in such a way that the image point still belongs to the Hirzebruch surface  $\mathbb{F}_n$ . We just set:

$$\forall \mathbf{g} \in SU(2) \quad : \quad \mathbf{g}(u,t) = \left( \frac{au+b}{cu+d}, \quad t(cu+d)^{-n} \right) \quad (10.7)$$

and we easily verify:

**a)** The transformation (10.7) respects the group product and provides a nonlinear representation since:

$$\mathbf{g}_1(\mathbf{g}_2(u,t)) = \mathbf{g}_1 \cdot \mathbf{g}_2(u,t) \quad (10.8)$$

**b)** The transformation (10.7) maps points of the Hirzebruch surface into points of the same surface since:

$$v(\mathbf{g}(u,t)) (s(\mathbf{g}(u,t)))^n - w(\mathbf{g}(u,t)) = 0 \quad (10.9)$$

if:

$$v(u,t) (s(u,t))^n - w(u,v) = 0 \quad (10.10)$$

On the Hirzebruch surface, as described in the current open chart (which is dense in the manifold), we can introduce nice Kähler metrics that are invariant under the action of  $SU(2)$  as given in eq. (10.7). In Section 7.3

we derive one of them (see eqs. (7.19) and (7.20)) induced on the compact exceptional divisor by the Kähler quotient construction.

## References

- [1] O. AHARONY, O. BERGMAN, D. L. JAFFERIS, AND J. MALDACENA, *N=6 superconformal Chern-Simons-matter theories, M2-branes and their gravity duals*, Journal of High Energy Physics, 2008 (2008), p. 091. doi:10.1088/1126-6708/2008/10/091 [[arXiv:0806.1218](#) [hep-th]].
- [2] D. ANSELMI, M. BILLÒ, P. FRÉ, L. GIRARDELLO, AND A. ZAFFARONI, *ALE manifolds and conformal field theories*, Int. J. Mod. Phys., A9 (1994), pp. 3007–3058.
- [3] M. BERTOLINI, V. L. CAMPOS, G. FERRETTI, P. SALOMONSON, P. FRÉ, AND M. TRIGIANTE, *BPS three-brane solution on smooth ALE manifolds with flux*, Fortsch. Phys., 50 (2002), pp. 802–807.
- [4] A. L. BESSE, *Einstein manifolds*, Classics in Mathematics, Springer-Verlag, Berlin, 2008. Reprint of the 1987 edition.
- [5] M. BIANCHI, U. BRUZZO, P. FRÉ, P. A. GRASSI AND D. MARTELLI, *work in progress*, to appear, (2019).
- [6] M. BIANCHI, F. FUCITO, AND J. F. MORALES, *D-brane instantons on the  $T^{**6}/Z(3)$  orientifold*, JHEP, 07 (2007), p. 038.
- [7] ———, *Dynamical supersymmetry breaking from unoriented D-brane instantons*, JHEP, 08 (2009), p. 040.
- [8] M. BIANCHI, F. FUCITO, AND G. ROSSI, *Instanton effects in supersymmetric Yang-Mills theories on ALE gravitational backgrounds*, Phys. Lett., B359 (1995), pp. 56–61.
- [9] M. BIANCHI, F. FUCITO, G. ROSSI, AND M. MARTELLINI, *ALE instantons in string effective theory*, Nucl. Phys., B440 (1995), pp. 129–170.
- [10] ———, *Explicit construction of Yang-Mills instantons on ALE spaces*, Nucl. Phys., B473 (1996), pp. 367–404.
- [11] M. BIANCHI AND J. F. MORALES, *Anomalies & tadpoles*, JHEP, 03 (2000), p. 030.
- [12] M. BILLÒ, D. FABBRI, P. FRÉ, P. MERLATTI, AND A. ZAFFARONI, *Rings of short  $\mathcal{N} = 3$  superfields in three dimensions and M-theory on  $\text{AdS}_4 \times \text{N}^{010}$* , Classical and Quantum Gravity, 18 (2001), p. 1269. doi:10.1088/0264-9381/18/7/310 [[hep-th/0005219](#)].
- [13] M. BILLÒ AND P. FRÉ, *N=4 versus N=2 phases, hyperKähler quotients and the 2-d topological twist*, Class. Quant. Grav., 11 (1994), pp. 785–848.
- [14] M. BILLÒ, P. FRÉ, L. GIRARDELLO, AND A. ZAFFARONI, *Stringy gravitational instantons, the H map and N=4 moduli deformations*, in International Workshop on String Theory, Quantum Gravity and the Unification of Fundamental Interactions Rome, Italy, September 21-26, 1992, 1992, pp. 28–40.

- [15] ———, *Gravitational instantons in heterotic string theory: The H map and the moduli deformations of (4,4) superconformal theories*, Int. J. Mod. Phys., A8 (1993), pp. 2351–2418.
- [16] M. BILLÒ, P. FRÉ, A. ZAFFARONI, AND L. GIRARDELLO, *Heterotic vacua including gravitational instantons*, in 10th Italian Conference on General Relativity and Gravitational Physics (It will include 4 workshops to take place in parallel sessions) Bardonecchia, Italy, September 1-5, 1992, 1992, pp. 601–606.
- [17] V. BOUCHARD, *Orbifold Gromov-Witten invariants and topological strings*, in Modular forms and string duality, vol. 54 of Fields Inst. Commun., Amer. Math. Soc., Providence, RI, 2008, pp. 225–246.
- [18] U. BRUZZO, A. FINO, AND P. FRÉ, *The Kähler Quotient Resolution of  $\mathbb{C}^3/\Gamma$  singularities, the McKay correspondence and  $D=3$   $\mathcal{N}=2$  Chern-Simons gauge theories*, Commun. Math. Phys., 365 (2019), pp. 93–214.
- [19] A. CERESOLE, G. DALL’AGATA, R. D’AURIA, AND S. FERRARA, *Spectrum of type IIB supergravity on  $AdS_5 \times T^{11}$ : predictions on  $\mathcal{N}=1$  SCFT’s*, Physical Review D, 61 (2000), p. 066001. [[hep-th/9905226](#)].
- [20] D. A. COX, J. B. LITTLE, AND H. K. SCHENCK, *Toric varieties*, vol. 124 of Graduate Studies in Mathematics, American Mathematical Society, Providence, RI, 2011.
- [21] A. CRAW, *The McKay correspondence and representations of the McKay quiver*, PhD thesis, Warwick University, United Kingdom, 2001.
- [22] ———, *An explicit construction of the McKay correspondence for A-Hilb  $\mathbb{C}^3$* , J. Algebra, 285 (2005), pp. 682–705.
- [23] A. CRAW AND A. ISHII, *Flops of G-Hilb and equivalences of derived categories by variations of GIT quotient*, Duke Math. J., 124 (2004), pp. 259–307.
- [24] A. DEGERATU AND T. WALPUSKI, *Rigid HYM connections on tautological bundles over ALE crepant resolutions in dimension three*, SIGMA Symmetry Integrability Geom. Methods Appl., 12 (2016), pp. Paper No. 017, 23.
- [25] T. EGUCHI AND A. J. HANSON, *Selfdual Solutions to Euclidean Gravity*, Annals Phys., 120 (1979), p. 82.
- [26] D. FABBRI, P. FRÉ, L. GUALTIERI, C. REINA, A. TOMASIELLO, A. ZAFFARONI, AND A. ZAMPA, *3D superconformal theories from Sasakian seven-manifolds: new non-trivial evidences for  $AdS_4/CFT_3$* , Nuclear Physics B, 577 (2000), pp. 547–608. [[hep-th/9907219](#)].
- [27] D. FABBRI, P. FRÉ, L. GUALTIERI, AND P. TERMONIA,  *$Osp(N|4)$  supermultiplets as conformal superfields on  $\partial AdS_4$  and the generic form of  $\mathcal{N}=2$ ,  $D=3$  gauge theories*, Classical and Quantum Gravity, 17 (2000), p. 55. [[hep-th/9905134](#)].
- [28] S. FERRARA AND C. FRONSDAL, *Gauge fields as composite boundary excitations*, Physics Letters B, 433 (1998), pp. 19–28. doi:10.1016/S0370-2693(98)00664-9 [[hep-th/9802126](#)].
- [29] S. FERRARA, C. FRONSDAL, AND A. ZAFFARONI, *On  $\mathcal{N}=8$  supergravity in  $AdS_5$  and  $\mathcal{N}=4$  superconformal Yang-Mills theory*, Nuclear Physics B, 532 (1998), pp. 153–162. doi:10.1016/S0550-3213(98)00444-1 [[hep-th/9802203](#)].

- [30] P. FRÉ AND P. A. GRASSI, *The Integral Form of D=3 Chern-Simons Theories Probing  $\mathbb{C}^n/\Gamma$  Singularities*, Fortsch. Phys., 65 (2017), p. 1700040.
- [31] P. FRÉ, L. GUALTIERI, AND P. TERMONIA, *The structure of  $\mathcal{N} = 3$  multiplets in AdS<sub>4</sub> and the complete  $\text{Osp}(3|4) \times \text{SU}(3)$  spectrum of M-theory on AdS<sub>4</sub>  $\times$  N<sup>0,1,0</sup>*, Physics Letters B, 471 (1999), pp. 27–38. [[hep-th/9909188](#)].
- [32] P. G. FRÉ, *Advances in Geometry and Lie Algebras from Supergravity*, Theoretical and Mathematical Physics book series, Springer, 2018.
- [33] D. GAIOTTO AND D. L. JAFFERIS, *Notes on adding D6 branes wrapping  $\mathbb{RP}^3$  in AdS(4)  $\times$   $\mathbb{CP}^3$* , JHEP, 11 (2012), p. 015.
- [34] D. GAIOTTO AND X. YIN, *Notes on superconformal Chern-Simons-Matter theories*, Journal of High Energy Physics, 2007 (2007), p. 056. doi:10.1088/1126-6708/2007/08/056 [[arXiv:0704.3740](#) [hep-th]].
- [35] G. W. GIBBONS AND S. W. HAWKING, *Gravitational Multi - Instantons*, Phys. Lett., 78B (1978), p. 430.
- [36] ———, *Classification of Gravitational Instanton Symmetries*, Commun. Math. Phys., 66 (1979), pp. 291–310.
- [37] A. HATCHER, *Algebraic topology*, Cambridge University Press, Cambridge, 2002.
- [38] M. HAUZER AND A. LANGER, *Moduli spaces of framed perverse instantons on  $\mathbb{P}^3$* , Glasg. Math. J., 53 (2011), pp. 51–96.
- [39] N. J. HITCHIN, A. KARLHEDE, U. LINDSTRÖM, AND M. ROČEK, *Hyperkahler metrics and supersymmetry*, Commun. Math. Phys., 108 (1987), p. 535.
- [40] Y. ITO AND M. REID, *The McKay correspondence for finite subgroups of  $SL(3, \mathbb{C})$* , in Higher dimensional complex varieties, Editors Marco Andreatta and Thomas Peternell, De Gruyter, 1994, pp. 221–240.
- [41] D. JOYCE, *Quasi-ALE metrics with holonomy  $SU(m)$  and  $Sp(m)$* , Ann. Global Anal. Geom., 19 (2001), pp. 103–132.
- [42] R. KALLOSH AND A. VAN PROEYEN, *Conformal symmetry of supergravities in AdS spaces*, Physical Review D, 60 (1999), p. 026001. doi:10.1103/PhysRevD.60.026001 [hep-th/9804099].
- [43] I. R. KLEBANOV AND E. WITTEN, *Superconformal field theory on three-branes at a Calabi-Yau singularity*, Nucl. Phys., B536 (1998), pp. 199–218.
- [44] P. B. KRONHEIMER, *The construction of ALE spaces as hyper-Kähler quotients*, J. Differential Geom., 29 (1989), pp. 665–683.
- [45] ———, *A Torelli-type theorem for gravitational instantons*, J. Differential Geom., 29 (1989), pp. 685–697.
- [46] J. MALDACENA, *The large-N limit of superconformal field theories and supergravity*, International Journal of Theoretical Physics, 4 (1999), pp. 1113–1133. doi:10.1023/A:1026654312961 [[hep-th/9711200](#)].
- [47] D. MARKUSHEVICH, *Resolution of  $\mathbb{C}^3/H_{168}$* , Math. Ann., 308 (1997), pp. 279–289.
- [48] J. MCKAY, *Graphs, singularities and finite groups*, Proc. Symp. Pure Math., 37 (1980), p. 183.

- [49] D. MUMFORD, J. FOGARTY, AND F. KIRWAN, *Geometric invariant theory*, vol. 34 of *Ergebnisse der Mathematik und ihrer Grenzgebiete (2)*, Springer-Verlag, Berlin, third ed., 1994.
- [50] P. E. NEWSTEAD, *Geometric invariant theory*, in *Moduli spaces and vector bundles*, vol. 359 of *London Math. Soc. Lecture Note Ser.*, Cambridge Univ. Press, Cambridge, 2009, pp. 99–127.
- [51] M. REID, *McKay correspondence*, in *Proc. of Algebraic Geometry Symposium, Kinoshita*, 1997, pp. 14–41. T. Katsura Ed.
- [52] S.-S. ROAN, *Minimal resolutions of Gorenstein orbifolds in dimension three*, *Topology*, 35 (1996), pp. 489–508.
- [53] A. V. SARDO INFIRRI, *Resolutions of orbifold singularities and representation moduli of McKay quivers*, PhD thesis, Kyoto U., RIMS, 1994.
- [54] ———, *Partial resolutions of orbifold singularities via moduli spaces of HYM type bundles*. [arXiv:alg-geom/9610004](https://arxiv.org/abs/alg-geom/9610004), 1996.
- [55] ———, *Resolutions of orbifold singularities and flows on the McKay quiver*. [arXiv:alg-geom/9610005](https://arxiv.org/abs/alg-geom/9610005), 1996.
- [56] H. J. S. SMITH, *On systems of linear indeterminate equations and congruences*, *Phil. Trans. R. Soc. Lond.*, 151 (1) (1861), pp. 293–326. Reprinted (pp. 367–409) in *The Collected Mathematical Papers of Henry John Stephen Smith, Vol. I*, edited by J. W. L. Glaisher. Oxford: Clarendon Press (1894), xcv+603 pp.
- [57] A. ZHIVKOV, *Resolution of degree = 6 algebraic equations by genus two theta constants*, *Journal of Geometry and Symmetry in Physics*, 11 (2008), pp. 77–93.